Examining Pathogenic and Mutualistic Regulatory Networks in the Bacterium *Xenorhabdus nematophila*

By

Xiaojun Lu

A dissertation submitted in partial fulfillment

of the requirements for the degree of

Doctor of Philosophy

(Microbiology)

at the

UNIVERSITY OF WISCONSIN-MADISON

2012

Date of final oral examination: 05/18/2012

The dissertation is approved by the following members of the Final Oral Committee:

Heidi Goodrich-Blair, Professor, Bacteriology

Jean-Michel Ané, Associate Professor, Agronomy

Margaret J. McFall-Ngai, Professor, Medical Microbiology and Immunology

John M. Mansfield, Professor, Bacteriology

Edward G. Ruby, Professor, Medical Microbiology and Immunology

Examining Pathogenic and Mutualistic Regulatory Networks in the Bacterium *Xenorhabdus nematophila*

Xiaojun Lu

Under the supervision of Professor Heidi Goodrich-Blair

At the University of Wisconsin-Madison

Xenorhabdus nematophila, a Gram-negative bacterium, forms a mutualistic association with the entomopathogenic nematode *Steinernema carpocapsae,* and also is a pathogen that can kill a wide range of insects, and therefore provides us an opportunity to study the underlying mechanisms of both types of interactions. The successful adaptation of *X. nematophila* to each of its hosts requires coordinated expression of cellular factors in response to changes in host environments. The work presented here examines the relationships among the known regulators involved in adaptation and reveals new factors that contribute to the regulatory network.

A microarray analysis was performed to examine the global transcriptomes of LrhA (LysR homologue A) and Lrp (leucine-responsive regulatory protein). It revealed that LrhA, which was initially regarded only as a regulator of activities involved in insect virulence and degradation has wider effects on cellular functions, including nutrient and energy metabolism, transport and secretion, and signal transduction. The analysis of Lrp regulon not only confirmed its global regulator function in mutualism through the regulation of nematode colonization genes *nilABC* and in pathogenesis through activation of LrhA, but also revealed that Lrp negatively regulates the transcription factor RpoS which is essential in mutualism, and the Cas system, a bacterial defense system against phage and other invading exogenous DNA elements.

Charcterization of the RpoS regulon suggests that it affects bacterial mutualism by mediating resistance to reactive-oxygen-species, growth under stress, and micro-aerobic conditions, and regulation of nutrient uptake and transport. Studies on the Cas system revealed its role in regulating bacterial mutualism potentially by affecting bacterial phenotypic variation and providing resistance to phage. They also suggest the Cas system may regulate the expression of endogenous *X. nematophila* genes.

Through the study of the regulatory networks of *X. nematophila*, this work provides useful information for us to understand the complex mechanisms of *X. nematophila*-host interactions, and allows us to gain valuable insights on both bacterial pathogenesis and mutualism in other systems. General knowledge obtained on how bacteria make the transition between pathogenic and mutualistic states will also help us control diseases involving human beings, animals and plants.

ACKNOWLEDGEMENTS

I have to admit that I never thought I would spend over 15 years studying microbiology before I reached this far. But science is just so fascinating and drags you into it without any notice.

It might be just for satisfying my own curiosity of seeing what's on the other side of the globe when I first traveled thousands of miles away from home to the US. But choosing the University of Wisconsin-Madison for my Ph.D. study was a more than apparent decision to make after finishing my M.S. in Hawaii, even though it was a dramatic change between two extremes (From a tropical paradise to a freezing cold-box). After so many years and finally reach the end of my Ph.D. training in Mad City, I would like to take this opportunity to thank all those people who have been helping me to make this achievement.

First, I would like to thank my advisor, Dr. Heidi Goodrich-Blair, who has been providing me all the warmhearted support and guidance since I first joined the lab. Science could be frustrating, but Heidi just always uses her knowledge and wisdom to shed light in front of me each time I reach a dead end in my research.

Second, I would like to express my gratitude to my committee members, Drs. Jean-Michel Anné, Margaret J. McFall-Ngai, John M. Mansfield, and Edward G. Ruby for offering their critical advice throughout the course of my Ph.D. study.

Third, I want to give my thanks to all my labmates for their generous help on my research, especially to Aaron Anderson who spent tremendous amount of time to help solve the mystery of RpoS.

Next, I would like to thank my friends who helped me fit in the life in Madison and made my experience of Ph.D. study more joyful.

Most importantly, I would like to thank my family for their never-ending support and care. I'm grateful to my parents Fengqin Xu and Qingchun Lu for their continuous encouragement during the course of my life, to my wife Yan Yue for her love and support, and to my new born daughter Sihan Lu who makes my life more meaningful and adds extra fun to the last part of my Ph.D. study in Madison. I would also like to thank two special family members, Jeff Smoller and Terry Shelton, who have been taking care of me like my American fathers and teaching me many things that I may never learn by myself.

Thank you all for everything!

Xiaojun Lu

TABLE OF CONTENTS

LIST OF FIGURES

Chapter 1

Chapter 2

Chapter 3

Chapter 4

LIST OF TABLES

CHAPTER 1

Introduction

Bacteria-Host Interactions

Bacteria, one of the most abundant and diverse life forms on earth, have been found in almost all environmental niches on our planet, from boiling deep sea thermal vents (Alain *et al*., 2002) to frozen glacier ice (Klassen *et al*., 2011), and from thin floating clouds in the sky (Kourteva *et al*., 2011) to miles down into the earth (Lin *et al*., 2006). With their wide distribution and an estimate of approximately five nonillion (5×10^{30}) total bacterial cells in our world, which form a biomass that exceeds that of all plants and animals (Whitman *et al*., 1998), bacteria are inevitably found to be associated with all other life forms, such as animals, plants, viruses, as well as other bacteria. The simple but mostly self-functional single cell structure of bacteria allows their quick reproduction, which provides the evolutionary advantages (Chou *et al.*, 2009) for them to develop different strategies to adapt to various interactions with other life forms.

Currently, bacteria-host interactions are classified in three major categories based on the effects of bacteria on their hosts. The first category is pathogenesis (or parasitism) in which the bacteria benefit from the relationship at the expense of their hosts and often cause detrimental effects on the hosts. This type of bacteria-host interaction has been most studied due to the diseases caused by various pathogenic bacteria in humans (de Vrankrijker *et al*., 2010), and animals (Marcé *et al*., 2010) or plants (Gonzalez *et al*., 2011) that have commercial value. But the disease-causing nature of pathogens, and the need to use complex animal and plant systems for their study have raised numerous concerns and challenges including the confinement of the pathogens, short workable time due to host death, and ethical issues on the test subjects used. The second form of interaction is mutualism where both the bacteria and their hosts benefit from

the relationship, and such association usually provides both parties advantages in their living environment. For example, the species of soil bacteria *Rhizobium* can mutualistically associate with legumes by stimulating the plants to form root nodules. Inside the nodules the plant hosts provide shelter and nutrients for the bacteria while the bacteria supply the hosts with extra nitrogen source by fixing the environmental nitrogen that cannot be directly utilized by the plants. This allows the plants to gain advantages in growth compared to others that are not associated with *Rhizobium* species (Sawada *et al*., 2003). Although the pathogenic and mutualistic relationships cause very different effects on the hosts, they both involve processes like host recognition, attachment and colonization, and suppression of host immunity. Increasing evidences show that the underlying molecular and cellular mechanisms for the bacteria to establish these two types of interactions can be fundamentally very similar (Soto *et al*., 2009). For example, derivatives of the ubiquitous microbial compound peptidoglycan induce disease symptoms during pathogenesis but also induce the squid, *Euprymna scolopes*, to produce a mucus that is necessary for colonization by its bacterial symbiont *Vibrio fischeri* (Cloud-Hansen *et al*., 2006). Thus the knowledge gained on either of the two interactions can shed lights on the other. Also, studying the mutualistic systems allows us to better utilize bacteria to benefit our own, instead of treating them all like enemies. For example, the artificial introduction of *Rhizobium* species during soybean cultivation improves the yields (Denison and Toby, 2004), and probiotic foods and treatments developed can help reduce the incidence of diarrhea and the risk of allergic disease in humans, such as atopic dermatitis (Salminen *et al*., 2005). The last category is the commensalism, which has been a controversial classification. Presumptively in this bacteria-host interaction one party benefits from the relationship without causing notable effects on the other. Although this relationship seems simple, recent development of technologies,

such as microarray analysis, have allowed more in-depth studies of this type of bacteria-host interaction, and the new findings have blurred the line between commensalism and pathogenesis or mutualism. One example is the microbiota on animal skins. Rather than the previous belief that the skin microbiota feed on the dead skin cells or skin-secreted products but do not affect the animals, the latest research showed that members of skin microbiota produce antimicrobial peptides that may help hosts defense against potential pathogenic microbes (Iwase *et al*., 2010). Studies on gut microbiota in human demonstrated that the originally thought commensal bacteria do benefit the hosts by synthesizing compounds, such as vitamins, that meet the host nutrient needs (Bik, 2010), and the discovery of opportunistic pathogens showed that members of commensal microbiota can be affected by the environmental changes and thus alter its relationship with their hosts (Rodr ǵuez-Rojas *et al*., 2012).

Xenorhabdus nematophila-Insect-Nematode Tripartite Model System

Although pathogenic and mutualistic bacteria-host interactions have been widely studied using different model systems, most of these systems only involve one of these two types of interactions, which makes it difficult to do the parallel study of both interactions with comparable backgrounds. In recent years, new models utilizing bacteria capable of forming both pathogenic and mutualistic relationships with different hosts were developed (Herbert and Goodrich-Blair, 2007; Goodrich-Blair and Clarke, 2007). This has allowed us to characterize the underlying mechanisms for both types of interactions and examine the relationship between host specificity and determinants that affect bacterial pathogenic and mutualistic phenotype switches.

Xenorhabdus nematophila, a Gram-negative bacterium, is able to form a species-specific mutualistic association with the entomopathogenic nematode *Steinernema carpocapsae*, and also is capable of acting as a pathogen to infect and kill a wide range of insect larvae, including many with impacts on agriculture and forestry (Forst *et al*., 1997). The mutualistic relationship between *X. nematophila* and *S. carpocapsae* is not obligate, as both the bacterium and the nematode can survive without the other, although *S. carpocapsae* reproduces more efficiently with the presence of *X. nematophila* (Sicard *et al*., 2003; Mitani *et al*., 2004). During its mutualistic life cycle, *X. nematophila* colonizes the nematode receptacle, a specialized lumenal region of the anterior end intestine of non-feeding infective juvenile (IJ) form of *S. carpocapsae* that develops when nutrients are limited (Bird and Akhurst, 1983). Prior to the IJ development, a few ingested *X. nematophila* cells colonize the pharyngeal-intestinal valve (unpublished findings), then move to and proliferate in the receptacle. The number of bacterial cells in the receptacle is maintained in a range of 30~200 per IJ once fully colonized (Orchard and Goodrich-Blair, 2005), which indicates a delicate balance between the nematode host and the bacterial guest. This balance not only prevents the uncontrolled bacterial growth that may cause host death, but also presumably ensures proper suppression of host defense system to support bacterial survival. The IJs serve as a vector to carry *X. nematophila* into susceptible insect hosts and release the bacterial cells in response to factors in insect hemolymph (Snyder *et al*., 2007). Once it enters the insect, the bacterium adapts to its new host by switching from its mutualistic state into a virulent form. Although the nematode alone can kill the insects, co-infection with *X. nematophila* makes the killing process more efficient as the bacterium itself is also pathogenic to the insects (Forst *et al*., 1997; Goodrich-Blair and Clarke, 2007). Within insect cadaver the bacterium produces various extracellular proteins, such as lipases (Richards and Goodrich-Blair,

2010) and proteases (Caldas *et al*., 2002), which help break down insect tissues for nutrients. When nutrients are depleted in the environment, *X. nematophila* re-associates with the nematode IJs, which start searching for new insect hosts to repeat the cycle (Figure 1.1).

This tripartite system as described above provides a simple model, relative to other systems involving complex animals, plants and microbial consortia, which can be used for understanding various aspects of bacteria-host interactions. As all three components of this system, the bacterium, nematode and insects, can be easily cultivated separately under laboratory conditions, their genetic, biochemical and developmental traits can be individually characterized. The bacterial pathogenic association with insects by direct injection and the mutualistic association with nematode *in vitro* using laboratory media allow us to investigate these two types of interactions separately without the interference from the other, but still within the same bacterial background, allowing parallel comparisons (Morgan *et al*., 1997; Herbert and Goodrich-Blair, 2007).

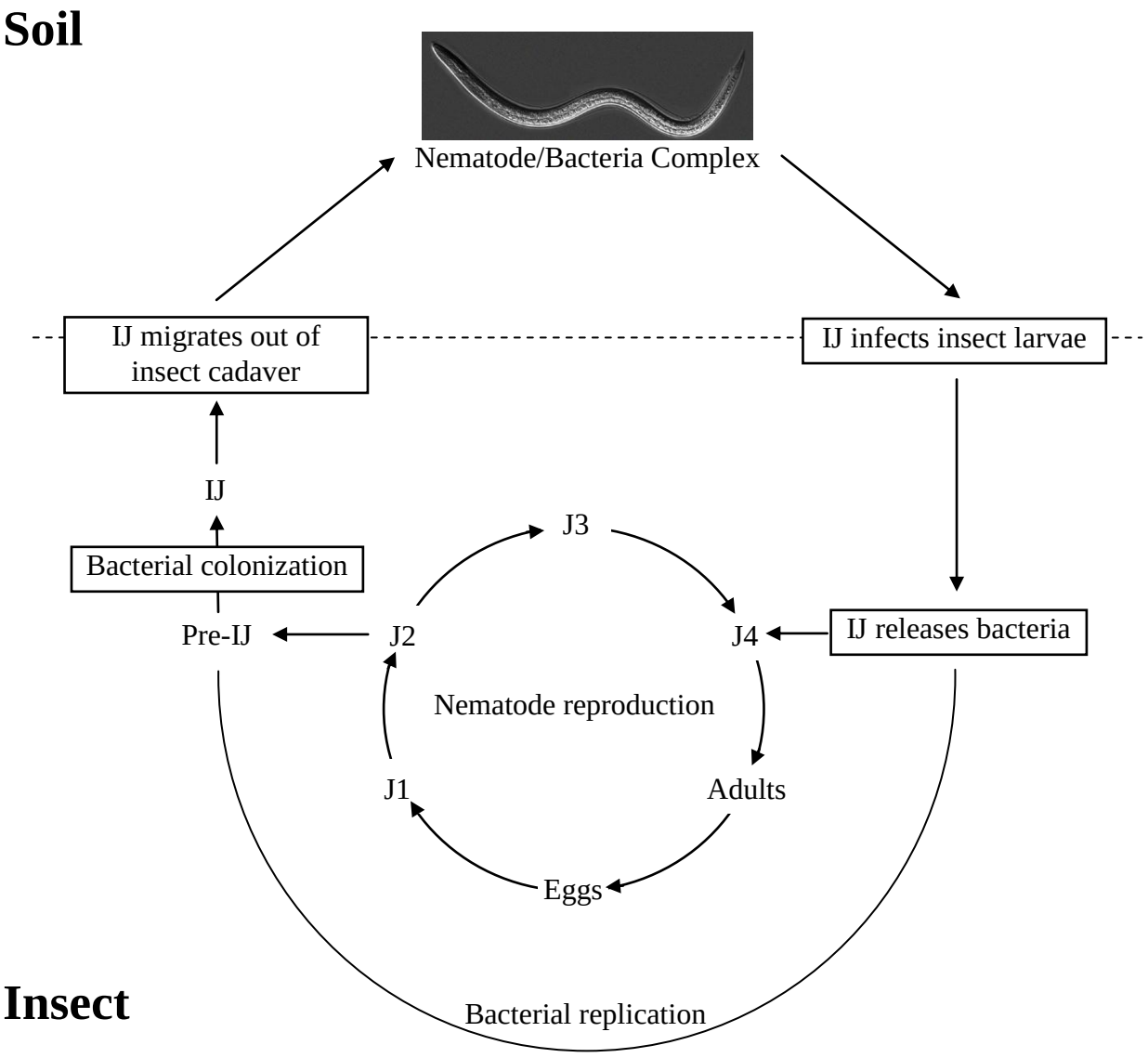

Figure 1.1. Life cycle of the nematode *S. carpocapsae* and the bacterium *X. nematophila*.

X. nematophila pathogenic and mutualistic regulatory networks

The successful adaptation of *X. nematophila* in both pathogenic and mutualistic hosts requires a finely controlled expression of various cellular factors in response to changes in host environments. In recent years, progress has been made for understanding the regulatory hierarchy of pathogenic and mutualistic interactions involved in the *X. nematophila*-hosts system (Herbert and Goodrich-Blair, 2007; Goodrich-Blair and Clarke, 2007). In particular, the global regulator Lrp has been found to be involved in almost all major regulatory pathways identified for pathogenic and mutualistic regulations (Figure 1.2; Cowles *et al*., 2007). The removal of the *lrp* gene causes pleiotropic defects in *X. nematophila* in both pathogenesis and mutualism, and high level expression of Lrp also causes attenuated virulence (Unpublished findings), which indicates a dosage-dependent regulation of bacterial cellular functions by Lrp.

Lrp activates the expression of virulence regulator LrhA (LysR homologue A), a member of the LysR-type transcriptional regulator family. The *lrhA* mutant has a severe virulence defect, demonstrated by an 8-10 times lower insect killing ability (Richards *et al*., 2008). LrhA positively regulates the gene encoding the flagellar master regulator FlhDC. Although bacterial motility is not required for virulence, LrhA-dependent regulation of *flhDC* may affect the transcription of virulence determinant genes and the secretion of their products via the flagellar apparatus (Givaudan and Lanois, 2000; Park and Forst, 2006). *flhD* has been found to be negatively regulated by the OmpR/EnvZ two-component system which also represses antibiotic activity and the expression of a non-ribosomal peptide synthetase operon (Park and Forst, 2006). The EnvZ component of the system acts as the membrane receptor, which detects and transfers external signals into the bacterial cell to influence the function of transcription factor OmpR.

Insect death may trigger the relief of OmpR/EnvZ repression of *flhDC*, which indicates that bacterial secreted enzymes, such as lipases, proteases and hemolysins, may serve more as facilitators for converting biomass into utilizable nutrients for nematode reproduction rather than solely acting as virulence factors for insect killing (Park and Forst, 2006).

For mutualistic regulation, Lrp also plays a central role. The *lrp* mutant is defective in colonizing nematode host, and *nilABC* genes that are necessary for bacterial mutualistic colonization are suppressed by Lrp (Cowles *et al*., 2007). Studies suggest that *nilA*, *nilB* and *nilC* encode an inner membrane protein, an outer membrane protein, and a periplasmically-oriented outer membrane lipoprotein, respectively. Expression of the *nil* genes in non-colonizing *Xenorhabdus* species confers upon the bacterium the ability to colonize *S. carpocapsae* nematodes, which suggests they are host specificity determinants. Synergistically with Lrp, the transcription factor NilR represses *nil* genes, but also is itself negatively regulated by Lrp (Heungens *et al*., 2002; Cowles and Goodrich-Blair, 2006; Cowles and Goodrich-Blair, 2008). The synergistic repression of *nil* genes by Lrp and NilR at first seems contradictory to the fact that both Lrp and Nil factors are necessary for colonization. The dosage-dependent effects of Lrp in bacterial virulence regulation may help explain this contradiction. In virulence regulation, low levels of Lrp expression is able to activate virulence functions and allows efficient insect killing, while high level of Lrp expression attenuates the bacterial virulence in insects (Unpublished findings). This may due to the ability of Lrp-like regulators to form different multimers that can provide variable binding affinities for the protein at regulatory binding sites (Brinkman *et al*., 2003). Lrp may repress Nil factors, likely as a mono- or dimer, when its level is kept low for virulence induction in insect hosts, and these same conditions may be permissive for NilR expression which adds an extra layer of Nil factor suppression. When Lrp level becomes higher,

multimers of the protein may have reversed effects on regulation: de-repression of *nil* genes and a tighter repression of *nilR* that further releases the repression of Nil factors.

In addition to its functions in pathogenesis and mutualism, Lrp is also involved in the regulation of a process called phenotypic variation, which takes place during prolonged stationary phase growth and causes *X. nematophila* to spontaneously switch between two cell types, primary and secondary (Volgyi *et al*., 1998). The switches are normally reversible while stable non-reversible secondary form can be obtained by extended long-term incubation and subculturing (Sicard *et al*., 2005; Cowles *et al*., 2007). The phenotypic differences demonstrated by these two types of cells are variable depending on *Xenorhabdus* species and strain. In general, primary form cells produce a wide range of extracellular factors, such as hemolysins, proteases, antibiotics and lipases, have the ability to agglutinate sheep erythrocytes, bind bromothymol blue dye, and are motile in both swimming and swarming assays. The secondary type cells of *X. nematophila* demonstrate a reduction in the levels of hemolysin, antibiotics and intracellular crystalline inclusion proteins and are non-motile on swim plates (Givaudan *et al*., 1995; Volgyi *et al*., 1998). The *lrp* mutant is phenotypically similar to secondary form bacterium except it is also defective in lipase production and motility. Despite the *in vitro* differences, both primary and secondary variants are capable of killing insects and colonizing nematode host to similar levels. Although the primary form bacterium is the mostly isolated form from *S. carpocapsae* nematode in nature, secondary form of the *X. nematophila* F1 strain generated by prolonged stationary-phase incubation has a competitive advantage in association with nematode host when co-injected into insect hosts with primary form bacterium (Sicard *et al*., 2005). In *X. nematophila* ATCC 19061 strain (HGB800), which was used in this work, the similar competitive effects in colonization were also observed when using stable secondary form strains obtained by long-term

growth through multiple passages. But in the tests using unstable reversible secondary form bacterium the primary form was the mostly isolated from colonized IJs (Cowles *et al*., 2007). The mechanisms for the selection of stable secondary form but not the unstable secondary form in nematode are still unclear and require further investigation.

Another factor that is involved in *X. nematophila* mutualism is RpoS, which was originally identified in other bacteria as a regulator for the expression of alkaline phosphatase (Touati *et al*., 1986) and catalase (Loewen and Triggs, 1984), as well as for protection from near-UV light (Sammartano *et al*., 1986) Other studies then made it clear that RpoS functions as a sigma factor regulating gene expression during the transition from exponential phase to stationary phase or in response to general stress, including oxidative stress such as that caused by peroxide challenge (Hengge-Aronis, 1993; Battesti *et al*., 2011). The *X. nematophila rpoS* mutant produces proteases, antibiotic, lipases, outer membrane proteins and crystal proteins at levels indistinguishable from those of the wild-type, and has no changes in exponential growth rate, stationary-phase cell morphology, or the ability to attach to an abiotic surface. However, it does display hyper-motility relative to wild type. With respect to host interactions, the *rpoS* mutant causes slightly, but significantly higher mortality in insects and completely loses the ability to colonize the nematode IJ, although it still supports nematode growth and reproduction *in vitro* (Vivas and Goodrich-Blair, 2001).

Previous attempts using hydrogen peroxide treatment, which causes cellular oxidative stress, revealed only a slight (4-7 fold) defect of the *rpoS* mutant in survival to peroxide challenge compared to wild type. In unpublished work, ectopic expression of the *E. coli* catalase gene partially restores the colonization ability of the mutant (Chapter 3). These data indicate that

RpoS may affect bacterial nematode colonization by supporting the stress response functions of the bacterium.

In the studies described in this thesis, the connections among the different known regulatory factors in *X. nematophila* were further explored using newly obtained genomic information of the bacterium and microarray technology. While new Lrp and LrhA dependent factors and regulatory pathways were identified and our knowledge on the regulatory networks was expanded, the microarray analysis provided much more complete information on gene expression profiles of Lrp and LrhA regulons. Analysis showed that these two regulons not only overlap in the functions for bacterial virulence but also co-regulate bacterial signal transduction, host interaction, and metabolism of energy and nutrients. The involvement of LrhA in these cellular functions in addition to its originally identified virulence modulation function helped change our opinion on this regulator. The revealed connections between Lrp and RpoS and potential anti-phage Cas system also provide directions for our future research on understanding the underlying mechanism of bacteria-host interactions.

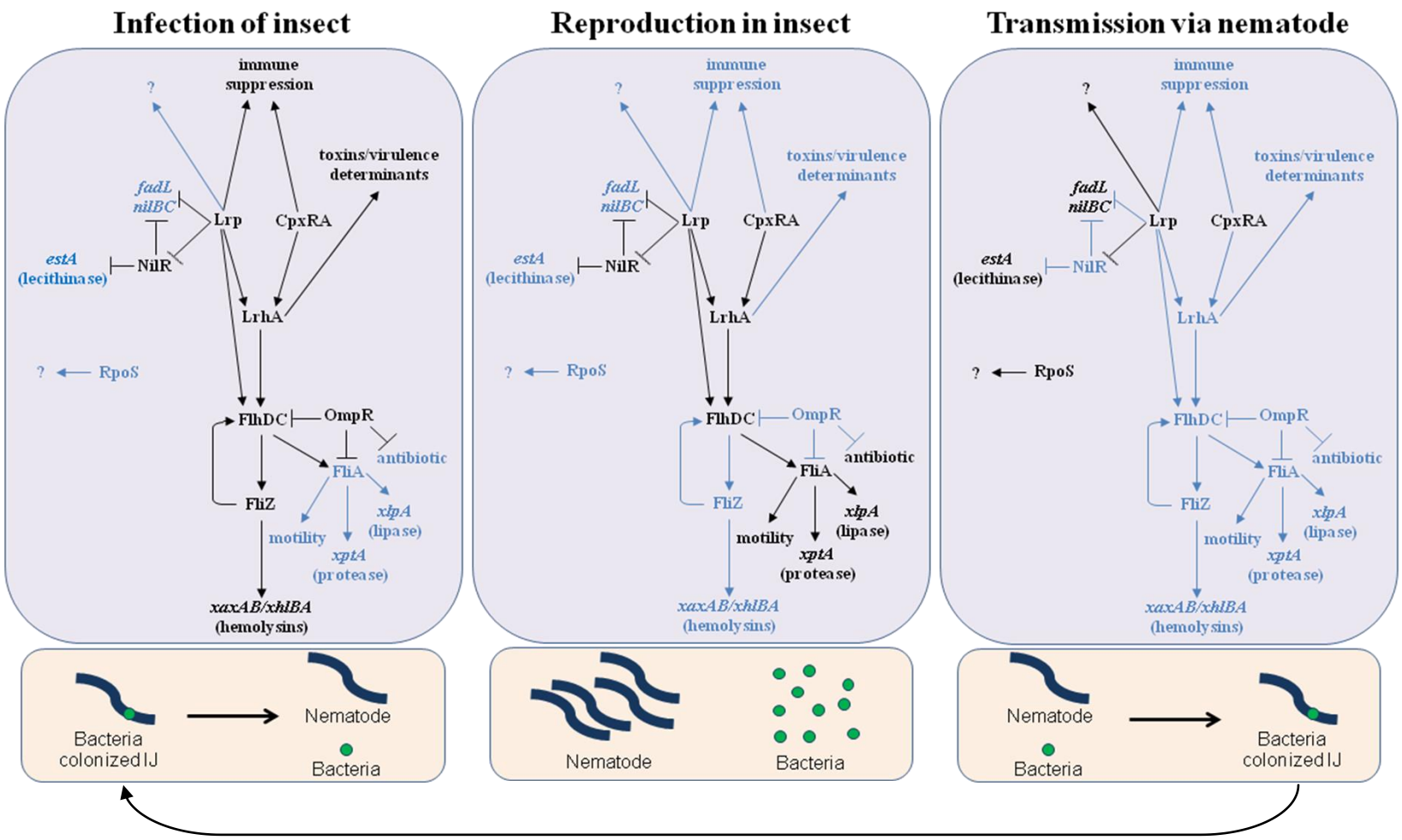

Figure 1.2. Previous predicted model of *X. nematophila* signal transduction cascades controlling mutualism and pathogenesis genes. Black lines indicated predicted active pathways; Blue lines indicate predicted inactive pathways. Arrows indicate positive regulations; Blunt arrows indicate negative regulations (Richards and Goodrich-Blair, 2009).

THESIS PLAN

Xenorhabdus nematophila is a Gram-negative enterobacterium that can mutualistically associate with the entomopathogenic soil nematode *Steinernema carpocapsae* and is pathogenic to a wide range of insects. It employs a series of regulators to mediate its mutualistic and pathogenic interactions with different hosts. This thesis describes the exploration of the regulatory networks involved in these two types of bacterium-host interactions and the characterization of two specific factors, RpoS and Cas system, that contribute to bacterial mutualism.

Chapter 2 describes the microarray analysis of the global effects of Lrp and LrhA on *X. nematophila* gene expression profile.

Chapter 3 describes the microarray analysis of the effects of RpoS on *X. nematophila* gene expression profile and characterizes the mechanisms for RpoS to affect bacterial mutualism.

Chapter 4 characterizes the functions of *X. nematophila* Cas system in bacterial mutualism and pathogenesis.

Chapter 5 contains a summary of this work and discussion of potential future directions.

REFERENCES

Alain K, Pignet P, Zbinden M, Quillevere M, Duchiron F, Donval JP, Lesongeur F, Raguenes G, Crassous P, Querellou J, Cambon-Bonavita MA. 2002. *Caminicella sporogenes* gen. nov., sp. nov., a novel thermophilic spore-forming bacterium isolated from an East-Pacific Rise hydrothermal vent. Int J Syst Evol Microbiol. 52(Pt 5):1621-8

Battesti A, Majdalani N, Gottesman S. 2011. The RpoS-mediated general stress response in *Escherichia coli*. Annu Rev Microbiol. 65:189-213

Bik EM. 2010. Composition and function of the human-associated microbiota. Nutr Rev. 68(3):189

Bird AF, Akhurst RJ. 1983. The nature of the intestinal vesicle in nematodes of the family *Steinernematidae*. Int J Parasitol. 13:599–606

Brinkman AB, Ettema TJ, de Vos WM, van der Oost J. 2003. The Lrp family of transcriptional regulators. Mol Microbiol. 48(2):287-94

Caldas C, Cherqui A, Pereira A, Simões N. 2002. Purification and characterization of an extracellular protease from *Xenorhabdus nematophila* involved in insect immunosuppression. Appl Environ Microbiol. 68:1297-1304

Chou HH, Berthet J, Marx CJ. 2009. Fast growth increases the selective advantage of a mutation arising recurrently during evolution under metal limitation. PLoS Genet. 5(9):e1000652

Cloud-Hansen KA, Peterson SB, Stabb EV, Goldman WE, McFall-Ngai MJ, Handelsman J. 2006. Breaching the great wall: peptidoglycan and microbial interactions. Nat Rev Microbiol. 4(9):710-6

Cowles CE, Goodrich-Blair H. 2006. *nilR* is necessary for co-ordinate repression of *Xenorhabdus nematophila* mutualism genes. Mol Microbiol. 62(3):760-71

Cowles KN, Cowles CE, Richards GR, Martens EC, Goodrich-Blair H. 2007. The global regulator Lrp contributes to mutualism, pathogenesis and phenotypic variation in the bacterium *Xenorhabdus nematophila*. Cell Microbiol. 9(5):1311-23

de Vrankrijker AM, Wolfs TF, van der Ent CK. 2010. Challenging and emerging pathogens in cystic fibrosis. Paediatr Respir Rev. 11(4):246-54.

Denison RF, Toby Kiers E. 2004. Why are most rhizobia beneficial to their plant hosts, rather than parasitic? Microbes Infect. 6(13):1235-9.

Forst S, Dowds B, Boemare N, Stackebrandt E. 1997. *Xenorhabdus* and *Photorhabdus* spp.: bugs that kill bugs. Annu Rev Microbiol. 51:47-72

Givaudan, A., Baghdiguian, S., Lanois, A., Boemare, N. 1995. Swarming and swimming changes concomitant with phase variation in *Xenorhabdus nematophilus*. Appl Environ Microbiol 61: 1408–1413

Gonzalez M, Pujol M, Metraux JP, Gonzalez-Garcia V, Bolton MD, Borrás-Hidalgo O. 2011. Tobacco leaf spot and root rot caused by *Rhizoctonia solani Kühn*. Mol Plant Pathol. 12(3):209-16

Goodrich-Blair H, Clarke DJ. 2007. Mutualism and pathogenesis in *Xenorhabdus* and *Photorhabdus*: two roads to the same destination. Mol Microbiol. 64(2):260-8

Hengge-Aronis R. 1993. Survival of hunger and stress: the role of *rpoS* in early stationary phase gene regulation in *E. coli*. Cell. 72(2):165-8

Herbert EE, Goodrich-Blair H. 2007. Friend and foe: the two faces of *Xenorhabdus nematophila*. Nat Rev Microbiol. 5(8):634-46

Heungens K, Cowles CE, Goodrich-Blair H. 2002. Identification of *Xenorhabdus nematophila* genes required for mutualistic colonization of *Steinernema carpocapsae* nematodes. Mol Microbiol. 45(5):1337-53

Ivanova AB, Glinsky GV, Eisenstark A. 1997. Role of *rpoS* regulon in resistance to oxidative stress and near-UV radiation in delta *oxyR* suppressor mutants of *Escherichia coli*. Free Radic Biol Med. 23(4):627-36

Iwase T, Uehara Y, Shinji H, Tajima A, Seo H, Takada K, Agata T, Mizunoe Y. 2010. *Staphylococcus epidermidis Esp* inhibits *Staphylococcus aureus* biofilm formation and nasal colonization. Nature. 465(7296):346-9

Klassen JL, Foght JM. 2011. Characterization of *Hymenobacter* isolates from Victoria Upper Glacier, Antarctica reveals five new species and substantial non-vertical evolution within this genus. Extremophiles. 15(1):45-57

Kourteva P, Hillb K,Shepsonb P, Konopka A. 2011. Atmospheric cloud water contains a diverse bacterial community. Atmospheric Environment. 45(30):5399–5405

Krajewska M, Kozińska M, Zwolska Z, Lipiec M, Augustynowicz-Kopeć E, Szulowski K. 2012. Human as a source of tuberculosis for cattle. First evidence of transmission in Poland. Vet Microbiol. Epub ahead of print

Lin LH, Wang PL, Rumble D, Lippmann-Pipke J, Boice E, Pratt LM, Sherwood Lollar B, Brodie EL, Hazen TC, Andersen GL, DeSantis TZ, Moser DP, Kershaw D, Onstott TC. 2006. Long-term sustainability of a high-energy, low-diversity crustal biome. Science. 314(5798):479-82

Loewen PC, Triggs BL. 1984. Genetic mapping of *katF*, a locus that with *katE* affects the synthesis of a second catalase species in *Escherichia coli*. J Bacteriol 160:668–675

Morgan W, Kuntzelmann V, Tavernor S, Ousley MA, Winstanley C. 1977. Survival of *Xenorhabdus nematophilus* and *Photorhabdus luminescens* in water and soil. J Appl Microbiol. 83, 665–670

Marcé C, Ezanno P, Weber MF, Seegers H, Pfeiffer DU, Fourichon C. 2010. Invited review: modeling within-herd transmission of Mycobacterium avium subspecies paratuberculosis in dairy cattle: a review. J Dairy Sci. 93(10):4455-70.

Richards GR and Goodrich-Blair H. **2009**. Masters of conquest and pillage: *Xenorhabdus nematophila* global regulators control transitions from virulence to nutrient acquisition. Cell Microbiol. 11(7):1025-33.

Richards GR, Goodrich-Blair H. 2010. Examination of *Xenorhabdus nematophila* lipases in pathogenic and mutualistic host interactions reveals a role for *xlpA* in nematode progeny production. Appl Environ Microbiol. 76(1):221-9

Rodríguez-Rojas A, Oliver A, Blázquez J. 2012. Intrinsic and environmental mutagenesis drive diversification and persistence of *Pseudomonas aeruginosa* in chronic lung infections. J Infect Dis. 205(1):121-7

Salminen SJ, Gueimonde M, Isolauri E. 2005. Probiotics that modify disease risk. J Nutr 135(5):1294-8

Sammartano LJ, Tuveson RW, Davenport R. 1986. Control of sensitivity to inactivation by H_2O_2 and broad-spectrum near-UV radiation by the *Escherichia coli katF* locus. J Bacteriol 168:13–21

Sawada H, Kuykendall LD, Young JM. 2003. Changing concepts in the systematics of bacterial nitrogen-fixing legume symbionts. J Gen Appl Microbiol. 49(3):155-79

Sicard M, Le Brun N, Pages S, Godelle B, Boemare N, Moulia C. 2003. Effect of native *Xenorhabdus* on the fitness of their *Steinernema* hosts: contrasting types of interactions. Parasitol Res. 91, 520–524

Soto MJ, Domínguez-Ferreras A, Pérez-Mendoza D, Sanjuán J, Olivares J. 2009. Mutualism versus pathogenesis: the give-and-take in plant-bacteria interactions. Cell Microbiol. 11(3):381-8

Toft C, Andersson SG. 2010. Evolutionary microbial genomics: insights into bacterial host adaptation. Nat Rev Genet. 11(7):465-75

Touati E, Dassa E, Boquet PL. 1986. Pleiotropic mutations in appR reduce pH 2.5 acid phosphatase expression and restore succinate utilisation in CRP-deficient strains of *Escherichia coli*. Mol Gen Genet 202:257–264

Vivas EI, Goodrich-Blair H. 2001. *Xenorhabdus nematophilus* as a model for host-bacterium interactions: *rpoS* is necessary for mutualism with nematodes. J Bacteriol. 183(16):4687-93

Volgyi A, Fodor A, Szentirmai A, Forst S. 1998. Phase Variation in *Xenorhabdus nematophilus*. Appl Environ Microbiol. 64(4):1188-93

Whitman WB, Coleman DC, Wiebe WJ. 1998. Prokaryotes: the unseen majority. Proc Natl Acad Sci U S A. 95(12):6578-83

CHAPTER 2

Microarray analysis of *Xenorhabdus nematophila* reveals new regulatory functions of global regulator Lrp and virulence regulator LrhA

All the works described in this chapter were performed by me with the support and guidance from Dr. Heidi Goodrich-Blair.

INTRODUCTION

Xenorhabdus nematophila is a Gram-negative enterobacterium that can mutualistically associate with the entomopathogenic soil nematode *Steinernema carpocapsae* and is pathogenic to a wide range of insects. When associated with nematode host, *X. nematophila* resides in a specialized structure of infective juvenile (IJ) nematode intestine, namely the receptacle. When IJs encounter susceptible insect hosts in the environment, they will invade the host's hemocoel and release the bacterial cells. Within the insects, the bacterium produces various virulence factors that suppress host immunity and eventually kill the insects. The exoenzymes secreted by the bacterium then facilitate the degradation of insect cadaver tissues to provide nutrients for the bacterium and nematode reproduction. When nutrients are depleted the bacterium and nematode re-associate together to look for new hosts (Bird and Akhurst, 1983; Forst *et al*., 1997; Snyder *et al*., 2007). This tripartite *X. nematophila*-nematode-insect system presents a convenient model for studying both mutualistic and pathogenic microbe-host interactions using a single bacterial species, and the transition between nematode and insect hosts indicates the needs for the bacterium to fine tune its cellular functions to ensure its proper adaptation to the processes of infection, reproduction and transmission in different hosts (Figure 2.1; Morgan *et al*., 1977; Herbert and Goodrich-Blair, 2007).

The recent genomic sequencing of *X. nematophila* type strain ATCC 19061 revealed that the bacterium has a 4,432,590 bp circular chromosome with 79 tRNA and 4,299 predicted protein-coding open reading frames, and a 155,327 bp plasmid that contains 175 predicted protein-coding open reading frames (Chaston *et al*., 2011). Although the functions of many of the predicted genes and non-coding intergenic sequences in *X. nematophila* are still unknown

and need further characterization, previous studies have identified 5 regulators that are involved in bacterial pathogenicity, mutualism or both (Figure 2.1): the nematode intestine localization gene regulator NilR (Cowles and Goodrich-Blair, 2006), the general stress response regular RpoS (Vivas and Goodrich-Blair, 2001), the LysR-type regulator LrhA (Richards *et al*., 2008), the two-component system CpxRA (Herbert *et al*., 2007) and the leucine-responsive regulatory protein Lrp (Cowles *et al*., 2007).

NilR is involved in the regulation of a small subset of genes (18 proteins, ~3% of the detectable proteome) including *nilABC* that are necessary in nematode colonization and host specificity; expression of *X. nematophila nilABC* in non-colonizing *Xenorhabdus* species confers upon them the ability to colonize *S. carpocapsae*. Consistent with the fact that NilR inhibits *nilABC* gene expression, ectopic *nilR* expression causes 60-fold lower levels of bacterial colonization in *S. carpocapsae* compared to wild type (Cowles and Goodrich-Blair, 2006; Cowles and Goodrich-Blair, 2008).

RpoS is a stationary phase sigma factor known to be involved in stress responses in bacteria. *rpoS* mutants are defective in colonization of the nematode host and display a slight, but significant, increase in virulence against *M. sexta* insects relative to wild type. Current evidence indicates that RpoS affects bacterial colonization by conferring upon bacterial cells the ability to deal with reactive-oxygen species and starvation, which are believed to be conditions within nematode receptacle (Chapter 3; Vivas and Goodrich-Blair, 2001).

LrhA, a member of the LysR-type transcriptional regulator family, is an activator of a series of bacterial virulence related functions including flagellar synthesis and motility, and production of toxin, hemolysin and extracellular enzymes like lipase and proteases for breaking down host tissues. An *X. nematophila lrhA* mutant has defects in supporting nematode

reproduction, virulence in *Manduca sexta* insects (Richards *et al*, 2008), and require aspartate, leucine, and glutamate for growth on minimal medium (G.R. Richards, Ph.D. thesis, UW-Madison). Another function of LrhA is to positively regulate the genes encoding the flagellar master regulator FlhDC. Although bacterial motility is not required for virulence, LrhA-dependent regulation of *flhDC* may affect the transcription of virulence determinant genes and the secretion of their products, such as lipases via the flagellar apparatus (Givaudan and Lanois, 2000; Park and Forst, 2006; Richards and Goodrich-Blair, 2008). The expression of *flhD* is negatively regulated by the OmpR/EnvZ two-component system that also represses antibiotic activity and the expression of a non-ribosomal peptide synthetase operon. The EnvZ component of the system is a membrane receptor, which detects and transfers external signals into the bacterial cell to affect the function of transcription factor OmpR. Evidence suggests that insect death may trigger the relief of OmpR/EnvZ repression of *flhDC*, which indicates that bacterial secreted enzymes, such as lipases, proteases and hemolysins, may help convert biomass into utilizable nutrients for bacterium and nematode reproduction in addition to their functions for insect killing (Park and Forst, 2006; Richards and Goodrich-Blair, 2010).

CpxRA, a two-component signal transduction system, has been found to affect both bacterial pathogenicity and mutualism; *cpxR* and *cpxA* mutants have attenuated virulence in *M. sexta* insects and reduced levels of colonization in nematodes, compared to wild type *X. nematophila*. Based on quantitative reverse transcriptase PCR (qRT-PCR) analysis, the CpxRA system was shown to activate expression of *lrhA* and genes for motility, lipase, and mutualistic colonization of nematodes, while suppressing the genes for hemolysin, protease, antibiotic activities, and pilin production (Herbert *et al*., 2007; Herbert *et al*., 2009; Herbert and Goodrich-Blair, 2009).

While the regulators described above affect different aspects of bacterium-host interactions, there is one global regulator Lrp that seems to coordinate most of these functions. Studies show that Lrp synergistically represses *nilABC* with NilR and thus affects bacterial mutualistic colonization, while it activates the LrhA pathway and other virulence functions, and stimulates immune suppression. Consistent with this role for Lrp in global regulation, *lrp* mutants are defective in virulence, immune suppression, nematode reproduction, nematode colonization, and the production of secreted activities, such as proteases, lipases, and antibiotics (Cowles and Goodrich-Blair, 2006; Cowles *et al*., 2007).

Based on targeted examination of the interactions among the regulators described above and the genes they regulate, a regulatory network dominated by Lrp was proposed (Figure 2.1; Richards and Goodrich-Blair, 2009). This regulatory network is hypothesized to allow *X. nematophila* to fine tune its gene expression to adapt to and exploit the different environments it encounters during its life cycle in pathogenic and mutualistic hosts.

Although previous findings have helped us obtain knowledge on the *X. nematophila* regulatory hierarchy controlling symbiosis factors, we are far from fully understanding the regulation mechanisms, especially with such a changing and complex contexts during transitions between hosts. Also, the connections among those known regulators, their effects on other cellular functions for pathogenicity and mutualism and if there are other components involved in the regulatory network still need to be explored.

In recent years, developments in sequencing and microarray technologies have made studies of whole gene expression profiles of an organism under various conditions feasible. In this study, with the available genome sequenceof *X. nematophila* (Chaston *et al*., 2011), we designed a microarray chip using the tiling array design (Figure 2.2; Mockler *et al*., 2005) and

performed the first microarray study on this bacterium to analyze the global effects of regulators Lrp and LrhA.

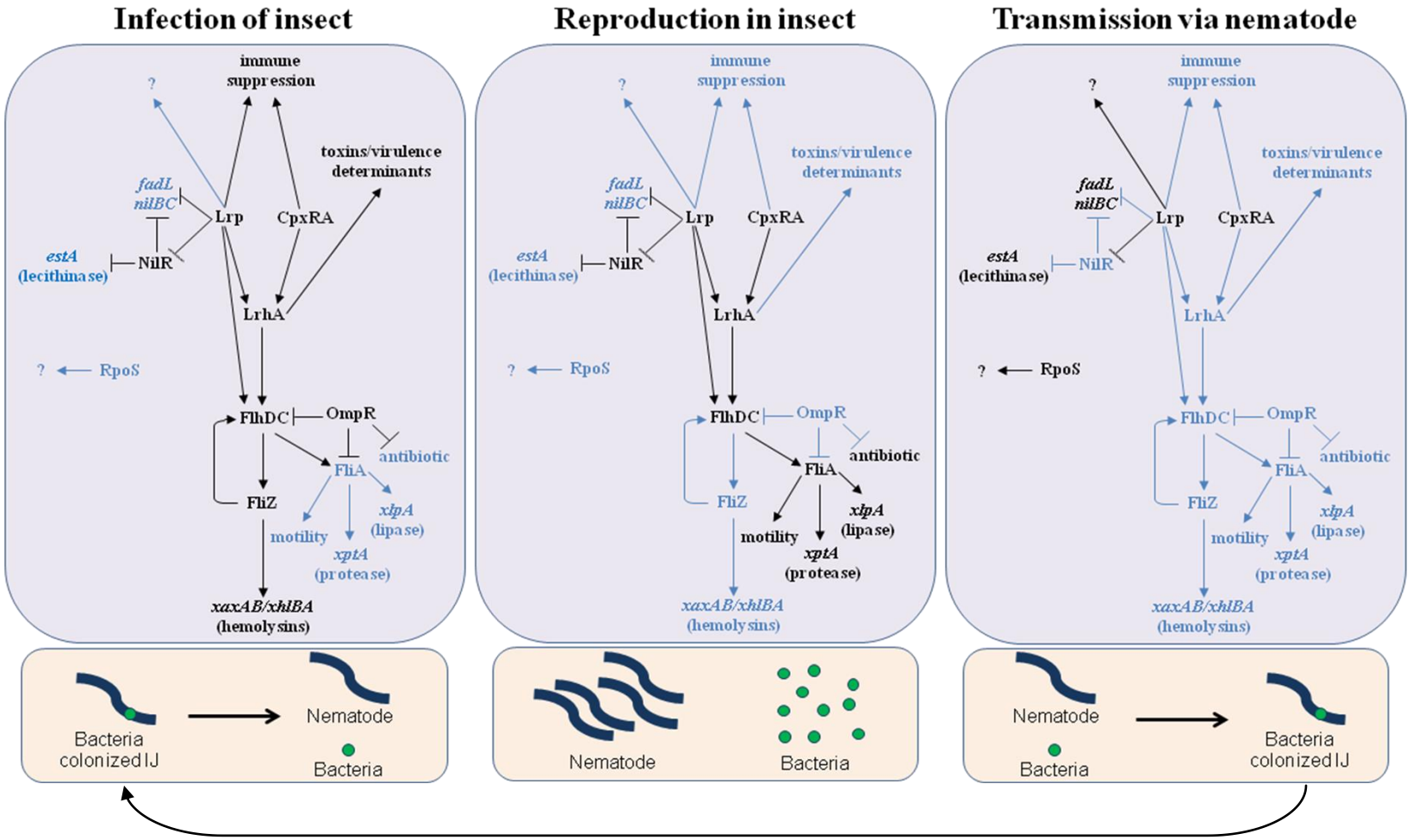

Figure 2.1. Previous predicted model of *X. nematophila* signal transduction cascades controlling mutualism and pathogenesis genes. Black lines indicated predicted active pathways; Blue lines indicate predicted inactive pathways. Arrows indicate positive regulations; Blunt arrows indicate negative regulations (Richards and Goodrich-Blair, 2009).

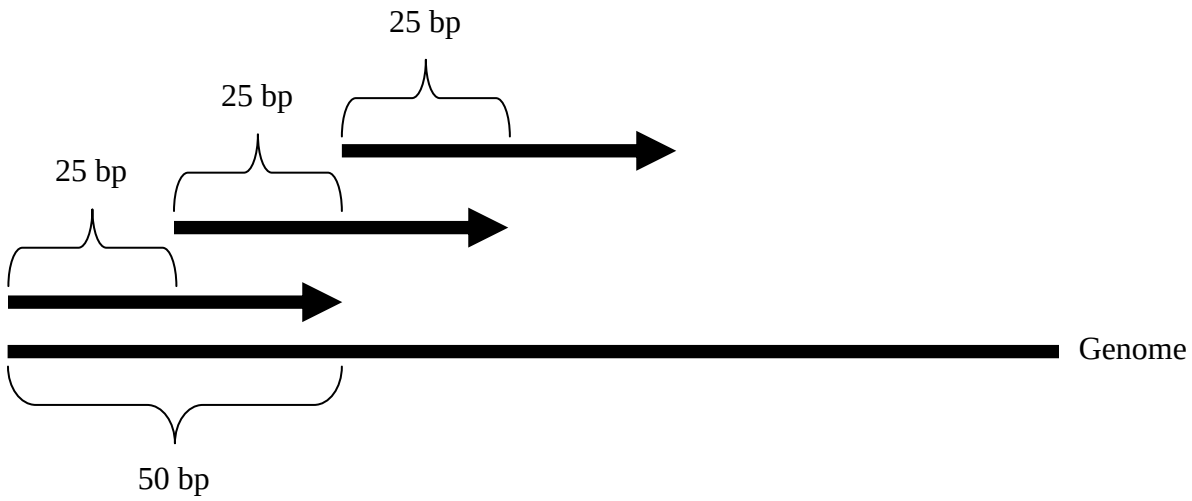

Figure 2.2. Tiling array design of *X. nematophila* microarray. Arrows indicate consecutive 50-bp probes that have 25-bp sequences on each end overlapping with adjacent probes.

RESULTS

Global effects of Lrp and LrhA on *X. nematophila* gene expression

Microarray analysis revealed that among the 4553 predicted ORFs of the bacterial genome, 4215 (93%) in wild-type *X. nematophila* HGB800, 3743 (82%) in *lrp* mutant HGB1059, and 3655 (80%) in *lrhA* mutant HGB3120 had average signal strength more than 5 fold of the baseline signal level, and thus were regarded to be expressed in early stationary phase growth in LB as tested in this study (Figure 2.3). By using wild type *X. nematophila* HGB800 as a comparison and the average signal strength of the *recA* gene for normalization, ORFs that showed differential expression in *lrp* and *lrhA* mutants were identified. Using 2.5 fold changes in average signal strength as a cut-off, analysis revealed that Lrp affected transcript levels of 263 ORFs positively and 53 ORFs negatively (7.5% of genes expressed in wild type) while LrhA affected 149 ORFs positively and 83 ORFs negatively (5.5% of genes expressed in wild type). Regulated genes were categorized based on their dependence on Lrp and LrhA, and by their predicted function (Figure 2.4 and Table 2.1).

Positive regulation by Lrp and LrhA

Consistent with their attenuated virulence (Richards *et al*., 2008) and nematode reproductive support phenotypes (Richards and Goodrich-Blair, 2010), as well as with previous qRT-PCR analysis (Cowles *et al*., 2007; Richards *et al*., 2008; Richards and Goodrich-Blair, 2010), both *lrp* and *lrhA* mutants had lower transcript levels for predicted virulence and "nematode reproduction" genes including those encoding flagellar regulon, lipases, hemolysin, toxin and proteases, which indicated the positive regulation of Lrp and LrhA on these functions.

They also both positively regulated a secretion system type VI cluster (one of two clusters encoded by *X. nematophila*), a chemotactic response regulon and a zinc transporter. Type VI secretion systems have been implicated in virulence in many bacteria (Mulder *et al*., 2012), consistent with the hypothesis that Lrp positively regulates genes involved in virulence. However, an *X. nematophila* deletion mutant lacking the entire Lrp-dependent Type VI secretion system, did not display virulence or mutualism defects compared to wild type. Similarly deletion of an Lrp and LrhA-dependent gene, XNC1_1469, encoding a VgrG homolog (a secreted component of Type VI secretion systems) had no effect on virulence in *M. sexta* insects (K. Cowles, E. Hussa, and H. Goodrich-Blair, unpublished). LrhA and Lrp also positively regulate members of the flagellar regulon, including the chemotactic flagellar motor component FliM, which helps tranduce environmental signals by working with CheBY, a two-component chemotactic regulatory system (Yuan *et al*., 2012), which is positively regulated by Lrp and LrhA. Another LrhA and Lrp regulated gene is predicted to encode a zinc transporter that is potentially involved in bacterial growth and virulence (Gielda and Dirita. 2012). Lrp-dependent, but LrhA-independent genes included those predicted to encode functions for the citric acid cycle, oligopeptide transport, chitin biodegradation, and production of insecticidal toxins, the antimicrobial compound xenocoumacin, the pigment pyoverdine, and a crystal inclusion protein. While LrhA is itself positively regulated by Lrp, LrhA-dependent genes that were independent of Lrp were also observed, including those predicted to encode pyruvate dehydrogenase, serine transport mechanisms, trehalose degradation enzymes, and fatty acid biosynthesis enzymes.

Negative regulation by Lrp and LrhA

Overall, Lrp and LrhA affected more genes positively than negatively, and only 5 genes were negatively regulated by both, including those predicted to encode a hydroxyphenylacetic acid monooxygenase (XNC1_0445) and one of four OppA homologs involved in oligopeptide transport. Note that LrhA also negatively regulates several other genes predicted to be in an operon with, or near XNC1_0445 (XNC1_0443, 0444, 0446, and 0449). Lrp was observed to have a negative effect on these genes as well, but these failed to reach the cut-off used in this analysis (Table 2.1). Other genes negatively regulated by LrhA, but independent of Lrp, were those predicted to encode functions for dipeptide and proline transport, glyoxylate cycle, growth on fatty acids (e.g. fatty acid degradation enzymes and isocitrate lyase). In previous proteomic and reporter fusion analyses *fadL* was identified as negatively regulated in stationary phase by both NilR and Lrp (Cowles and Goodrich-Blair, unpublished). It was therefore surprising that the microarray analysis, while indicating LrhA negatively regulates *fadL* (and other *fad* genes), suggest Lrp does not negatively impact *fadL* transcript levels under the tested conditions. LrhA negatively influences the expression of 8 clusters of genes (XNC1_0238-0246, XNC1_0443-0449, XNC1_0819-0821, XNC1_2270-2273, XNC1_2534-2536, XNC1_2534-2536, and XNC1_3185-3187) that are predicted to encode metabolic biosynthesis or degradation pathways, suggesting that LrhA could suppress secondary metabolism. LrhA also suppressed expression of the gene encoding the structural subunit (MrxA) of type I fimbriae and chitin binding protein, both of which are positively regulated by Lrp.

While LrhA appears to suppress functions mainly involved in nutrient metabolism, Lrp demonstrated a wider range of regulatory effects. As previously reported, Lrp negatively regulated bacterial colonization factors NilABC, as well as the gene encoding the transcription factor NilR, which synergistically with Lrp represses *nilABC* (Cowles and Goodrich-Blair, 2006).

The microarray data presented here revealed Lrp also negatively regulates functions predicted to play a role in anaerobic growth (NrdD), virulence (PagC), stress response (RpoS and Dps), and the Cas system (YgcBLKJIH, YgbTF) that was discovered in recent years as a phage defense system in bacteria and archaea.

The *lrhA* mutant (but not the *lrp* mutant) is defective for growth on minimal medium, and this growth can be rescued by addition of casamino acids, and to a lesser extent by a combination of aspartate, glutamate, and leucine (GR Richards, Ph.D. thesis, UW-Madison). The microarray revealed that LrhA-induced, but Lrp-independent genes include *gltX*, predicted to encode a glutamyl tRNA synthetase, *leuO* predicted to encode a transcriptional regulator of leucine biosynthesis, and a putative aspartate racemase. Furthermore, an *lrhA* mutant displayed higher levels of a transcript predicted to encode a glutamate-aspartate transporter.

A.

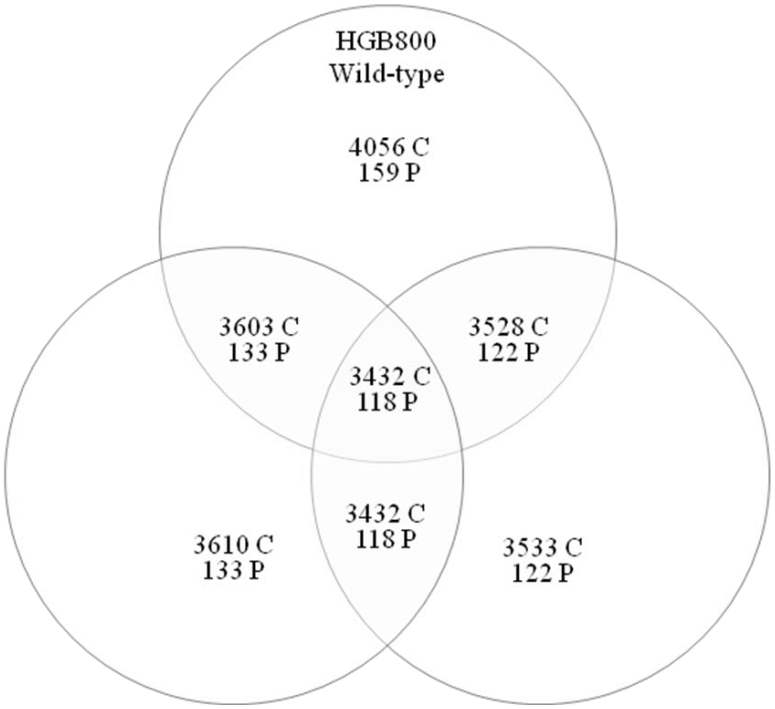

B.

	HGB800	HGB1059	HGB1320
Chromosome ORFs	**4378**		
Expressed chromosome ORFs	**4056 (92.6%)**	**3610 (82.5%)**	**3533 (80.7%)**
Plasmid ORFs	**175**		
Expressed plasmid ORFs	**159 (90.9%)**	**133 (76%)**	**122 (69.7%)**
Total expressed genomic ORFs	**4215 (92.6%)**	**3743 (82.2%)**	**3655 (80.3%)**
Regulated by Lrp	**316 (6.9%)**		
Regulated by LrhA	**232 (5.1%)**		

Figure 2.3. A. Numbers of ORFs expressed in wild type *X. nematophila* HGB800, *lrp* mutant HGB1059, and *lrhA* mutant HGB3120 (C: Chromosome encoded; P: Plasmid encoded). Overlapping regions shows ORFs expressed in 2 or 3 strains. **B.** Percentages of ORFs expressed in bacterial strains and number of genes affected by Lrp and LrhA.

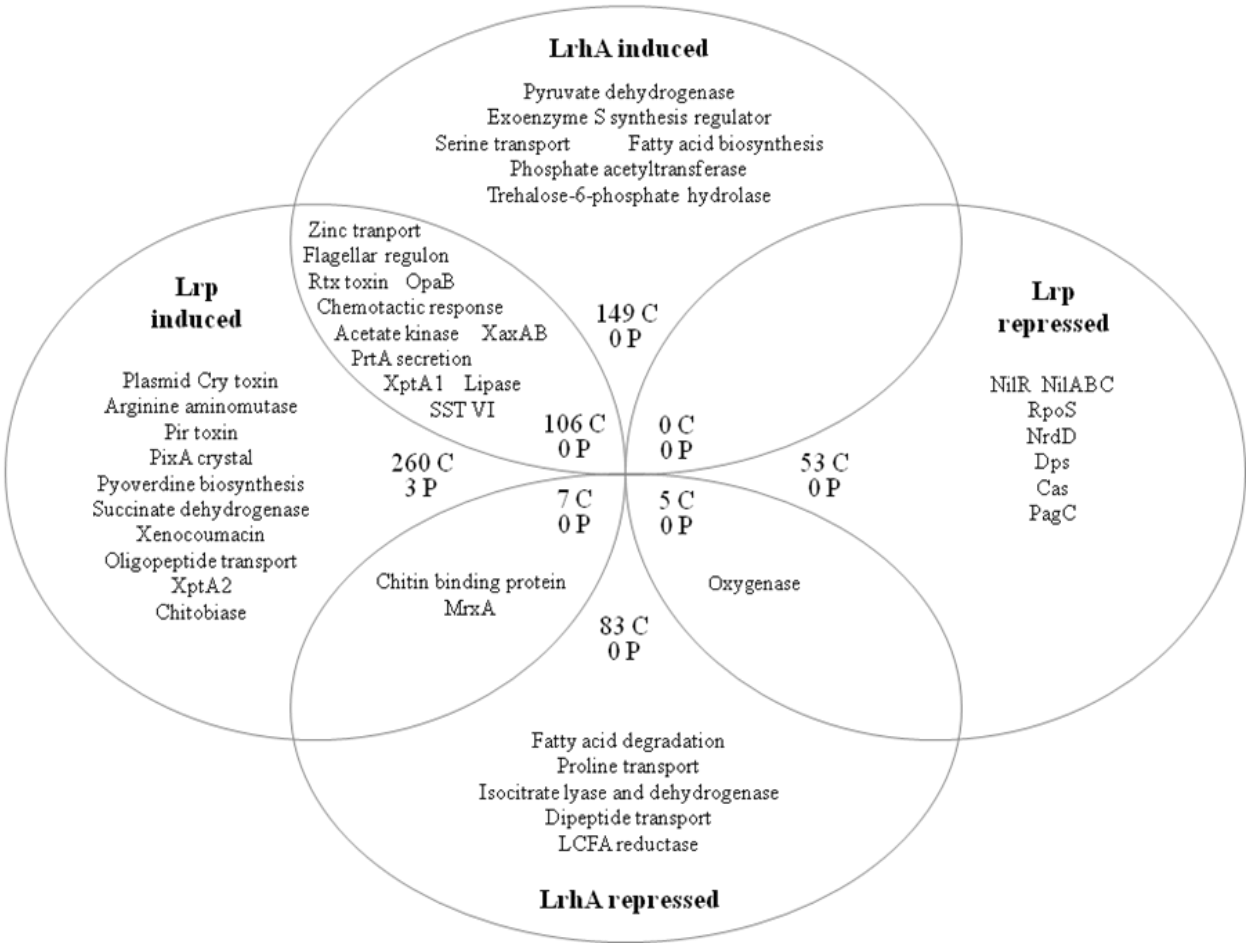

Figure 2.4. Effects of Lrp and LrhA on *X. nematophila* gene expression. C: Chromosome encoded ORFs; P: Plasmid encoded ORFs. Functions and activities listed in each category are based on predicted annotation or experimental evidence and represent only a subset of genes regulated.

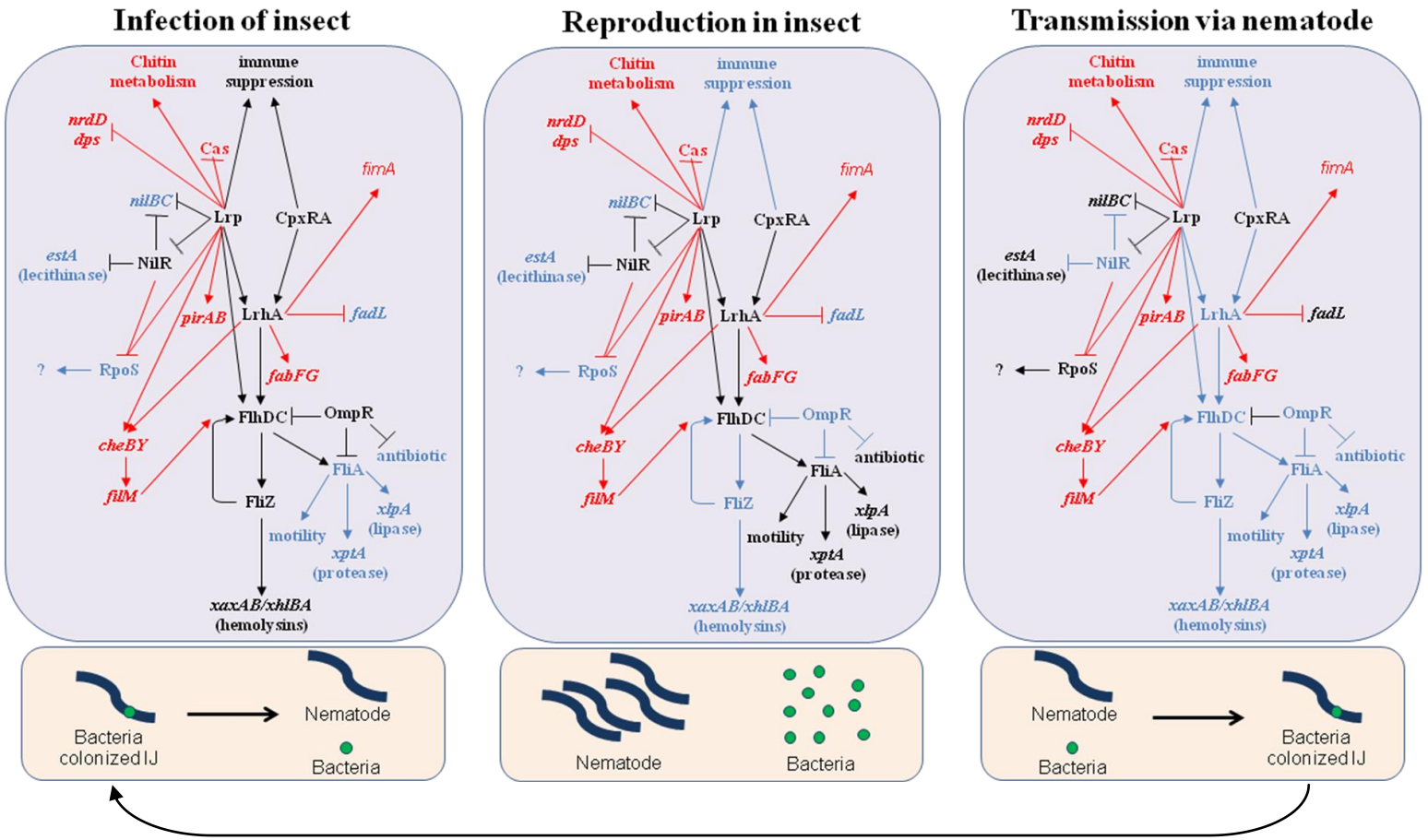

Figure 2.5. New predicted model of *X. nematophila* signal transduction cascades among previously and newly indentified factors controlling mutualism and pathogenesis genes. Red lines indicate new regulatory connections identified via microarray analysis; Black lines indicated predicted active pathways; Blue lines indicate predicted inactive pathways. Arrows indicate positive regulations; Blunt arrows indicate negative regulations.

Table 2.1. Effects of Lrp and LrhA on gene expression profile. Genes are grouped according to predicted functions. Red color indicates genes that are predicted to be expressed in operons. 2.5-fold differences of mutant expression levels relative to wild-type were used as the cut-off.

LrhA induced, independent of Lrp						
ORF ID	**Start Position**	**End Position**	**ORF Length**	**Annotation**	***lrp* mutant**	***lrhA* mutant**
				Virulence factors		
XNC1_1176	1048584	1049399	816	Exoenzyme S synthesis regulatory protein exsA	0.63	0.40
XNC1_1371	1230676	1231173	498	Alkaline protease secretion protein (fragment)	0.50	0.39
XNC1_1735	1636951	1637457	507	fimA, pilA, fimD, putative Fimbrial subunit (pilin)	0.65	0.32
XNC1_2687	2649415	2650791	1377	yegQ, putative protease	0.43	0.38
				Fatty acid metabolism		
XNC1_0643	555717	556793	1077	glpQ, glycerophosphodiester phosphodiesterase, periplasmic, glycerophospholipid metabolism	0.50	0.33
XNC1_2733	2707837	2709078	1242	fabF, fabJ, cvc, vtr, 3-oxoacyl-[acyl-carrier-protein] synthase II	0.62	0.38
				Transport		
XNC1_0874	741937	743214	1278	dctA, out (S.t.), citrate and C4-dicarboxylic acids transport protein	0.40	0.28

				(DAACS family)		
XNC1_1484	1362525	1364120	1596	ybiT, putative transport protein (ABC superfamily, atp_bind)	0.48	0.35
XNC1_1525	1408312	1409616	1305	sdaC, dcrA, putative serine transport protein (HAAAP family)	0.93	0.37
XNC1_1945	1846825	1848222	1398	uhpT, hexose phosphate transport protein (MFS family)	1.03	0.33
XNC1_1987	1878525	1878716	192	putative efflux transport protein (PET family) (fragment)	0.55	0.38
XNC1_2697	2658180	2659628	1449	yaaJ, putative alanine/glycine transport protein (AGCS family)	0.48	0.32
XNC1_3227	3166835	3167680	846	cysW, thiosulfate permease W protein (ABC superfamily, membrane)	0.49	0.36
XNC1_3228	3167680	3168510	831	cysU, cysT, thiosulfate transport protein (ABC superfamily, membrane)	0.44	0.35
XNC1_3293	3220772	3222007	1236	hcaT, yfhS, putative 3-phenylpropionic acid transport protein (MFS family)	0.54	0.36
XNC1_3809	3666973	3668223	1251	yeiM, putative transport protein (NUP family)	0.59	0.38
				Nutrient and energy metabolism		
XNC1_0945	812489	813799	1311	gsk, inosine-guanosine kinase, purine metabolism	0.56	0.38
XNC1_1043	916933	917880	948	leuO, putative transcriptional regulator of leucine biosynthesis with periplasmic binding protein domain (LysR family)	1.24	0.29

XNC1_1080	956870	959533	2664	aceE, pyruvate dehydrogenase, decarboxylase subunit, thiamin-binding	0.95	0.38
XNC1_1305	1172659	1174242	1584	putative L-2,4-diaminobutyrate decarboxylase	0.55	0.38
XNC1_1556	1438305	1439045	741	pflA, act, pyruvate formate lyase activating enzyme 1, anaerobic glucose metabolism	1.66	0.38
XNC1_1954	1852801	1854378	1578	guaA, GMP synthetase (glutamine aminotransferase)	0.89	0.39
XNC1_2201	2130898	2131674	777	1-(5-phosphoribosyl)-5-[(5-phosphoribosylamino)methylideneamino] imidazole-4-carboxamide isomerase 2 (Phosphoribosylformimino-5-aminoimidazole carboxamide ribotide isomerase 2)	0.47	0.24
XNC1_2801	2800866	2802932	2067	pta, phosphotransacetylase (phosphate acetyltransferase)	0.70	0.35
XNC1_3205	3149119	3150534	1416	gltX, glutamate tRNA synthetase, catalytic subunit	0.46	0.31
XNC1_4228	4073153	4073845	693	putative aspartate racemase	0.56	0.39
XNC1_4409	4229031	4230440	1410	glnA, glutamine synthetase	0.96	0.32
XNC1_4588	4381844	4383508	1665	treC, olgH, treE, trehalose-6-P hydrolase, alternative inducer of maltose system, cytoplasmic	0.81	0.38
				Others		

XNC1_3414	3322721	3323098	378	putative antitermination protein Q	0.48	0.40
XNC1_4645	4431506	4431832	327	rnpA, RNase P, protein C5 component, processes tRNA, 4.5S RNA	0.48	0.35
				Unknown functions		
XNC1_0939	806216	806377	162	conserved hypothetical protein	0.52	0.37
XNC1_1402	1279615	1280736	1122	conserved hypothetical protein; putative membrane protein	0.60	0.39
XNC1_1614	1506202	1506360	159	hypothetical protein	0.41	0.36
XNC1_1791	1727903	1727977	75	hypothetical protein	0.50	0.29
XNC1_2064	1986104	1986256	153	hypothetical protein	0.61	0.39
XNC1_2200	2129711	2130895	1185	conserved hypothetical protein	0.45	0.27
XNC1_2565	2530402	2530785	384	conserved hypothetical protein	0.42	0.26
XNC1_3446	3345024	3345281	258	conserved hypothetical protein	0.61	0.40
XNC1_3842	3698487	3698720	234	hypothetical protein	0.50	0.38
XNC1_4152	4009908	4010057	150	hypothetical protein	0.54	0.37
XNC1_4277	4113527	4113694	168	hypothetical protein	0.58	0.40
XNC1_4607	4405009	4405140	132	hypothetical protein	0.75	0.37

XNC1_4644	4431285	4431479	195	conserved hypothetical protein	0.53	0.38
LrhA repressed, independent of Lrp						
ORF ID	**Start Position**	**End Position**	**ORF Length**	**Annotation**	***lrp* mutant**	***lrhA* mutant**
				Virulence factors		
XNC1_0518	453933	454184	252	conserved hypothetical protein; putative exported protein	1.08	2.66
XNC1_1113	994502	994786	285	conserved hypothetical protein; putative exported protein	0.22	1.25
XNC1_1215	1082789	1083265	477	eco, eti, ecotin, a serine protease inhibitor	1.07	6.58
XNC1_1883	1805487	1805924	438	slyA, transcriptional activator for hemolysin (MarR family)	0.42	2.98
XNC1_2535	2490760	2492499	1740	conserved hypothetical protein; putative exported protein	2.17	5.68
				Fatty acid metabolism		
XNC1_2184	2103179	2104870	1692	fadD, oldD, acyl-CoA synthetase (long-chain-fatty-acid--CoA ligase)	0.83	2.78
XNC1_3041	3014876	3017323	2448	fadE, yafH, fadF (S.t.), acyl coenzyme A dehydrogenase	0.62	6.20
XNC1_3197	3143396	3144757	1362	fadL, ttr, outer membrane porin, transport of long-chain fatty acids, sensitivity to phage T2	0.62	4.84

XNC1_3875	3732677	3734863	2187	fadB, oldB, multifunctional: 3-hydroxybutyryl-CoA epimerase, delta(3)-cis-delta(2)-trans-enoyl-CoA isomerase, enoyl-CoA hydratase (N-terminal); 3-hydroxyacyl-CoA dehydrogenase (C-terminal)	0.46	9.83
XNC1_3876	3734875	3736038	1164	fadA, oldA, 3-ketoacyl-CoA thiolase; (thiolase I, acetyl-CoA transferase), in complex with FadB catalyzes	0.54	8.26
XNC1_4145	4003928	4005949	2022	fadH, ygjL, 2,4-dienoyl-CoA reductase, NADH and FMN-linked	0.85	2.52
XNC1_4601	4396555	4398990	2436	putative Long-chain-fatty-acyl-CoA reductase	0.96	4.60
XNC1_4602	4398992	4400122	1131	putative Long-chain-fatty-acid--luciferin-component ligase	0.82	3.38
				Antibiotics		
XNC1_4355	4182554	4183939	1386	putative N-acetylpuromycin N-acetylhydrolase precursor	1.21	4.57
XNC1_4360	4188156	4188749	594	Puromycin N-acetyltransferase	1.40	2.95
				Transport		
XNC1_1342	1204340	1205227	888	gltI, ybeJ, yzzK, glutamate/aspartate transport protein (ABC superfamily, peri_bind)	0.64	3.48
XNC1_3185	3129353	3130717	1365	proY, yajM, proline transport protein (APC family)	0.71	3.37

XNC1_4494	4296673	4298283	1611	dppA, fpp, dpp, alu, dipeptide transport protein (ABC superfamily, peri_bind)	0.93	3.66
				Nutrient and energy metabolism		
XNC1_0052	55744	57699	1956	acs, acsA, yfaC, acetyl-CoA synthetase, has propionyl-CoA synthetase activity	1.12	3.71
XNC1_0238	210479	211390	912	putative Dihydrodipicolinate synthase	0.71	4.41
XNC1_0240	211811	212842	1032	putative Homocitrate synthase	0.74	5.33
XNC1_0241	212902	213597	696	putative Phosphoglycolate phosphatase, glyoxylate and dicarboxylate metabolism	0.76	6.37
XNC1_0242	213621	214364	744	putative Short-chain dehydrogenase/reductase SDR	1.04	3.82
XNC1_0243	214388	215140	753	putative short chain dehydrogenase	1.30	2.55
XNC1_0246	217570	218709	1140	putative Sarcosine oxidase	0.92	2.71
XNC1_0377	309682	310797	1116	Histone deacetylase-like amidohydrolase (HDAC-like amidohydrolase) (HDAH)	0.87	3.09
XNC1_0444	376643	378046	1404	tnaA, ind, tryptophan deaminase, PLP-dependent	1.84	3.06
XNC1_0449	381232	382665	1434	putative 4-hydroxyphenylacetate 3-monooxygenase, oxygenase component (4-HPA 3-monooxygenase large component) (4-HPA	0.57	4.01

				3- hydroxylase)		
XNC1_0604	514790	515803	1014	putative Gamma-butyrobetaine dioxygenase	2.14	5.51
XNC1_0605	515816	516772	957	Aldo/keto reductase	1.46	3.54
XNC1_0819	705354	705743	390	5-carboxymethyl-2-hydroxymuconate delta-isomerase (5-carboxymethyl-2-hydroxymuconic acid isomerase) (CHM isomerase) (CHMI)	0.62	2.55
XNC1_0820	705811	706662	852	3,4-dihydroxyphenylacetate 2,3-dioxygenase (Homoprotocatechuate 2,3-dioxygenase) (HPC dioxygenase)	0.55	2.75
XNC1_0821	706729	708195	1467	betB, NAD+-dependent betaine aldehyde dehydrogenase	0.51	2.60
XNC1_1083	962852	963868	1017	putative Cysteine synthase	0.91	2.55
XNC1_1141	1018232	1019299	1068	yeiC, putative sugar kinase with ribokinase-like domain	0.42	3.95
XNC1_2270	2214668	2216125	1458	ydcW, putative aldehyde dehydrogenase	2.39	6.22
XNC1_2272	2216979	2218268	1290	goaG, 4-aminobutyrate aminotransferase, PLP-dependent	2.13	4.99
XNC1_3186	3130810	3132342	1533	Histidine ammonia-lyase (Histidase)	0.57	8.28
XNC1_3187	3132358	3134031	1674	Urocanate hydratase (Urocanase) (Imidazolonepropionate hydrolase)	0.60	6.40

XNC1_3948	3811147	3812928	1782	aceK, isocitrate dehydrogenase kinase/phosphatase	0.97	8.88
XNC1_3949	3812948	3814255	1308	aceA, icl, isocitrate lyase	1.64	6.46
XNC1_3950	3814318	3815913	1596	aceB, mas, malate synthase A	2.40	7.86
XNC1_4045	3913215	3914894	1680	putative Clavaminate synthase	0.55	3.37
XNC1_4325	4155276	4156160	885	lsrF, yneB, putative aldolase with ribulose-phoshate binding barrel	0.80	2.53
XNC1_4358	4186646	4187350	705	N-methyl-transferase	1.23	3.91
XNC1_4359	4187352	4188149	798	Mono-phosphatase	1.30	3.20
XNC1_4600	4395296	4396540	1245	Putative AMP-dependent synthetase/ligase	0.95	3.36
XNC1_1766	1706452	1707240	789	putative Enoyl-CoA hydratase	0.70	2.58
XNC1_1880	1803847	1804254	408	gloA, glyoxalase I, nickel isomerase	0.95	2.50
				Others		
XNC1_0051	55226	55537	312	Inner membrane protein yjcH	1.13	3.18
XNC1_0603	514311	514724	414	putative Metallothiol transferase fosB (Fosfomycin resistance protein)	1.94	4.76
XNC1_1188	1057991	1058626	636	Baseplate assembly protein V (GpV)	1.32	2.53
XNC1_2273	2218346	2218693	348	yhaI, putative membrane protein	1.24	3.53

XNC1_2622	2587498	2588169	672	pspA, cog, negative regulatory gene for the psp opreon, phage shock protein	0.96	2.53
XNC1_4357	4185414	4186649	1236	AtaP4 protein	1.13	3.79
				Unknown functions		
XNC1_0239	211441	211821	381	conserved hypothetical protein	0.68	6.02
XNC1_0244	215140	216159	1020	hypothetical protein	1.45	2.78
XNC1_0443	375897	376601	705	hypothetical protein	1.65	2.71
XNC1_0445	378057	379274	1218	hypothetical protein	1.79	2.84
XNC1_0602	513181	514314	1134	hypothetical protein	2.00	5.16
XNC1_0606	516798	517694	897	hypothetical protein	1.29	2.72
XNC1_1208	1076202	1076519	318	conserved hypothetical protein	1.74	2.58
XNC1_1654	1535362	1535616	255	conserved hypothetical protein	1.74	2.53
XNC1_2089	2006288	2006971	684	hypothetical protein	0.76	2.53
XNC1_2271	2216142	2216915	774	conserved hypothetical protein	2.24	6.26
XNC1_2534	2490360	2490647	288	hypothetical protein	1.48	2.73
XNC1_2536	2492572	2494053	1482	conserved hypothetical protein(fragment)	2.09	5.54

XNC1_2564	2529708	2530118	411	hypothetical protein	0.76	3.40
XNC1_2998	2983754	2984149	396	conserved hypothetical protein	0.76	2.51
XNC1_3947	3810332	3810898	567	conserved hypothetical protein	0.59	3.69
XNC1_4356	4183932	4185401	1470	hypothetical protein	1.19	4.08
XNC1_4361	4188752	4190878	2127	hypothetical protein	1.35	2.98
Lrp induced independent of LrhA						
ORF ID	**Start Position**	**End Position**	**ORF Length**	**Annotation**	***lrp* mutant**	***lrhA* mutant**
				Virulence factors		
XNC1_0005	6274	6897	624	conserved hypothetical protein; putative exported protein	0.15	1.33
XNC1_0220	193410	193940	531	hslV, htpO, clpQ, yiiC, peptidase component of the HslUV protease	0.38	0.42
XNC1_1112	994129	994257	129	hypothetical protein; putative exported protein	0.18	1.35
XNC1_1142	1019735	1021024	1290	pirB, JHE-like toxin, "Photorhabdus insecticidal related" toxin, PirB	0.21	1.59
XNC1_1143	1021093	1021500	408	pirA, JHE-like toxin, "Photorhabdus insecticidal related" toxin,	0.16	1.47

				PirA		
XNC1_1170	1043577	1044134	558	pixA, Methionine-rich PixA inclusion body protein	0.33	1.33
XNC1_2567	2538951	2542001	3051	xptB1, tccC, C component of insecticidal toxin complex (Tc)	0.27	1.12
XNC1_2568	2542055	2546482	4428	xptC1, tcaC, tcdB, B component of insecticidal toxin complex (Tc)	0.22	1.20
XNC1_2569	2546604	2554178	7575	xptA2, A component of insecticidal toxin complex (Tc)	0.18	1.40
XNC1_3045	3020787	3021671	885	Putative exported protein	0.35	0.78
XNC1_3766	3624314	3625540	1227	xaxA, XaxA	0.02	0.45
XNC1_4025	3886931	3888367	1437	Secreted alkaline metalloproteinase	0.05	0.56
XNC1_4425	4244528	4245007	480	putative Hcp-like protein of Escherichia coli	0.39	0.72
XNC1_4538	4336814	4338214	1401	Conserved Hypothetical protein with ImpA domain (probable component of SST VI cluster)	0.27	0.42
XNC1_4547	4349682	4350236	555	conserved hypothetical protein (probable lipoprotein of SST VI cluster)	0.24	0.50
XNC1_4551	4354370	4354810	441	conserved hypothetical protein (probable component of the SST VI cluster; lysozyme-related protein)	0.19	0.46

XNC1_4552	4354813	4356291	1479	conserved hypothetical protein (probable component of the SST VI cluster)	0.20	0.48
XNC1_4553	4356311	4356808	498	conserved hypothetical protein (probable component of the SST VI cluster)	0.27	0.65
XNC1_4554	4357739	4358257	519	hcp, Hemolysin-coregulated protein Hcp(probable Type VI secreted cytotoxin system component)	0.06	0.64
XNC1_4555	4358887	4360560	1674	xhlB, XhlB, XhlA hemolysin secretion/activation protein (TpsB)	0.17	0.41
XNC1_4556	4360676	4365088	4413	xhlA, XhlA, Cell surface associated hemolysin (TpsA)	0.04	0.56
XNC1_p0077	66062	66403	342	hypothetical protein; putative exported protein	0.19	1.72
				Antibiotics		
XNC1_1698	1572674	1573756	1083	xcnN, Fatty acid desaturase involved in xenocoumacin synthesis	0.20	1.01
XNC1_1699	1574084	1575169	1086	xcnM, Saccharopine dehydrogenase involved in xenocoumacin synthesis	0.08	0.99
XNC1_1700	1575318	1579781	4464	xcnL, Polyketide synthase involved in xenocoumacin synthesis	0.06	1.08
XNC1_1701	1579884	1582457	2574	xcnK, Non-ribosomal peptide synthase involved in xenocoumacin synthesis	0.06	0.96

XNC1_1702	1582639	1582962	324	xcnJ, Conserved hypothetical protein involved in xenocoumacin synthesis	0.06	0.65
XNC1_1703	1582971	1583702	732	xcnI, Thioesterase involved in xenocoumacin synthesis	0.06	0.62
XNC1_1704	1583908	1589691	5784	xcnH, Polyketide synthase involved in xenocoumacin synthesis	0.06	0.96
XNC1_1705	1589816	1591285	1470	xcnG, Beta-lactamase class C involved in xenocoumacin synthesis	0.07	0.69
XNC1_1706	1591422	1601687	10266	xcnF, Polyketide synthase involved in xenocoumacin synthesis	0.06	0.89
XNC1_1707	1601892	1603043	1152	xcnE, Acyl-CoA dehydrogenase involved in xenocoumacin synthesis	0.05	0.83
XNC1_1708	1603051	1603308	258	xcnD, Putative acyl carrier protein potentially involved in xenocoumacin synthesis	0.06	0.77
XNC1_1709	1603342	1604403	1062	xcnC, Methoxymalonate biosynthesis protein involved in xenocoumacin synthesis	0.04	0.75
XNC1_1710	1604406	1605263	858	xcnB, 3-hydroxyacyl-CoA dehydrogenase involved in xenocoumacin synthesis	0.04	0.78
XNC1_1711	1605964	1613982	8019	xcnA, nrps1, Non-ribosomal peptide synthase involved in Xenocoumacin synthesis	0.06	0.86

				Flagellar		
XNC1_1676	1553520	1554461	942	Flagellin	0.004	0.48
XNC1_1694	1569426	1569695	270	fliQ, flaQ, flagellar biosynthesis	0.34	0.70
				Transport		
XNC1_0427	357490	358887	1398	ydfJ, putative transport protein (MFS family)	0.34	1.12
XNC1_1006	877489	878715	1227	Major facilitator family transporter	0.35	1.62
XNC1_2165	2085467	2086423	957	znuA, yebL, yzzP, high-affinity Zn transport protein (ABC superfamily, peri_bind)	0.25	0.42
XNC1_2479	2431482	2433122	1641	oppA1, oligopeptide transport protein (ABC superfamily, peri_bind)	0.24	1.76
XNC1_2762	2737663	2739150	1488	lysP, cadR, lysine-specific permease (APC family)	0.40	0.54
XNC1_4460	4270633	4271982	1350	yhfT, putative transport protein	0.23	1.02
				Chitin metabolism		
XNC1_1359	1222208	1224907	2700	Chitobiase precursor (N-acetyl-beta-glucosaminidase) (Beta-N-acetylhexosaminidase)	0.19	2.19
				Nutrient and energy metabolism		

XNC1_0012	10181	11629	1449	putative monooxygenase, flavin-binding family	0.39	1.37
XNC1_0077	80396	81160	765	putative transferase enzyme	0.16	2.00
XNC1_0428	358966	359973	1008	putative transcriptional repressor for ribose metabolism (GalR/LacI family)	0.33	1.42
XNC1_0646	559887	563051	3165	Putative non-ribosomal peptide synthetase (fragment)	0.06	0.92
XNC1_0653	566074	567822	1749	putative Cytochrome-c oxidase	0.16	1.25
XNC1_0682	590376	591104	729	putative Phosphonate-transporting ATPase	0.13	1.02
XNC1_0792	685172	686149	978	yhdH, putative dehydrogenase, NAD(P)-binding domain and GroES-like domain	0.30	1.45
XNC1_0910	781728	782381	654	yadF, putative beta-carbonic anhydrase	0.32	0.42
XNC1_0954	822311	822862	552	apt, adenine phosphoribosyltransferase	0.21	1.20
XNC1_1004	875384	876745	1362	Similar to Biotin carboxylase	0.19	1.62
XNC1_1090	973506	976103	2598	acnB, yacI, yacJ, bifunctional: aconitate hydratase 2; 2-methylisocitrate dehydratase	0.28	1.48
XNC1_1172	1045065	1046672	1608	putative AMP-dependent synthetase/ligase	0.34	1.31
XNC1_1173	1046965	1047705	741	fabG, 3-oxoacyl-[acyl-carrier-protein] reductase	0.11	1.01

XNC1_1221	1086139	1087146	1008	Pyoverdine biosynthesis protein	0.23	0.60
XNC1_1222	1087180	1088070	891	Pyoverdine biosynthesis protein	0.25	0.61
XNC1_1384	1258667	1259410	744	Methyltransferase	0.26	1.46
XNC1_1405	1283732	1284121	390	sdhC, cybA, succinate dehydrogenase, hydrophobic subunit, cytochrome b556 with SdhD	0.40	1.31
XNC1_1406	1284115	1284462	348	sdhD, succinate dehydrogenase, hydrophobic subunit, cytochrome b556 with SdhC	0.32	1.19
XNC1_1407	1284463	1286229	1767	sdhA, succinate dehydrogenase, catalytic and NAD/flavoprotein subunit	0.33	1.25
XNC1_1424	1304549	1305601	1053	aroG, 3-deoxy-D-arabinoheptulosonate-7-phosphate synthase (DAHP synthetase, phenylalanine-repressible)	0.32	0.89
XNC1_1561	1445711	1448770	3060	putative Nonribosomal peptide synthase (NRPS)	0.05	0.78
XNC1_2038	1931447	1949431	17985	Non-ribosomal peptide synthetase	0.36	1.63
XNC1_2039	1949443	1956171	6729	Non-ribosomal peptide synthetase (fragment)	0.28	2.07
XNC1_2040	1956186	1972628	16443	putative Phenylalanine racemase (ATP-hydrolyzing)	0.34	2.11
XNC1_2153	2062080	2063258	1179	Arginine aminomutase	0.02	1.01

XNC1_2154	2063292	2064461	1170	Aminotransferase, class I and II precursor	0.04	1.01
XNC1_2155	2064487	2065449	963	putative Clavaminate synthase	0.07	1.02
XNC1_2156	2065493	2070427	4935	Long-chain-fatty-acid--CoA ligase (polyketide synthase)	0.08	0.82
XNC1_2157	2070432	2076113	5682	Phenylalanine racemase (ATP-hydrolyzing)(polyketide synthase)	0.14	0.60
XNC1_2159	2077362	2078366	1005	putative 2-dehydropantoate 2-reductase	0.20	0.72
XNC1_2161	2079592	2082900	3309	putative Phenylalanine racemase (ATP-hydrolyzing)	0.27	0.75
XNC1_2162	2083185	2083709	525	Thioesterase (fragment)	0.31	0.59
XNC1_2166	2086444	2087763	1320	putative peptidase protein YebA	0.39	0.75
XNC1_2228	2154724	2159406	4683	peptide synthetase	0.12	1.06
XNC1_2229	2159403	2164067	4665	Peptide synthetase	0.09	1.19
XNC1_2230	2164064	2170060	5997	peptide synthetase	0.10	1.26
XNC1_2233	2170947	2175158	4212	Peptide synthetase (Phenylalanine racemase)	0.39	0.79
XNC1_2299	2235579	2241581	6003	putative Peptide synthetase	0.22	1.08
XNC1_2300	2241578	2245621	4044	putative Peptide synthetase	0.17	1.41
XNC1_2317	2259620	2260621	1002	add, adenosine deaminase	0.38	0.40
XNC1_2466	2402479	2412318	9840	putative Ornithine racemase	0.30	1.12

XNC1_2467	2412309	2420630	8322	putative Ornithine racemase	0.28	1.42
XNC1_2470	2422128	2423435	1308	Diaminobutyrate--2-oxoglutarate transaminase (Diaminobutyrate--2-oxoglutarate aminotransferase) (L-2,4- diaminobutyric acid transaminase) (DABA aminotransferase)	0.12	2.25
XNC1_2492	2443315	2444163	849	purU, tgs, ychI, formyltetrahydrofolate hydrolase	0.28	1.11
XNC1_2652	2612258	2612893	636	narP, response regulator in two-component regulatory system with NarQ (or NarX), regulates anaerobic respiratory gene expression	0.39	0.72
XNC1_2713	2674287	2689136	14850	putative Non-ribosomal peptide synthase	0.14	1.03
XNC1_2781	2753210	2763988	10779	Peptide synthetase XpsB	0.09	0.84
XNC1_2782	2763993	2773973	9981	Peptide synthetase XpsB	0.07	0.75
XNC1_2783	2774010	2777249	3240	Peptide synthetase XpsA	0.07	1.04
XNC1_2784	2777892	2779517	1626	putative ATP-binding protein	0.07	0.61
XNC1_3338	3261979	3263025	1047	putative 3-oxoacyl-[acyl-carrier-protein] synthase	0.10	0.98
XNC1_3737	3597698	3598972	1275	metY, homocysteine synthase	0.12	1.24
XNC1_3750	3609809	3610828	1020	ybjS, NAD-dependent epimerase/dehydratase	0.12	1.28
XNC1_3751	3610825	3611823	999	putative 3-oxoacyl-[acyl-carrier-protein] synthase III (Beta-	0.17	1.31

				ketoacyl-ACP synthase III) (KAS III)		
XNC1_3857	3712568	3714019	1452	cysG, multifunctional siroheme synthase: uroporphyrinogen methyltransferase; 1,3-dimethyluroporphyriongen III dehydrogenase; siroheme ferrochelatase	0.36	0.55
XNC1_3898	3756959	3759409	2451	putative Acy-homoserine lactone acylase	0.37	1.24
XNC1_4080	3952751	3953527	777	ygiD, putative enzyme with aromatic-ring-opening dioxygenase domain	0.28	1.53
XNC1_4459	4269543	4270628	1086	yhfS, putative enzyme with PLP-dependent tansferase domain	0.31	0.99
XNC1_4462	4272501	4273526	1026	php, yhfV, putative phosphotriesterase with metallo-dependent hydrolase domain	0.26	0.96
XNC1_4622	4415526	4416323	798	paaG, ydbT, acyl-CoA hydratase, phenylacetic acid degradation (strain W)	0.38	1.10
				Others		
XNC1_1458	1335359	1336369	1011	ybhG, putative multidrug resistance membrane protein	0.39	1.41
XNC1_1459	1336466	1337143	678	ybiH, putative transcriptional repressor with homeodomain-like DNA binding domain (TetR/AcrR family)	0.34	1.32

XNC1_1548	1428876	1429370	495	lrp, alsB, livR, lss, lstR, mbf, oppI, ihb, lrs, rblA, Leucine-responsive regulatory protein	0.18	0.96
XNC1_1967	1862961	1863824	864	e14 prophage; putative tail fiber protein (modular protein)	0.24	1.58
XNC1_2404	2330757	2332700	1944	rnb, RNase II, mRNA degradation	0.26	0.50
XNC1_3903	3762985	3764553	1569	Efflux pump component MtrF (antibiotic resistance)	0.38	0.69
XNC1_p0079	66965	67303	339	transposase (fragment)	0.29	1.25
				Unknown functions		
XNC1_0095	93927	95336	1410	conserved hypothetical protein; putative membrane protein	0.37	1.00
XNC1_0573	492121	492273	153	hypothetical protein	0.37	0.82
XNC1_0647	563048	563230	183	conserved hypothetical protein	0.06	0.79
XNC1_1003	874117	875286	1170	conserved hypothetical protein	0.25	1.34
XNC1_1005	876758	877474	717	conserved hypothetical protein	0.26	1.62
XNC1_1038	910950	911348	399	hypothetical protein	0.35	0.68
XNC1_1111	993862	994035	174	hypothetical protein	0.17	1.33
XNC1_1223	1088074	1089360	1287	conserved hypothetical protein	0.29	0.55
XNC1_1389	1263395	1264417	1023	hypothetical protein	0.30	0.77

XNC1_1779	1715245	1716324	1080	putative surface protein	0.09	1.46
XNC1_1781	1720864	1721226	363	hypothetical protein	0.20	1.73
XNC1_1952	1851480	1851761	282	hypothetical protein	0.24	0.78
XNC1_2025	1916127	1916588	462	hypothetical protein	0.06	0.78
XNC1_2061	1983380	1983694	315	hypothetical protein	0.36	2.49
XNC1_2102	2014624	2014755	132	hypothetical protein	0.34	0.96
XNC1_2152	2061905	2062024	120	hypothetical protein	0.16	0.98
XNC1_2158	2076110	2077360	1251	hypothetical protein; putative membrane protein	0.14	0.55
XNC1_2160	2078366	2079595	1230	hypothetical protein	0.29	0.81
XNC1_2203	2132829	2132951	123	hypothetical protein	0.24	1.26
XNC1_2280	2224845	2225438	594	conserved hypothetical protein	0.27	1.36
XNC1_2445	2374061	2374798	738	conserved hypothetical protein	0.04	1.48
XNC1_2446	2374802	2374927	126	conserved hypothetical protein	0.13	1.73
XNC1_2465	2399063	2402479	3417	conserved hypothetical protein	0.36	1.22
XNC1_2468	2420775	2421230	456	conserved hypothetical protein	0.19	1.66
XNC1_2469	2421249	2422106	858	conserved hypothetical protein	0.15	1.97

XNC1_2491	2442790	2443242	453	conserved hypothetical protein	0.31	0.89
XNC1_2494	2444696	2445559	864	conserved hypothetical protein	0.16	1.35
XNC1_2550	2507763	2508314	552	conserved hypothetical protein	0.12	1.03
XNC1_2796	2786510	2786653	144	hypothetical protein	0.12	1.76
XNC1_3736	3597474	3597659	186	hypothetical protein	0.08	1.22
XNC1_3748	3607736	3609013	1278	conserved hypothetical protein	0.16	1.60
XNC1_3749	3609010	3609816	807	conserved hypothetical protein	0.13	1.31
XNC1_4047	3915655	3916494	840	conserved hypothetical protein	0.35	1.16
XNC1_4278	4114012	4114611	600	conserved hypothetical protein	0.34	0.42
XNC1_4440	4258051	4258584	534	hypothetical protein	0.03	1.05
XNC1_4461	4271993	4272355	363	conserved hypothetical protein	0.18	0.99
XNC1_p0080	67351	69318	1968	hypothetical protein	0.12	1.59
Lrp repressed, independent of LrhA						
ORF ID	**Start Position**	**End Position**	**ORF Length**	**Annotation**	***lrp* mutant**	***lrhA* mutant**
				Virulence factors		

XNC1_1254	1118100	1118501	402	crl, transcriptional regulator of cryptic genes for curli formation and fibronectin binding	5.25	0.64
XNC1_2700	2661502	2661873	372	hypothetical protein; putative exported protein	6.44	0.92
XNC1_3735	3596659	3597237	579	pagC, Virulence membrane protein pagC precursor	3.10	0.77
XNC1_4587	4381134	4381613	480	hypothetical protein; putative exported protein	3.32	0.45
XNC1_1236	1102330	1102851	522	hypothetical protein; putative exported protein	5.52	1.20
				Mutulistic factors		
XNC1_0845	723637	723942	306	nilR, NilR transcription factor	5.45	1.42
XNC1_0846	724013	724228	216	nilQ, NilQ	6.89	1.40
XNC1_2792	2784653	2785501	849	nilC, Outer membrane protein NilC	5.27	1.77
XNC1_3846	3702548	3703543	996	rpoS, appR, csi2, katF, nur, otsX, sigS, abrD, dpeB, sigma S (sigma 38) factor of RNA polymerase, major sigma factor during stationary phase	4.35	1.28
				Cas System		
XNC1_3717	3580652	3583402	2751	conserved hypothetical protein (Similar to unknown protein YgcB of Escherichia coli)	4.56	1.02

XNC1_3718	3583402	3585018	1617	conserved hypothetical protein (Similar to unknown protein YgcL of Escherichia coli)	4.82	1.07
XNC1_3719	3585011	3585562	552	conserved hypothetical protein	4.58	1.11
XNC1_3720	3585612	3586649	1038	conserved hypothetical protein (Similar to unknown protein YgcJ of Escherichia coli)	4.27	1.25
XNC1_3721	3586663	3587427	765	conserved hypothetical protein (similar to protein ygcI precursor of E. coli)	3.49	1.25
XNC1_3722	3587414	3588091	678	conserved hypothetical protein (Similar to unknown protein YgcH of Escherichia coli)	8.13	1.22
XNC1_3723	3588091	3589011	921	conserved hypothetical protein (Uncharacterized protein ygbT)	6.36	1.05
XNC1_3724	3589014	3589307	294	conserved hypothetical protein (similar to protein ygbF of E. coli)	8.17	1.03
				Transport		
XNC1_3833	3690036	3691361	1326	yhaO, putative transport protein (HAAAP family)	2.75	0.55
				Nutrient and energy metabolism		
XNC1_0136	125204	125815	612	Putative glycosyltransferase	2.69	0.95
XNC1_0521	455236	457110	1875	nrdD, anaerobic ribonucleoside-triphosphate reductase	3.14	1.45

XNC1_2512	2459837	2460904	1068	dadX, alnB, dadB (S.t.), msuA?, alanine racemase 2, PLP-binding, catabolic	4.11	1.10
XNC1_2513	2460927	2462228	1302	dadA, dadR, D-amino acid dehydrogenase subunit	5.95	1.54
XNC1_2078	1997624	1998412	789	Phosphate starvation-inducible protein	4.57	2.20
XNC1_2826	2830208	2830651	444	putative phosphotransferase enzyme II, A component SgcA	5.00	0.66
XNC1_2827	2830695	2830982	288	putative sugar phosphotransferase component II B	6.06	0.51
XNC1_2828	2830995	2832251	1257	ulaA, sgaT, yjfS, PTS family enzyme IIC, ascorbate-specific	4.16	0.58
XNC1_3252	3180999	3181679	681	ung, uracil-DNA-glycosylase	3.07	0.70
XNC1_3716	3580201	3580599	399	Glyoxalase	4.34	0.86
XNC1_4091	3964383	3965423	1041	putative alcohol dehydrogenase	4.24	1.32
				Others		
XNC1_1480	1359239	1359742	504	dps, pexB, vtm, stress response DNA-binding protein with ferritin-like domain	2.70	0.94
XNC1_1941	1844986	1845240	255	relB, RC, Qin prophage; part of two-component toxin-antitoxin system with RelE, transcriptional repressor of relBE operon	3.04	0.74
XNC1_2765	2741514	2742356	843	nfo, endonuclease IV, with intrinsic 3'-5' exonuclease activity	2.91	1.72

XNC1_2835	2837427	2837912	486	yfiB, putative outer membrane protein	2.85	1.29
XNC1_3158	3103554	3104468	915	yfcH, putative cell division inhibitor, NAD(P)-binding	8.35	0.90
XNC1_2839	2840365	2841693	1329	ycdQ, hmsR (Y.p.), Haemin storage system (HmsS protein of hmsHFRS Operon)	2.73	0.91
XNC1_2840	2841686	2843722	2037	ycdR, hsmF/pgaB, lipoprotein (HmsF protein of hmsHFRS Operon)	3.11	1.00
XNC1_3715	3579672	3579971	300	transposase	12.51	0.91
XNC1_3773	3629800	3630438	639	putative transcriptional regulator, TetR family	4.38	1.68
XNC1_3928	3790193	3793447	3255	putative type I restriction-modification system (HsdR)	2.53	0.62
XNC1_3930	3793624	3794913	1290	Type I restriction-modification	3.22	0.62
XNC1_3931	3794913	3797195	2283	putative type I restriction-modification system DNA methylase (HsdM)	5.33	0.80
				Unknown functions		
XNC1_0844	723384	723539	156	hypothetical protein	8.79	0.78
XNC1_2957	2945032	2945361	330	hypothetical protein	3.22	0.73
XNC1_3725	3589489	3589851	363	hypothetical protein	3.28	0.83

XNC1_3726	3590092	3590208	117	conserved hypothetical protein	3.09	0.80
XNC1_3891	3749794	3750186	393	conserved hypothetical protein	5.19	0.82
XNC1_4069	3939800	3939955	156	hypothetical protein	3.57	0.69
XNC1_4586	4380807	4381133	327	putative periplasmic protein	2.59	0.44
LrhA and Lrp induced						
ORF ID	**Start Position**	**End Position**	**ORF Length**	**Annotation**	***lrp* mutant**	***lrhA* mutant**
				Virulence factors		
XNC1_1369	1229715	1229852	138	Proteases secretion ATP-binding protein prtD (partial)	0.22	0.29
XNC1_1376	1234148	1236277	2130	ABC transporter RTX toxin	0.24	0.18
XNC1_1377	1236280	1237707	1428	RtxD, RTX toxin ABC transporter protein RtxD	0.27	0.21
XNC1_1378	1237700	1239757	2058	RTX toxin ABC transporter	0.30	0.23
XNC1_1381	1241044	1255956	14913	rtxA, toxin RtxA	0.15	0.08
XNC1_1469	1347268	1349382	2115	VgrG	0.09	0.24
XNC1_2036	1928862	1929419	558	opaB, ail, Attachment invasion locus protein precursor	0.30	0.24
XNC1_2566	2531280	2538851	7572	xptA1, tcdA, tcbA, A component of insecticidal toxin complex	0.10	0.11

				(Tc)		
XNC1_2771	2746387	2746704	318	conserved hypothetical protein; putative exported protein	0.35	0.37
XNC1_2809	2810628	2811620	993	lrhA, genR, Positive transcriptional regulator for motility, lipase activity, toxin and virulence; LysR family	0.08	0.01
XNC1_2911	2906157	2908271	2115	VgrG	0.09	0.23
XNC1_2908	2902796	2904562	1767	Rhs-family protein (fragment)	0.23	0.26
XNC1_3767	3625581	3626633	1053	xaxB, XaxB	0.02	0.39
XNC1_3828	3683257	3684222	966	Putative lipase/esterase	0.34	0.26
XNC1_4021	3881811	3883208	1398	Alkaline protease secretion protein aprF	0.30	0.30
XNC1_4022	3883214	3884551	1338	Alkaline protease secretion protein aprE	0.25	0.28
XNC1_4023	3884603	3886399	1797	Alkaline protease secretion ATP-binding protein aprD	0.14	0.25
XNC1_4024	3886414	3886746	333	Alkaline proteinase inhibitor precursor (PrtA-specific inhibitor) (fragment)	0.13	0.29
XNC1_4539	4338297	4341902	3606	Conserved hypothetical protein (probable component of SST VI cluster)	0.20	0.33
XNC1_4540	4341899	4343341	1443	Conserved hypothetical protein with ImpA domain(probable	0.22	0.32

				component of SST VI cluster)		
XNC1_4541	4343347	4344018	672	conserved hypothetical protein (probable component of SST VI cluster)	0.20	0.31
XNC1_4544	4344812	4347547	2736	putative ClpA/B-type chaperone (Putative ATPase with chaperone activity; probable component of SST VI cluster)	0.18	0.31
XNC1_4545	4347557	4348324	768	conserved hypothetical protein (probable component of SST VI cluster)	0.19	0.34
XNC1_4546	4348327	4349679	1353	conserved hypothetical protein (probable component of SST VI cluster)	0.19	0.37
XNC1_4548	4350220	4351515	1296	Conserved hypothetical protein with FHA domain (probable component of SST VI cluster)	0.18	0.38
XNC1_4549	4351521	4352573	1053	conserved hypothetical protein (probable component of the SST VI cluster)	0.16	0.33
XNC1_4550	4352537	4354369	1833	conserved hypothetical protein (probable component of the SST VI cluster)	0.18	0.39
XNC1_4560	4367398	4367811	414	putative Type VI secretion system Vgr family protein (fragment)	0.13	0.30

				Flagellar		
XNC1_1624	1515992	1516993	1002	motB, flaJ, enables flagellar motor rotation, linking torque machinery to cell wall	0.05	0.15
XNC1_1625	1516996	1517877	882	motA, flaJ, proton conductor component of motor, torque generator	0.06	0.15
XNC1_1626	1518013	1518597	585	flhC, flaI, transcriptional regulator of flagellar class II biosynthesis, anaerobic respiration and the Entner-Doudoroff pathway, tetramer with FlhD	0.19	0.26
XNC1_1627	1518600	1518950	351	flhD, flbB, transcriptional regulator of flagellar class II biosynthesis, anaerobic respiration and the Entner-Doudoroff pathway, tetramer with FlhC	0.11	0.20
XNC1_1674	1551969	1552481	513	fliZ, yedH, putative regulator of FliA	0.13	0.17
XNC1_1675	1552533	1553255	723	fliA, flaD, rpoF, sigma F (sigma 28) factor of RNA polymerase, transcription of late flagellar genes (class 3a and 3b operons)	0.03	0.12
XNC1_1677	1554737	1556209	1473	fliD, flbC, rfs, flagellar biosynthesis; filament capping protein, enables filament assembly	0.02	0.24

XNC1_1678	1556222	1556632	411	fliS, flagellar biosynthesis; repressor of class 3a and 3b operons (RflA activity)	0.04	0.13
XNC1_1679	1556632	1557006	375	fliT, putative flagellar biosynthesis; export chaperone for FliD	0.05	0.11
XNC1_1682	1558751	1559062	312	fliE, flaN, flaAI, flagellar biosynthesis; basal-body component	0.03	0.10
XNC1_1683	1559346	1561070	1725	fliF, flaBI, flaAII.1, flagellar biosynthesis; basal-body MS(membrane and supramembrane)-ring and collar protein	0.17	0.11
XNC1_1684	1561067	1562059	993	fliG, flaBII, flaAII.2, flagellar biosynthesis; component of motor switching and energizing	0.20	0.14
XNC1_1685	1562052	1562756	705	fliH, flaBIII, flaAII.3, putative flagellar biosynthesis; export of flagellar proteins	0.20	0.13
XNC1_1686	1562756	1564132	1377	fliI, flaC, flagellum-specific ATP synthase	0.23	0.15
XNC1_1687	1564167	1564613	447	fliJ, flaO, flagellar fliJ protein	0.26	0.17
XNC1_1688	1564610	1565977	1368	Flagellar hook-length control protein FliK	0.17	0.14
XNC1_1689	1566196	1566672	477	fliL, cheC1, flaAI, flaQI, flagellar biosynthesis	0.07	0.12
XNC1_1690	1566678	1567685	1008	fliM, cheC2, flaA, flaAII, flaQII, flagellar biosynthesis; component of motor switch and energizing	0.08	0.13

XNC1_1691	1567678	1568085	408	fliN, motD, flagellar biosynthesis; component of motor switch and energizing	0.11	0.16
XNC1_1692	1568088	1568549	462	fliO, flbD, flagellar biosynthesis	0.14	0.21
XNC1_1693	1568560	1569378	819	fliP, flaR, flagellar biosynthesis	0.21	0.35
XNC1_1717	1620395	1621363	969	flgL, flaT, flagellar biosynthesis; hook-filament junction protein	0.03	0.20
XNC1_1718	1621399	1623039	1641	flgK, flaS, flagellar biosynthesis; hook-filament junction protein 1	0.02	0.23
XNC1_1719	1623260	1624237	978	flgJ, flaZ, flagellar biosynthesis	0.05	0.09
XNC1_1722	1625371	1626162	792	flgH, flaY, flagellar biosynthesis; basal-body outer-membrane L (lipopolysaccharide layer) ring protein	0.02	0.07
XNC1_1723	1626229	1627011	783	flgG, flaL, flagellar biosynthesis; cell-distal portion of basal-body rod	0.02	0.09
XNC1_1724	1627029	1627784	756	flgF, flaX, flagellar biosynthesis; cell-proximal portion of basal-body rod	0.02	0.13
XNC1_1725	1627821	1629017	1197	flgE, flaK, flagellar biosynthesis; hook protein	0.02	0.18
XNC1_1726	1629033	1629734	702	flgD, flaV, flagellar biosynthesis; initiation of hook assembly	0.02	0.08
XNC1_1727	1629748	1630152	405	flgC, flaW, flagellar biosynthesis; cell-proximal portion of basal-	0.02	0.10

				body rod		
XNC1_1728	1630158	1630574	417	flgB, flbA, flagellar biosynthesis; cell-proximal portion of basal-body rod	0.02	0.05
XNC1_1729	1630791	1631462	672	flgA, flaU, flagellar biosynthesis; assembly of basal-body periplasmic P ring	0.07	0.10
XNC1_1730	1631585	1631884	300	flgM, anti-FliA (anti-sigma) factor; also known as RflB protein	0.08	0.25
XNC1_1731	1631911	1632351	441	flgN, flagellar biosynthesis; believed to be export chaperone for FlgK and FlgL	0.09	0.24
XNC1_1736	1638470	1640557	2088	flhA, flaH, putative export protein for flagellar biosynthesis	0.21	0.22
XNC1_1737	1640550	1641569	1020	flhB, flaG, yecQ, putative part of export apparatus for flagellar proteins	0.18	0.17
				Signal transduction		
XNC1_1615	1506589	1507227	639	cheZ, chemotactic response, CheY protein phophatase	0.06	0.15
XNC1_1616	1507255	1507644	390	cheY, chemotactic response regulator in two-component regulatory system with CheA, transmits signals to FliM flagelllar motor component	0.05	0.14

XNC1_1617	1507726	1508778	1053	cheB, chemotactic response regulator; methylesterase, in two-component regulatory system with CheA, regulates chemotactic response	0.07	0.19
XNC1_1618	1508771	1509658	888	cheR, cheX, glutamate methyltransferase, chemotactic response regulator	0.05	0.13
XNC1_1619	1509674	1511236	1563	tsr, cheD, methyl-accepting chemotaxis protein I, serine sensor receptor	0.03	0.15
XNC1_1620	1511353	1513056	1704	tsr, cheD, methyl-accepting chemotaxis protein I, serine sensor receptor	0.02	0.10
XNC1_1622	1513246	1513743	498	cheW, purine-binding chemotaxis protein; regulation	0.08	0.15
XNC1_1623	1513838	1515985	2148	cheA, chemotactic sensory histidine kinase (soluble) in two-component regulatory system with CheB and CheY, senses chemotactic signal	0.06	0.16
				Transport		
XNC1_2164	2084632	2085381	750	znuC, yebM, high-affinity Zn transport protein (ABC superfamily, atp_bind)	0.20	0.18

XNC1_3229	3168510	3169541	1032	cysP, thiosulfate transport protein (ABC superfamily, peri_bind)	0.37	0.32
XNC1_4279	4114626	4115735	1110	putative transport protein (permease)	0.21	0.27
				Nutrient and energy metabolism		
XNC1_0037	39827	40819	993	asnA, asparagine synthetase A	0.35	0.22
XNC1_1079	955866	956630	765	pdhR, yacB, transcriptional repressor for pyruvate dehydrogenase complex (GntR family)	0.39	0.22
XNC1_1320	1185352	1185816	465	ogt, methylated-DNA--protein-cysteine methyltransferase (6-O-methylguanine-DNA methyltransferase) (O-6-methylguanine-DNA- alkyltransferase)	0.15	0.15
XNC1_2022	1902005	1914421	12417	Non Ribosomal peptide synthetase (-succinylbenzoate--CoA ligase)	0.37	0.34
XNC1_2802	2803194	2804396	1203	ackA, acetate kinase A (propionate kinase 2)	0.30	0.21
XNC1_2807	2808616	2809830	1215	yfbQ, putative PLP-dependent aminotransferase	0.26	0.36
XNC1_3860	3716756	3718576	1821	cysJ, sulfite reductase, alpha subunit (flavoprotein)	0.32	0.35
XNC1_4280	4115930	4116583	654	putative Inorganic diphosphatase	0.09	0.26
XNC1_4281	4116609	4117670	1062	putative L-iditol 2-dehydrogenase	0.06	0.30

XNC1_4282	4117670	4118920	1251	putative 4-aminobutyrate aminotransferase, PLP-dependent	0.04	0.26
XNC1_4544	4344812	4347547	2736	putative ClpA/B-type chaperone (Putative ATPase with chaperone activity; probable component of SST VI cluster)	0.18	0.31
				Unknown functions		
XNC1_1130	1007907	1008002	96	hypothetical protein	0.34	0.33
XNC1_1177	1050657	1051151	495	conserved hypothetical protein	0.39	0.16
XNC1_1178	1051248	1051517	270	conserved hypothetical protein	0.39	0.21
XNC1_1379	1240227	1240592	366	conserved hypothetical protein	0.12	0.06
XNC1_1465	1340982	1343807	2826	Conserved hypothetical protein (fragment)	0.27	0.26
XNC1_1466	1343952	1345667	1716	Conserved hypothetical protein (fragment)	0.10	0.22
XNC1_1467	1345680	1346036	357	conserved hypothetical protein	0.09	0.19
XNC1_1468	1346134	1347252	1119	conserved hypothetical protein	0.09	0.21
XNC1_1555	1436943	1437758	816	conserved hypothetical protein; putative membrane protein	0.38	0.34
XNC1_1621	1513082	1513210	129	hypothetical protein	0.21	0.28
XNC1_1680	1557332	1557565	234	hypothetical protein	0.09	0.20
XNC1_1681	1557592	1558329	738	conserved hypothetical protein	0.23	0.36

XNC1_1798	1734218	1734346	129	hypothetical protein	0.33	0.22
XNC1_2808	2810335	2810475	141	conserved hypothetical protein	0.20	0.24
XNC1_2830	2833304	2833579	276	putative lipoprotein	0.21	0.14
XNC1_2831	2833831	2834295	465	hypothetical protein	0.16	0.13
XNC1_2832	2834500	2834775	276	conserved hypothetical protein	0.29	0.19
XNC1_2833	2834768	2836018	1251	conserved hypothetical protein	0.34	0.27
XNC1_2909	2904575	2904931	357	conserved hypothetical protein	0.09	0.19
XNC1_2910	2904924	2906141	1218	conserved hypothetical protein	0.09	0.22
XNC1_4543	4344639	4344782	144	hypothetical protein	0.19	0.30
LrhA and Lrp repressed						
ORF ID	**Start Position**	**End Position**	**ORF Length**	**Annotation**	***lrp* mutant**	***lrhA* mutant**
				Virulence factors		
XNC1_2249	2190494	2191969	1476	conserved hypothetical protein; putative exported protein	5.01	9.79
				Transport		
XNC1_0744	638542	640191	1650	oppA4, oligopeptide transport protein (ABC superfamily,	4.47	2.52

				peri_bind)		
				Nutirent and energy metabolism		
XNC1_0446	379308	380741	1434	putative 4-hydroxyphenylacetate 3-monooxygenase, oxygenase component (4-HPA 3-monooxygenase large component) (4-HPA 3- hydroxylase)	2.55	3.28
				Unknown functions		
XNC1_0906	778482	779738	1257	hypothetical protein	3.51	4.50
XNC1_1819	1746382	1747245	864	conserved hypothetical protein	5.16	2.85
Lrp induced and LrhA repressed						
ORF ID	**Start Position**	**End Position**	**ORF Length**	**Annotation**	***lrp* mutant**	***lrhA* mutant**
				Virulence factors		
XNC1_3803	3661001	3661540	540	mrxA, yfcV, Major fimbrial subunit polypeptide, MrfA	0.09	3.64
				Mutualistic factors		
XNC1_2997	2983011	2983610	600	Chitin-binding protein(CBP21 precursor)	0.23	5.11
				Nutrient and energy metabolism		

XNC1_1045	920184	921911	1728	ilvI, acetolactate synthase III, valine-sensitive, large subunit	0.35	3.15
XNC1_3619	3496914	3498233	1320	putative oxidoreductase with FAD/NAD(P)-binding domain	0.36	3.06
				Unknown functions		
XNC1_1088	971808	972050	243	hypothetical protein	0.27	2.96
XNC1_2126	2036859	2038058	1200	hypothetical protein (Similarities with unknown protein from a prophage)	0.24	2.73
XNC1_4099	3973702	3974898	1197	hypothetical protein	0.34	4.67

DISCUSSION

In this study we performed the first global transcriptome analysis for *X. nematophila* and extended our knowledge of the regulatory hierarchy of pathogenic and mutualistic functions of the bacterium. Previous research had established Lrp as a global regulator mediating pathogenic, mutualistic and other cellular functions of *X. nematophila*. The microarray data presented here confirm that Lrp regulates many genes, including those predicted to be involved in each stage of *X. nematophila* symbiosis (Figure 2.1). However, the percentage of Lrp-regulated ORFs detected by microarray was much lower than that revealed in a previous proteomic study (Cowles *et al*., 2007) which indicated 65% of detected protein products affected by Lrp. This difference may due to the fact that 2-D gel analysis only targeted on protein products in certain molecular weight range, which may have been disproportionately affected by Lrp, whereas microarray analysis can theoretically monitor transcript levels of all genes. Also, gene expression at transcriptional level may not necessarily affect gene expression at translational level, and Lrp may indirectly influence protein through post-translational regulation.

The results showed that 160 genes (marked in red color in Table 2.1) of the 430 coordinately regulated by Lrp and LrhA are within operons encoding functions such as flagellar synthesis, toxin production, type IV secretion system, chemotaxis, fatty acid metabolism, and peptide metabolism. The detection of the co-expression of all or most of the genes in the operons indicates the reliability and robustness of the microarray analysis performed. LrhA and Lrp together positively regulated a higher number of genes (106 out of 263 of Lrp and 149 of LrhA) than they did negatively (5 out of 53 of Lrp and 83 of LrhA) (Figure 2.4). This suggests that much of Lrp and LrhA function together in positively regulating gene expression, but that their

negative influence on genes is largely independent. Lrp positive regulation may be mediated through its activation of *lrhA* transcription (Richards *et al*., 2008) or both transcription factors may directly activate the same promoters..

The majority of genes identified by microarray as being positively regulated by both Lrp and LrhA are predicted to have a role in insect killing or bioconversion. Previous work had demonstrated a positive influence of Lrp and LrhA on motility (Cowles *et al*., 2007; Richards *et al*., 2008), and LrhA positive regulation of the flagellar genes *flhD, fliA, flgE,* and *fliC* (Richards *et al*., 2008). Strikingly, microarray analysis showed Lrp and LrhA both positively regulate a total of 90 flagellar genes in two loci (XNC1_1624-1693 and XNC1_1717-1737), including those encoding *flhD, flgE,* and *fliA*. The *fliC* (XNC1_1676) and *fliQ* (XNC1_1694) genes were positively regulated by Lrp, but did not meet the 2.5X cutoff to be considered LrhA regulated (they were 2.1 and 1.4 fold lower in the *lrhA* mutant respectively), in contrast to previous qRT-PCR data that had indicated *lrhA* mutants had 20% of wild type levels of *fliC* (Richards *et al*., 2008). Microarrays also revealed Lrp and LrhA positively regulate 9 chemotaxis genes (XNC1_1615-1623), including the only two *X. nematophila* genes predicted to encode receptors (both are the Tsr serine receptor type). These data establish that both Lrp and LrhA regulate the majority of genes encoding the flagellar and chemosensory apparati, and suggest these processes provide a competitive advantage to *X. nematophila* in its life cycle. The flagellar export apparatus, but not motility is necessary for bacterial virulence (Givaudan *et al*., 2000; Park and Forst, 2007; Richards *et al*., 2008), but the involvement of chemotaxis in *X. nematophila* virulence has not been tested. Also, the results presented here and those of others (Park and Forst, 2006; Richards *et al*., 2008) warrant an investigation of the role for motility, flagellar export, and chemotaxis during insect bioconversion.

In *Photorhabdus luminescens* and *X. nematophila,* addition of L-proline causes the bacteria to undertake a metabolic switch that mimics the switch triggered by insect hemolymph. Study using proline transpoter mutants showed that L-proline both regulates the metabolic shift and maintains the bacterial proton motive force that ultimately regulates the downstream bacterial pathways affecting virulence and antibiotic production (Crawford *et al*., 2010). Inhibition of proline transport by LrhA suggests a role of LrhA in signal transduction for virulence induction.

LrhA positively regulates two genes involved in cellular fatty acid biosynthesis (*glpQ* and *fabF*) and and negatively regulates several involved in fatty acid uptake and degradation (*fadA, fadB, fadD,fadE*, *fadL,* and *fadH*. Previously, LrhA was predicted to be active during bacterial infection and reproduction inside insect hosts and inactive when bacterial cells colonize nematode host (Richards *et al*., 2008). The association of LrhA and fatty acid metabolism further supports this prediction because production or conversion of certain type(s) of fatty acids by the bacterium may provide necessary nutrients for nematode reproduction in insect hosts. When cultivated on bacterial lawn *in vitro* on lipid agar (Volgyi *et al*., 1998), supplementation of fatty acid is still necessary for nematode reproduction, which indicates that the bacterium may need specific or more complex nutrient source to produce or convert the right type(s) of lipid to support nematode reproduction. When inside nematode host, release of LrhA suppression of fatty acid biodegradation may allow the bacterium to directly or indirectly utilize the nutrients stored in nematode intestinal cells. Activation of amino acid transport, zinc transport and trehalose degradation by LrhA further indicate that LrhA plays important roles in bacterial nutrient uptake and metabolism, which may in turn be essential for virulence. No well defined virulence determinants were identified as being independently regulated by LrhA, suggesting that the

virulence defect of the *lrhA* mutant is either due to the interruption of the activation pathway of Lrp which uses LrhA as an intermediating signal transporter, or because the predicted dysregulation of metabolism itself is sufficient to cause a virulence defect. The induction of components of pyruvate metabolism and TCA cycle along with the suppression of the components of glyoxylate metabolism indicate that LrhA regulates simple carbon metabolism and energy generation. These new findings regarding LrhA suggest it is not only a virulence regulator but also plays a more global role in the regulatory hierarchy regarding pathogenic and mutualistic regulations although most of its functions, especially in virulence regulation, are still under the supervision of Lrp.

Both previous data (Cowles *et al*., 2007) and the data presented here indicate Lrp is a master regulator at the top of a complex regulatory hierarchy. Lrp, independent of LrhA, induces predicted virulence factors in addition to those also induced by LrhA. It activates oligopeptide transport and chitin degradation, indicating that it is responsible for the handling of more complex compounds for nutrient and energy metabolism. The up-regulation of chitin binding protein suggest a potential role of Lrp and this protein in bacterial attachment during bacterial colonization in nematode host since chitin and its oligomers are known to be predominant surface molecules that are specifically recognized by microbial symbionts in their invertebrate hosts (Chaston and Goodrich-Blair, 2010). On the other hand, LrhA inhibits the chitin binding protein and chitin degradation (over 2-fold suppression of chitinase gene expression was detected by microarray but less than the 2.5 fold cut off level). This opposite effect and the metabolism genes that are independently regulated by Lrp or LrhA indicate that these two regulators are differentially regulating bacterial metabolism to help the bacterium adapt to host environment changes during various stages of bacterial life cycle. A working model is that during initial

infection in insects, Lrp and LrhA synergistically regulate bacterial virulence and host immune suppression to ensure efficient insect killing. Once the insect is dead, Lrp and LrhA differentially regulate bacterial metabolism pathways to meet the needs for nutrient acquisition and reproduction; then during the re-association with nematode host, changes in the Lrp regulon leads to activation of mutualism genes and suppression of virulence genes. Continued coordination between Lrp and LrhA causes expression of metabolic pathways that are different from those expressed during insect infection and allow adaptation to changing nutrient availability in the insect cadaver.

Lrp negatively regulated functions revealed two interesting findings that may help us better understand the mutualistic microbe-host interactions in this model system. First, the stress response and stationary phase sigma regulator RpoS (Hengge-Aronis, 1993) along with stress response factor Dps (Nair and Finkel. 2004), anaerobic growth factor Nrd (Garriga *et al*., 1996) and oxygenases (Fuchs, 2008) for catabolism of various compounds were found to be negatively regulated by Lrp. The fact that RpoS is essential for bacterial mutualistic colonization of the nematode and has subtle but significant negative impacts on bacterial virulence (Vivas and Goodrich-Blair, 2001) leads to the prediction that within the nematode, the bacterium is in a stationary phase under a micro-aerobic condition since the bacterium cannot grow anaerobically as tested in our studies (Chapter 3). Second, Lrp negatively regulates expression of the Cas system (Bhaya *et al*., 2011), which is involved in bacterial defense against phage and other exogenous genetic elements and also potentially regulates endogenous gene expression. The Cas system utilizes bacterial encoded Clustered Regularly Interspaced Short Palindromic Repeats (CRISPR) and short spacer sequences to recognize and degrade exogenous elements that are complementary to spacer sequences. This indicates that host source phages might affect the

ability of bacterial survival in nematode or insect hosts. Recent preliminary studies in *Caenorhabditis elegans* also showed that the *E. coli* Cas system can affect nematode development via a RNAi like mechanism (Samuels *et al*., 2012 NemaSym). Similarly, the *X. nematophila* Cas system may also have effects on nematode host development. Although the genome of *S. carpocapsae* does not have homologs of the *sid-1* and *sid-2* genes (A. Dillman and P. Sternberg, pers. comm.) that are necessary for *C. elegans* systemic RNAi effects, a homolog of the *C. elegans sid-1*-like gene *tag-130* was present. *C. elegans* Tag-130 does not have known effects on nematode systemic RNAi, but its homolog in *S. carpocapsae* may function more like *C. elegans* Sid-1 since it is structurally more similar to Sid-1 than Tag-130 (Hunter *et al*., 2006; Tomoyasu *et al*., 2008; A. Dillman and P. Sternberg, pers. comm.). Thus RNAi and Cas-system-mediated effects on nematode development may also occur in *S. carpocapsae*, and defects in such RNAi/Cas-system dependent development may cause the nematode fail to associate with *X. nematophila* for proper bacterial colonization in the nematode.

The microarray analysis presented here was a useful tool for extending our knowledge of *X. nematophila* physiology and gene regulation and how these may be linked to different stages of host interactions (Figure 2.5). It expanded the known functions of LrhA from virulence regulator to a global regulator that has wider than expected impacts on bacterial functions, including nutrient metabolism and signal transduction. The new findings on the relationship between Lrp and RpoS helped connect the known factors that are involved in the bacterial regulation of mutualism and pathogenicity. Identification of Cas system also points us to a new direction for understanding how a conserved class of bacterial small RNAs may play a role in mutualistic nematode-bacterium interactions

MATERIALS AND METHODS

Bacterial strains and culture conditions

Table 2.2 lists bacteria strains for this study. Unless specifically mentioned, *X. nematophila* strains were grown in LB broth or on LB plates supplemented with 0.1% pyruvate at 30℃ and kept in dark. Where appropriate, the following antibiotic concentrations were used: ampicillin, 50 μg/ml; and kanamycin, 50 μg/ml.

Microarray design

The tiling array was designed by Roche NimbleGen (Madison, WI) based on the genomic sequences of *X. nematophila* strain ATCC19061. 50 bp long consecutive probes were used to map through the whole bacterial genome. For both ends of each probe there were 25 bp long sequences overlapping with the adjacent probes (Figure 2.2). After removing repetitive probe sequences from the array a total of 192509 probes (176235 probes for chromosome sequences, 6166 probes for plasmid sequences, 10000 random sequence probes, and 108 probes for external control genes were synthesized in duplicates on 385K chips.

Microarray experiment

Bacteria cultures were grown overnight in 3 ml of LB supplemented with 0.1% pyruvate and appropriate antibiotics in culture tubes at 30^{o}C on roller, subcultured 1:100 into 30 ml of LB supplemented with 0.1% pyruvate and 50 μg/ml ampicilin in 125 ml glass flasks and grown for 12 hours to early stationary phase (OD 2-2.1) at 30^{o}C at 150 rpm on shaker. 1 ml of each culture

was used to extract total RNA using Qiagen RNeasy Mini Kit, and on-column DNA digestion was performed using Qiagen RNase-Free DNase Set according to manufacturer's protocol (Qiagen, Valencia, CA). The RNA purity was tested by measuring 260 nm/280 nm and 260 nm/230 nm ratios in TE buffer and the values should be over 1.8. RNA integrity was verified by running 2 μg of RNA samples on 1% denaturing agarose gel. The samples were then submitted to Roche NimbleGen.for processing and microarray analysis.

Microarray data analysis

For each strain, the average signal strength of all random probes was used as the baseline signal level and genes with average signal strength higher than 5 times of this value were deemed as being expressed. The baseline signal strength value was subtracted from the average signal strength of each gene, and the resulted values were normalized using the values for *recA* gene across the strains. The normalized values were then used for comparison between different strains, and 2.5-fold change in average signal strength was used as the cut-off level for determining the significance of changes in gene transcript levels.

Table 2.2. List of strains

Strain	Description	Reference
HGB007	Amp^r; *X. nematophila* wild-type ATCC 19061	ATCC
HGB151	Amp^r; Kan^r; *ΔrpoS::kan*; HGB007	Vivas *et al.*, 2001
HGB800	Amp^r; *X. nematophila* wild-type ATCC 19061	ATCC
HGB1059	Amp^r; Kan^r; *lrp-2::kan*; HGB800	Cowles *et al.*, 2006; Cowles *et al.* 2007
HGB1320	Amp^r; Kan^r; *ΔlrhA2;* HGB800	Richards and Goodrich-Blair, 2010

REFERENCE

Bhaya D, Davison M, Barrangou R. 2011. CRISPR-Cas systems in bacteria and archaea: versatile small RNAs for adaptive defense and regulation. Annu Rev Genet. 45:273-97

Bird, AF and Akhurst RJ. 1983. The nature of the intestinal vesicle in nematodes of the family *Steinernematidae*. Int J Parasitol. 13:599–606

Brinkman AB, Ettema TJ, de Vos WM, van der Oost J. 2003. The Lrp family of transcriptional regulators. Mol Microbiol. 48(2):287-94

Chaston J, Goodrich-Blair H. 2010. Common trends in mutualism revealed by model associations between invertebrates and bacteria. FEMS Microbiol. Rev. 34(1):41-58

Chaston JM, Suen G, Tucker SL, Andersen AW, Bhasin A, Bode E, Bode HB, Brachmann AO, Cowles CE, Cowles KN, Darby C, de León L, Drace K, Du Z, Givaudan A, Herbert Tran EE, Jewell KA, Knack JJ, Krasomil-Osterfeld KC, Kukor R, Lanois A, Latreille P, Leimgruber NK, Lipke CM, Liu R, Lu X, Martens EC, Marri PR, Médigue C, Menard ML, Miller NM, Morales-Soto N, Norton S, Ogier JC, Orchard SS, Park D, Park Y, Qurollo BA, Sugar DR, Richards GR, Rouy Z, Slominski B, Slominski K, Snyder H, Tjaden BC, van der Hoeven R, Welch RD, Wheeler C, Xiang B, Barbazuk B, Gaudriault S, Goodner B, Slater SC, Forst S, Goldman BS, Goodrich-Blair H. 2011. The entomopathogenic bacterial endosymbionts *Xenorhabdus* and *Photorhabdus*: convergent lifestyles from divergent genomes. PLoS ONE 6(11):e27909

Cowles CE, Goodrich-Blair H. 2006. *nilR* is necessary for co-ordinate repression of *Xenorhabdus nematophila* mutualism genes. Mol Microbiol. 62(3):760-71

Cowles KN, Cowles CE, Richards GR, Martens EC, Goodrich-Blair H. 2007. The global regulator Lrp contributes to mutualism, pathogenesis and phenotypic variation in the bacterium *Xenorhabdus nematophila*. Cell Microbiol. 9(5):1311-23

Crawford JM, Kontnik R, Clardy J. 2010. Regulating alternative lifestyles in entomopathogenic bacteria. Curr Biol. 20(1):69-74

Fuchs G. 2008. Anaerobic metabolism of aromatic compounds. Ann N Y Acad Sci. 1125:82-99

Garriga X, Eliasson R, Torrents E, Jordan A, Barb é J, Gibert I, Reichard P. 1996. nrdD and nrdG genes are essential for strict anaerobic growth of Escherichia coli. Biochem Biophys Res Commun. 229(1):189-92

Gielda LM, Dirita VJ. 2012. Zinc Competition among the Intestinal Microbiota. MBio. 3(4). pii: e00171-12.

Givaudan, A., Baghdiguian, S., Lanois, A., and Boemare, N. 1995. Swarming and swimming changes concomitant with phase variation in *Xenorhabdus nematophilus*. Appl Environ Microbiol 61: 1408–1413

Hengge-Aronis R. 1993. Survival of hunger and stress: the role of rpoS in early stationary phase gene regulation in *E. coli*. Cell. 72(2):165-8

Herbert EE, Cowles KN, Goodrich-Blair H. 2007. CpxRA regulates mutualism and pathogenesis in *Xenorhabdus nematophila*. Appl Environ Microbiol. 73(24):7826-36

Herbert EE, Goodrich-Blair H. 2007. Friend and foe: the two faces of *Xenorhabdus nematophila*. Nat Rev Microbiol. 5(8):634-46

Herbert Tran EE, Andersen AW, Goodrich-Blair H. 2009. CpxRA influences *Xenorhabdus nematophila* colonization initiation and outgrowth in Steinernema carpocapsae nematodes through regulation of the *nil* locus. Appl Environ Microbiol. 75(12):4007-14

Herbert Tran EE, Goodrich-Blair H. 2009. CpxRA contributes to *Xenorhabdus nematophila* virulence through regulation of lrhA and modulation of insect immunity. Appl Environ Microbiol. 75(12):3998-4006

Hunter CP, Winston WM, Molodowitch C, Feinberg EH, Shih J, Sutherlin M, Wright AJ, Fitzgerald MC. 2006. Systemic RNAi in *Caenorhabditis elegans*. Cold Spring Harb Symp Quant Biol. 71:95-100

Mockler TC, Chan S, Sundaresan A, Chen H, Jacobsen SE, Ecker JR. 2005. Applications of DNA tiling arrays for whole-genome analysis. Genomics. 85(1):1-15

Morgan W, Kuntzelmann V, Tavernor S, Ousley MA, Winstanley C. 1977. Survival of *Xenorhabdus nematophilus* and *Photorhabdus luminescens* in water and soil. J Appl Microbiol. 83, 665–670

Mulder DT, Cooper CA, Coombes BK. 2012. Type VI Secretion System Associated Gene Clusters Contribute to Pathogenesis of *Salmonella enterica* serovar Typhimurium. Infect Immun. Epub ahead of print

Park D and Forst S 2006. Co-regulation of motility, exoenzyme and antibiotic production by the EnvZ-OmpR-FlhDC-FliA pathway in *Xenorhabdus nematophila*. Mol Microbiol. 61:1397-412

Richards GR, Goodrich-Blair H. 2010. Examination of *Xenorhabdus nematophila* lipases in pathogenic and mutualistic host interactions reveals a role for *xlpA* in nematode progeny production. Appl. Environ. Microbiol. 76(1):221-9

Richards GR and Goodrich-Blair H. **2009**. Masters of conquest and pillage: *Xenorhabdus nematophila* global regulators control transitions from virulence to nutrient acquisition. Cell Microbiol. 11(7):1025-33.

Richards GR, Herbert EE, Park Y, Goodrich-Blair H. 2008. *Xenorhabdus nematophila lrhA* is necessary for motility, lipase activity, toxin expression, and virulence in *Manduca sexta* insects. J Bacteriol. 190(14):4870-9

Snyder, H., Stock, P., Kim, S., Flores-Lara, Y. and Forst, S. 2007. New insights into the colonization and release processes of *Xenorhabdus nematophila* and the morphology and ultrastructure of the bacterial receptacle of its nematode host, *Steinernema carpocapsae*. Appl Environ Microbiol. 66: 1622-1628

Tomoyasu Y, Miller SC, Tomita S, Schoppmeier M, Grossmann D, Bucher G. 2008. Exploring systemic RNA interference in insects: a genome-wide survey for RNAi genes in *Tribolium*. Genome Biol. 9(1):R10

Vivas EI, and Goodrich-Blair H. 2001. *Xenorhabdus nematophilus* as a model for host-bacterium interactions: rpoS is necessary for mutualism with nematodes. J Bacteriol. 183(16):4687-93

Volgyi A, Fodor A, Szentirmai A, Forst S. 1998. Phase variation in *Xenorhabdus nematophilus*. Appl Environ Microbiol. 64(4):1188-93

Yuan J, Branch RW, Hosu BG, Berg HC. 2012. Adaptation at the output of the chemotaxis signalling pathway. Nature. 484(7393):233-6.

CHAPTER 3

RpoS-dependent stress response is necessary for *Xenorhabdus nematophila* colonization of the nematode *Steinernema carpocapsae*

Aaron W. Anderson, Eugenio I. Vivas, Charles E. Cowles, and Dr. Heidi Goodrich-Blair also provided contributions to the studies described in this chapter.

My contributions included writing the manuscript, microarray analysis of *rpoS* mutant, construction of *rpoS-lacZ* fusion strains and related β-gal assays, aerobic and anaerobic growth tests, and qRT-PCT tests for gene expressions. Eugenio Vivas constructed the *rpoS'-'lacZ* reporter fusion. Charles E. Cowles constructed the Tn*7/katE* plasmids for catalase complementation experiments. Aaron Anderson contributed to the UV exposure test and colonization assays. Heidi Goodrich-Blair contributed to the writing of the manuscript and provided advices on the experiment design and implementation.

INTRODUCTION

Although pathogenic and mutualistic microbial interactions cause dramatically different effects in hosts, the underling mechanisms for both types of interactions share many common features, including for host recognition, evasion of host defense, and nutrient uptake (Soto *et al*., 2009). Also in some cases, one microbe can be both pathogenic and mutualistic when interacting with different hosts (Herbert and Goodrich-Blair, 2007; Goodrich-Blair and Clarke, 2007). Such microbes may require precise regulation and coordination between the pathogenic and mutualistic functions, to ensure the activities necessary for each are expressed only in the appropriate environment.

Xenorhabdus nematophila, a γ-proteobacterium, forms a species-specific beneficial symbiotic relationship with the nematode *Steinernema carpocapsae*. The bacteria colonize the receptacle, a specialized intestinal region present in the infective juvenile (IJ) stage of the nematode (Bird and Akhurst, 1983). In cooperation with its nematode host, *X. nematophila* can kill and reproduce within a wide variety of insect larvae (Forst *et al*., 1997). Although the bacterium alone can efficiently kill insects when directly injected into insect hosts, a nematode host is required as a vector to deliver the bacterial cells into insects in nature. Conversely, while the nematode host can infect insects, it requires the bacterium for efficient killing and reproduction (Forst *et al*., 1997; Goodrich-Blair and Clarke, 2007). Being both pathogenic and mutualistic to different hosts (insects and nematodes respectively) during its life cycle, *X. nematophila* is a model for studying both types of microbe-host interactions, and the regulation of the transition between pathogenic and mutualistic stages. Insights gained from such model systems may have important medical implications, by shedding light on how opportunistic

pathogens of humans regulate the switch from non-pathogenic to pathogenic behaviors when necessary conditions are met.

During the mutualistic part of its life cycle, *X. nematophila* bacteria specifically colonize *S. carpocapsae* IJ stage nematodes and persist there at a relatively stable number, despite limiting nutrients, while the IJ seeks a new insect host (Orchard and Goodrich-Blair, 2005). Bacterial colonization of the nematode IJ requires that both partners distinguish each other from other potential partners. Furthermore, the bacterium likely encounters nematode host defenses system, despite the fact that the association is mutualistic. Once inside an insect cadaver, the bacterium encounters the insect's immune system, and adapts to the changing nutritive environment as the insect dies and is digested. To date, several *X. nematophila* regulators have been found to play important roles in regulating mutualistic interactions of the bacterium, including the transcription factor RpoS (Vivas and Goodrich-Blair, 2001; Cowles and Goodrich-Blair, 2006; Cowles *et al*., 2007; Herbert *et al*., 2007). RpoS was originally identified in other bacteria as a regulator for the expression of alkaline phosphatase (Touati *et al*., 1986) and catalase (Loewen and Triggs, 1984), as well as for protection from near-UV light (Sammartano *et al*., 1986). It was then identified as a sigma factor regulating gene expression during the transition from exponential phase to stationary phase or in response to general stress, including oxidative stress such as that caused by peroxide challenge (Hengge-Aronis, 1993; Battesti *et al*., 2011). The *X. nematophila rpoS* mutant produces proteases, antibiotic, lipases, outer membrane proteins and crystal proteins at levels similar to those of the wild-type, and has no changes in exponential growth rate, stationary-phase cell morphology, or the ability to attach to an abiotic surface. However, it does display hyper-motility relative to wild type. With respect to host interactions, the *rpoS* mutant causes slightly, but significantly higher mortality in insects and

completely loses the ability to colonize the nematode IJ, although it still supports nematode growth and reproduction *in vitro* in insects (Vivas and Goodrich-Blair, 2001).

Although the details about the role of RpoS in regulating *X. nematophila* mutualistic interactions remain unclear, previous studies have provided useful information on its potential functions. Genomic sequencing revealed that *X. nematophila* lacks a catalase gene(s) and contains a limited number of genes encoding anti-reactive-oxygen-species (ROS) function: *ahpC* (an alkyl hydroperoxide reductase), *sodB* (a superoxide dismutase) and *dps* (a ferritin-like protein). ROS, as shown in other bacteria-host interaction studies, is a potent tool for hosts to defend against bacterial infections (Fones and Preston, 2012). One major target of ROS is DNA (Imlay JA and Linn S, 1988) on which it causes base oxidation leading to mutations or lethal strand breaks (Lloyd *et al*., 1998). ROS also target oxygen sensitive proteins, such as iron-sulfur cluster-containing proteins, and disrupt the functions of metabolic pathways (Imlay, 2006). The limited anti-ROS functions encoded by *X. nematophila* suggest it is sensitive to host generated or environmental ROS, despite the fact that it is a successful symbiont of host niches. This hypothesis is supported by the fact that the bacterium cannot grow in light-exposed LB medium and adding reducing reagents in the medium, such as pyruvate, eliminates this inhibitory effect (Xu and Hurlbert, 1990).

Given the regulatory role of RpoS on anti-ROS functions in other bacteria (Tarassova *et al*., 2009; Eisenstark *et al*., 1996), the defect of *X. nematophila rpoS* mutant in mutualism may due to its dysfunction in regulating anti-ROS functions. The *rpoS* mutant has a 4-7 fold defect in survival to hydrogen peroxide challenge (which causes oxidative stress) compared to wild type (Vivas and Goodrich-Blair, 2001). Also in unpublished work, ectopic expression of the *E. coli* catalase gene partially restores the colonization ability of the mutant (A. Andersen, X. Lu, and H.

Goodrich-Blair, unpubl.). These data further support the hypothesis that RpoS may affect bacterial nematode colonization by promoting ROS stress resistance. In addition, other RpoS regulated cellular functions such as adaptation to varying nutrient sources, dormant state cell metabolism, biofilm formation, and virulence may also play a role in bacterial mutualism (Vivas and Goodrich-Blair, 2001; Dong and Schellhorn, 2009; Battesti *et al*., 2011).

Previous work showed that the global regulator Lrp negatively regulates *rpoS* expression (Chapter 2; Cowles *et al*., 2007). Lrp synergistically activates virulence functions with the transcription factor LrhA (Richards *et al*., 2008) and synergistically represses bacterial mutualistic genes with the transcription factor NilR (Cowles and Goodrich-Blair, 2006). Studies of the interactions among RpoS and these regulators will also help elucidate the regulatory networks involved in the bacterium-host interactions.

To begin to understand the requirement for RpoS in nematode colonization we elucidated the *X. nematophila* RpoS-dependent regulon by comparing, using microarrays, wild type and *rpoS* mutant transcripts, and examining the integration of RpoS in the cellular regulatory hierarchy. Our findings demonstrate that RpoS is required for colonization at least partially due to its role in protection from ROS. We also determined that the expression of RpoS is repressed by two factors: the leucine responsive regulatory protein (Lrp), a global regulator that regulates mutualism, pathogenesis and phenotypic variation in *X. nematophila*, and NilR, a repressor of colonization genes.

RESULTS

Effects of RpoS on gene expression profile.

Microarray analysis of an *rpoS* mutant revealed that RpoS regulates 114 predicted chromosomal ORFs out of 4553 genomic ORFs predicted for the bacterium (4378 encoded by bacterial chromosome and 175 encoded by the plasmid). The 27 genes positively regulated (directly or indirectly) by RpoS are predicted to encode proteins involved in anaerobic nutrient and energy metabolism (e.g. the pyruvate metabolism pathway), anaerobic dicarboxylate transport, the carbon starvation response, and virulence (e.g. the insecticidal Pir toxins). On the other hand, *rpoS* mutation leads to elevated expression of 87 genes, which involve the functions for aerobic metabolism and energy production, such as the citric acid cycle pathway, amino acid metabolism, fatty acid degradation, and a large number of transporters for the transportation of peptides, long-chain fatty acids, and amino acids. Except for the Pir toxins, neither virulence nor mutualism factors were revealed by microarray to be regulated by RpoS. Also, contrary to our prediction, none of the three known anti-ROS genes were regulated by RpoS (Table 3.1).

Lrp and NilR regulate *rpoS* expression.

Microarray analysis indicated *rpoS* transcript levels are 4.5-fold higher in *lrp* mutant cells than in wild type, suggesting Lrp negatively regulates (directly or indirectly) *rpoS* expression (Chapter 2; Figure 3.1). To verify and expand upon this finding, quantitative reverse transcriptase-PCR (qRT-PCR) analyses were performed to compare *rpoS* transcript levels among various *X. nematophila* strains. The microarray analysis also revealed 6.9-fold more expression of the *nilR* gene in *lrp* mutants relative to wild type, consistent with previous reports (Chapter 2;

Cowles and Goodrich-Blair, 2006), and so *nilR* transcript levels were also monitored as a positive control. Despite the negative impact of Lrp on NilR expression, these two proteins act synergistically to repress expression of the colonization factors *nilA, nilB,* and *nilC* (Cowles and Goodrich-Blair, 2006). To determine if Lrp and NilR similarly influence *rpoS* expression, *rpoS* transcript levels in a *nilR* mutant was also tested, with *nilC* expression used as a positive control. Consistent with the microarray data and previous studies (Chapter 2; Cowles and Goodrich-Blair, 2006), *nilR* transcript levels in the *lrp* mutant were 30 times higher than wild type, and *nilC* transcript levels in the *nilR* and *lrp* mutants were 17 and 37 fold higher than wild-type levels respectively. *rpoS* gene transcript levels in the *lrp* mutant and *nilR* mutant were both 7-fold greater than wild-type levels respectively, indicating that, like the *nil* colonization factors *rpoS* is negatively regulated by both Lrp and NilR transcription factors, either directly or indirectly (Figure 3.2). qRT-PCR of *nilR* transcript levels in the *rpoS* mutant showed no significant difference from wild-type (data not shown), indicating RpoS does not regulate *nilR* expression. The inability of RpoS to affect *nilC* expression (Figure 3.2; Cowles and Goodrich-Blair, 2004) suggests that Lrp and NilR do not negatively regulate *nil* mutualism genes through their influence on *rpoS* expression.

Effects of Lrp on growth-phase induction of RpoS expression.

In *E. coli, rpoS* expression is induced upon entry into stationary phase (Hirsch and Elliott, 2005). We sought to determine if *X. nematophila rpoS* expression is similarly growth-phase regulated, and what role Lrp plays in this expression profile. We monitored β-galactosidase activity in wild type and *lrp* mutant cells expressing an *rpoS'-'lacZ* fusion construct integrated at the Tn*7* site of the bacterial genome. Control strains with the empty Tn*7* insertions had

undetectable β-galactosidase activity (data not shown). When grown in LB, β-galactosidase activity was induced as cells entered stationary phase (Fig. 3.3A and B), indicating that as in *E. coli, X. nematophila rpoS* expression increases in stationary phase. The *lrp* mutant displayed higher levels of β-galactosidase activity throughout the growth curve, and showed similar induction upon entry into stationary phase as wild-type cells. Therefore, Lrp represses *rpoS* expression throughout the growth curve, and Lrp de-repression is not responsible for stationary phase induction of *rpoS* expression. Similar trends were observed when cells were grown in defined medium (Figure 3.3C and D). During growth in minimal medium, elevated levels of *rpoS'-'lacZ* expression in the *lrp* mutant may be explained in part by the reduced growth rate of this strain relative to wild type. However, during growth in LB, the *lrp* mutant has elevated *rpoS'-'lacZ* expression even during exponential phase when both strains are growing similarly.

Expression of exogenous catalase gene rescues the colonization ability of *rpoS* mutant.

RpoS is known to be involved in regulation of stress response genes in many bacteria, and host generated ROS is a common component of host defenses against microbial colonization (both mutualistic and pathogenic) (Ruby and McFall-Ngai, 1999; Fones and Preston, 2012; Chávez *et al*., 2007). An *X. nematophila rpoS* mutant is 4-7 fold more sensitive to peroxide challenge than wild type (Vivas and Goodrich-Blair, 2001), indicating that *X. nematophila* RpoS may confer resistance to ROS. However, *X. nematophila* lacks catalase activity for detoxification of peroxide, and must rely on other mechanisms for ROS resistance. We reasoned that if the colonization defect of *rpoS* mutant is due to its relative sensitivity to ROS, then this phenotype might be rescued by expression of the *E.coli katE* gene encoding catalase. *E. coli katE* was introduced into wild type and the *rpoS* mutant genomes using Tn*7* insertion. As expected,

colonies of both wild type and the *rpoS* mutant carrying Tn*7-katE* "bubbled" upon exposure to peroxide, indicating expression of the catalase. The presence of *E. coli katE* partially rescued the colonization defect of the *rpoS* mutant at a level of about 30% of wild-type *X. nematophila*, indicating that ROS is an inhibitory factor for bacterial colonization in nematode hosts, and that catalase expression is sufficient to partially overcome the colonization defect of the *rpoS* mutant (Figure 3.4).

The *X. nematophila rpoS* mutant is more sensitive to near ultra violet (UV) radiation and expression of exogenous catalase gene rescues such defect.

The data described above indicate that the *rpoS* colonization defect may be caused by its relative sensitivity to ROS. In *E. coli*, the *rpoS* gene was originally designated as *nur* (Tuveson, 1981), since mutations in this gene caused sensitivity to near UV radiation, a known cause of ROS and cell damage. To test if *X. nematophila* RpoS is required for near UV-resistance, UV exposure assays were performed on wild type *X. nematophila*, the *rpoS* mutant and *rpoS* mutant expressing *E.coli* catalase gene. The ability of UV resistance was measured as the survival rate of the cells using wild type *X. nematophila* level as 100%. After 60 seconds of UV exposure, *rpoS* mutant had an average survival of 11% that of wild-type *X. nematophila* and expression of *E. coli* catalase gene in *rpoS* mutant increased the survival rate to 165% of wild-type (Figure 3.5), which indicates that the defect of near UV resistance can be rescued by exogenous catalase. These data support the model that *X. nematophila* RpoS is required for resistance to ROS and cell damage that it may encounter in nematode hosts.

RpoS does not regulate known anti-ROS genes *in vitro*.

To test which gene(s) are the regulatory target(s) of RpoS for anti-ROS functions in *X. nematophila*, transcript levels of *X. nematophila* homologs of known anti-ROS genes were measured using qRT-PCR. As high iron concentration is known to be involved in the generation of ROS (through the Fenton reaction), transcript levels were measured in cells grown in LB, in LB depleted for iron using the chelator 1,2-dipyridyl (DP), and in DP-treated LB supplemented with iron. Among the 5 genes tested, transcript levels of *cpxP* (a stress-combative member of the *cpx* regulon), *ahpC* (an alkyl hydroperoxide reductase), and *sodB* (a superoxide dismutase) were present at significant lower levels under iron-limiting conditions than during growth in LB in both wild-type *X. nematophila* HGB007 (49%, 24% and 22% respectively) and *rpoS* mutant (43%, 27% and 15% respectively). The influence of chelation on transcript levels was reversed by re-supplementation with iron. Transcript levels of *dps* (a ferritin-like protein) and *nilB* (a known colonization gene that is not regulated by RpoS) were not significantly affected by iron-depleted or iron re-supplemented conditions. The transcript levels of all 5 genes had no significant differences between the wild type *X. nematophila* and *rpoS* mutant, indicating their expression is not RpoS dependent, at least under *in vitro* conditions tested (Figure 3.6).

Iron concentrations do not affect Lrp-dependent RpoS regulation.

As iron concentration affected expression of putative stress response genes in both wild type *X. nematophila* and the *rpoS* mutant, β-galactosidase assays were performed to test if iron concentrations impact *rpoS* expression, and if any iron-dependent regulation occurs through Lrp. While iron-depleted conditions caused slower growth rate than the normal or iron re-supplemented conditions in both wild type *X. nematophila* and the *lrp* mutant, the *lrp* mutant showed more severe growth rate decrease when iron was depleted. RpoS expression, detected by

β-galactosidase activity expressed from the *rpoS'-'lacZ* fusion, showed no significant difference among different conditions (Figure 3.7A, B), except metal chelation caused RpoS expression to be higher in stationary phase for both strains tested (Figure 3.7C). This indicates that Lrp regulation of RpoS expression is not affected by iron concentrations, and metal depletion is an inducing factor for RpoS expression.

X. nematophila and the _rpoS_ mutant have no differences in oxygen requirements but RpoS expression is induced when oxygen is limited.

One hypothesis derived from examining the RpoS-dependent genes revealed by microarray is that the *rpoS* mutant may be defective in shifting metabolism to micro-aerobic growth. To test this idea, we determined if oxygen availability differentially affected the growth of the *rpoS* mutant. Wild-type *X. nematophila* and the *rpoS* mutant were grown in boiled LB in sealed 100 ml glass bottles, which created a micro-aerobic condition or in boiled LB in sealed 100 ml glass bottles that had air replaced by N_2, which created an anaerobic condition. Neither strain showed significant growth under anaerobic condition (The initial levels of growth are most likely due to the residue oxygen left in the sealed bottle during media preparation), both wild type *X. nematophila* and *rpoS* mutant behaved similarly under micro-aerobic condition and showed no difference in growth density or rates. Similar results were observed for growth in minimal medium (Figure 3.8).

The impact of oxygen levels on Lrp-dependent regulation of *rpoS* was also tested (Figure 3.9). Neither strain showed significant growth under anaerobic conditions. Regardless of condition, the *lrp* mutant displayed higher levels of reporter expression than the wild type (Figure 3.3) and levels of reporter activity of *lrp* mutant cells grown in anaerobic and micro-

aerobic conditions were similar to those of cells grown in aerobic condition (Figure 3.3). The β-galactosidase activities detected under anaerobic condition may due to the limited growth based on trace amount of oxygen left in the medium, but the highest levels of RpoS expression in wild-type *X. nematophila* under anaerobic and micro-aerobic conditions were significantly higher than the level under aerobic condition, indicating that RpoS expression is induced when oxygen availability is limited (Figure 3.9 C).

CO_2 has no effects on *X. nematophila* anaerobic growth.

Since the anaerobic growth tests showed that *X. nematophila* cannot grow without oxygen, we tested the effects of high concentration of bicarbonate/CO_2 on *X. nematophila* anaerobic growth by adding CO_2 into the medium. Maintaining a proper intracellular bicarbonate/CO_2 concentration is important for bacterial carboxylation and growth, and supplementing higher CO_2 concentration can support better growth of *E.coli* (Kozliak *et al*., 1995). Since RpoS is a regulator involved in the responses to stresses including anaerobic conditions (King and Ferenci T, 2005), high concentration of bicarbonate/CO_2 may affect its function. *X. nematophila* and *rpoS* mutant were grown in boiled minimum medium in sealed 100 ml glass bottles with air replaced by CO_2, as well as in micro-aerobic and anaerobic conditions. Neither wild-type *X. nematophila* nor *rpoS* mutant showed significant growth when CO_2 was supplemented which indicates that high bicarbonate/CO_2 concentration has no effect on *X. nematophila* anaerobic growth (Figure 3.10).

Table 3.1. Effects of RpoS on gene expression detected by microarray analysis. Genes are grouped according to predicted functions. Red color indicates genes that are predicted to be expressed in operons. 2.5-fold differences were used as the cut-off.

RpoS induced					
ORF ID	**Start Position**	**End Position**	**ORF Length**	**Annotation**	**Fold changes**
				Virulence factors	
XNC1_1142	1019735	1021024	1290	pirB, JHE-like toxin, "Photorhabdus insecticidal related" toxin, PirB	0.38
XNC1_1143	1021093	1021500	408	pirA, JHE-like toxin, "Photorhabdus insecticidal related" toxin, PirA	0.40
				Transport	
XNC1_1558	1441516	1442373	858	focA, ycaE, formate transport protein (formate channel 1) (FNT family)	0.29
XNC1_3601	3485931	3487232	1302	dcuA, genA, anaerobic dicarboxylate transport protein (Dcu family)	0.29
XNC1_4279	4114626	4115735	1110	putative transport protein (permease)	0.31
				Nutrient and energy metabolism	
XNC1_0037	39827	40819	993	asnA, asparagine synthetase A	0.36
XNC1_1079	955866	956630	765	pdhR, yacB, transcriptional repressor for pyruvate dehydrogenase complex (GntR family)	0.39
XNC1_1080	956870	959533	2664	aceE, pyruvate dehydrogenase, decarboxylase subunit, thiamin-binding	0.31

XNC1_1081	959547	961106	1560	aceF, pyruvate dehydrogenase, dihydrolipoyltransacetylase subunit	0.28
XNC1_1556	1438305	1439045	741	pflA, act, pyruvate formate lyase activating enzyme 1	0.27
XNC1_1557	1439175	1441457	2283	pflB, pfl, pyruvate formate lyase I, induced anaerobically	0.27
XNC1_2801	2800866	2802932	2067	pta, phosphotransacetylase (phosphate acetyltransferase)	0.39
XNC1_2802	2803194	2804396	1203	ackA, acetate kinase A (propionate kinase 2)	0.29
XNC1_3840	3694715	3696868	2154	yjiY, carbon starvation protein	0.10
XNC1_4280	4115930	4116583	654	putative Inorganic diphosphatase	0.20
XNC1_4281	4116609	4117670	1062	putative L-iditol 2-dehydrogenase	0.33
XNC1_4282	4117670	4118920	1251	putative 4-aminobutyrate aminotransferase, PLP-dependent	0.28
XNC1_4285	4122280	4124730	2451	malP, malA, blu, maltodextrin phosphorylase	0.32
XNC1_4409	4229031	4230440	1410	glnA, glutamine synthetase	0.26
				Others	
XNC1_1205	1072815	1073894	1080	e14 prophage; putative tail fiber protein (modular protein)	0.09
XNC1_3066	3037190	3037798	609	Tail protein I (GpI)	0.38
				Unknown functions	
XNC1_1130	1007907	1008002	96	hypothetical protein	0.31
XNC1_2973	2958055	2958180	126	hypothetical protein	0.04

XNC1_3149	3099192	3099536	345	conserved hypothetical protein	0.37
XNC1_3838	3693379	3694371	993	protein of unknown function (similar to YjiA of E. coli)	0.38
XNC1_3839	3694430	3694633	204	conserved hypothetical protein	0.21
XNC1_4109	3982669	3982875	207	hypothetical protein	0.36
RpoS repressed					
ORF ID	**Start Position**	**End Position**	**ORF Length**	**Annotation**	**Fold changes**
				Virulence factors	
XNC1_2974	2958295	2961417	3123	Extracellular serine protease precursor	2.71
				Transport	
XNC1_0050	53574	55229	1656	yjcG, putative transporter of the sodium symport superfamily (SSS family); putative transmembrane protein	4.16
XNC1_1339	1202072	1202797	726	gltL, glutamate/aspartate transport protein (ABC superfamily, atp_bind)	2.56
XNC1_1340	1202797	1203471	675	gltK, glutamate/aspartate transport protein (ABC superfamily, membrane)	2.92
XNC1_1341	1203476	1204216	741	gltJ, glutamate/aspartate transport protein (ABC superfamily, membrane)	3.63
XNC1_1342	1204340	1205227	888	gltI, ybeJ, yzzK, glutamate/aspartate transport protein (ABC superfamily, peri_bind)	4.69

XNC1_1612	1503640	1505016	1377	putative amino-acid transport protein	3.81
XNC1_1672	1545897	1547381	1485	putP, putC, major sodium:proline symporter (SSS family)	5.64
XNC1_2474	2425776	2426777	1002	oppF, oligopeptide transport protein (ABC superfamily, atp_bind)	3.78
XNC1_2475	2426774	2427772	999	oppD, oligopeptide transport protein (ABC superfamily, atp_bind)	4.31
XNC1_2476	2427782	2428690	909	oppC, oligopeptide transport protein (ABC superfamily, membrane)	2.91
XNC1_2477	2428705	2429625	921	oppB, oligopeptide transport protein (ABC superfamily, membrane)	3.17
XNC1_2478	2429711	2431357	1647	oppA2, oligopeptide transport protein (ABC superfamily, peri_bind)	3.81
XNC1_2479	2431482	2433122	1641	oppA1, oligopeptide transport protein (ABC superfamily, peri_bind)	4.99
XNC1_2697	2658180	2659628	1449	yaaJ, putative alanine/glycine transport protein (AGCS family)	2.65
XNC1_2982	2970085	2971758	1674	yidK, putative myo-inositol transport protein (SSS family)	4.25
XNC1_3185	3129353	3130717	1365	proY, yajM, proline transport protein (APC family)	3.09
XNC1_3197	3143396	3144757	1362	fadL, ttr, outer membrane porin, transport of long-chain fatty acids, sensitivity to phage T2	6.91
XNC1_4146	4006004	4007248	1245	sstT, ygjU, Na+:serine/threonine symporter (DAACS family)	4.77
XNC1_4230	4075019	4076299	1281	putative glutamate symport transmembrane protein	3.52
XNC1_4490	4292578	4293594	1017	dppF, dipeptide transport protein (ABC superfamily, atp_bind)	2.85
XNC1_4491	4293591	4294571	981	dppD, dipeptide transport protein (ABC superfamily, atp_bind)	3.16

XNC1_4492	4294584	4295501	918	dppC, dipeptide transport protein 2 (ABC superfamily, membrane)	2.69
XNC1_4493	4295512	4296531	1020	dppB, dipeptide transport protein 1 (ABC superfamily, membrane)	3.62
XNC1_4494	4296673	4298283	1611	dppA, fpp, dpp, alu, dipeptide transport protein (ABC superfamily, peri_bind)	4.47
				Nutrient and energy metabolism	
XNC1_0051	55226	55537	312	Inner membrane protein yjcH	5.90
XNC1_0052	55744	57699	1956	acs, acsA, yfaC, acetyl-CoA synthetase, has propionyl-CoA synthetase activity	6.18
XNC1_0241	212902	213597	696	putative Phosphoglycolate phosphatase	2.61
XNC1_0753	651362	653122	1761	ggt, gamma-glutamyltranspeptidase	3.74
XNC1_0810	696225	696743	519	ycdH, putative oxidoreductase component with FMN-binding split barrel domain	3.46
XNC1_0811	696765	698360	1596	4-hydroxyphenylacetate 3-monooxygenase, oxygenase component (4-HPA 3-monooxygenase large component) (4-HPA 3- hydroxylase)	7.17
XNC1_0820	705811	706662	852	3,4-dihydroxyphenylacetate 2,3-dioxygenase (Homoprotocatechuate 2,3-dioxygenase) (HPC dioxygenase)	2.62
XNC1_0821	706729	708195	1467	betB, NAD+-dependent betaine aldehyde dehydrogenase	2.55
XNC1_1040	912927	914096	1170	leuB, 3-isopropylmalate dehydrogenase	4.25
XNC1_1041	914099	915718	1620	leuA, 2-isopropylmalate synthase	5.20
XNC1_1045	920184	921911	1728	ilvI, acetolactate synthase III, valine-sensitive, large subunit	7.75

XNC1_1046	921914	922405	492	ilvH, brnP, acetolactate synthase III, valine-sensitive, small subunit	2.91
XNC1_1228	1092212	1093675	1464	prpD, acnC, yahT, 2-methyl citrate dehydratase	2.62
XNC1_1229	1093695	1094870	1176	prpC, yahS, yzzD, methylcitrate synthase (citrate synthase 2)	3.00
XNC1_1230	1094863	1095768	906	prpB, yahQ, 2-methylisocitrate lyase	5.27
XNC1_1405	1283732	1284121	390	sdhC, cybA, succinate dehydrogenase, hydrophobic subunit, cytochrome b556 with SdhD	3.16
XNC1_1406	1284115	1284462	348	sdhD, succinate dehydrogenase, hydrophobic subunit, cytochrome b556 with SdhC	2.84
XNC1_1407	1284463	1286229	1767	sdhA, succinate dehydrogenase, catalytic and NAD/flavoprotein subunit	3.72
XNC1_1408	1286267	1286983	717	sdhB, succinate dehydrogenase, Fe-S protein	2.81
XNC1_1673	1547894	1551874	3981	putA, poaA, putC, multifunctional: transcriptional repressor of proline utilization; proline dehydrogenase; pyrroline-5-carboxylate dehydrogenase	7.49
XNC1_2083	2001516	2003036	1521	putative Alkaline phosphatase	3.05
XNC1_2184	2103179	2104870	1692	fadD, oldD, acyl-CoA synthetase (long-chain-fatty-acid--CoA ligase)	2.65
XNC1_2270	2214668	2216125	1458	ydcW, putative aldehyde dehydrogenase	3.88
XNC1_2272	2216979	2218268	1290	goaG, 4-aminobutyrate aminotransferase, PLP-dependent	2.97
XNC1_2512	2459837	2460904	1068	dadX, alnB, dadB (S.t.), msuA, alanine racemase 2, PLP-binding, catabolic	4.67

XNC1_2513	2460927	2462228	1302	dadA, dadR, D-amino acid dehydrogenase subunit	7.34
XNC1_2979	2966316	2967146	831	Protein iolB	4.63
XNC1_2980	2967169	2968059	891	Rhizopine catabolism protein mocC	4.22
XNC1_2981	2968166	2970073	1908	putative Fructokinase	3.69
XNC1_2983	2971920	2972912	993	Inositol 2-dehydrogenase	5.19
XNC1_2984	2973198	2975162	1965	putative malonic semialdehyde oxidative decarboxylase	5.21
XNC1_2985	2975171	2976682	1512	mmsA, methylmalonate-semialdehyde dehydrogenase, oxidoreductase protein	4.19
XNC1_3041	3014876	3017323	2448	fadE, yafH, fadF (S.t.), acyl coenzyme A dehydrogenase	2.61
XNC1_3186	3130810	3132342	1533	Histidine ammonia-lyase (Histidase)	19.08
XNC1_3187	3132358	3134031	1674	Urocanate hydratase (Urocanase) (Imidazolonepropionate hydrolase)	15.62
XNC1_3491	3378037	3379881	1845	putative carbamoyltransferase protein	4.02
XNC1_3493	3382063	3383991	1929	nodQ, Nodulation protein Q, putative bifunctional enzyme: sulfate adenylyltransferase and Adenylyl-sulfate kinase	2.69
XNC1_3619	3496914	3498233	1320	putative oxidoreductase with FAD/NAD(P)-binding domain	3.90
XNC1_3621	3498724	3500217	1494	feaB, padA, ydbG, phenylacetaldehyde dehydrogenase	2.56
XNC1_3774	3630982	3632130	1149	opnS, ynaG, growth-phase-regulated outer membrane protein OpnS	8.34

XNC1_3875	3732677	3734863	2187	fadB, oldB, multifunctional: 3-hydroxybutyryl-CoA epimerase, delta(3)-cis-delta(2)-trans-enoyl-CoA isomerase, enoyl-CoA hydratase (N-terminal); 3-hydroxyacyl-CoA dehydrogenase (C-terminal)	8.85
XNC1_3876	3734875	3736038	1164	fadA, oldA, 3-ketoacyl-CoA thiolase; (thiolase I, acetyl-CoA transferase), in complex with FadB catalyzes	7.38
XNC1_3948	3811147	3812928	1782	aceK, isocitrate dehydrogenase kinase/phosphatase	4.22
XNC1_3949	3812948	3814255	1308	aceA, icl, isocitrate lyase	3.71
XNC1_3950	3814318	3815913	1596	aceB, mas, malate synthase A	4.68
XNC1_4323	4153153	4154745	1593	ydeV, putative sugar kinase, actin-like ATPase domain	5.24
XNC1_4614	4408565	4410637	2073	maoC, paaZ, tynP?, ydbN, putative aldehyde dehydrogenase, phenylacetic acid degradation	3.46
				Other functions	
XNC1_1202	1070462	1070920	459	stfE, ycfE, putative e14 prophage; tail fiber protein	22.48
XNC1_1203	1070920	1071513	594	tfaE, ycfA, putative e14 prophage; tail fiber assembly	8.72
				Unknown functions	
XNC1_0239	211441	211821	381	conserved hypothetical protein	2.57
XNC1_0770	665623	666639	1017	conserved hypothetical protein; putative membrane protein	3.20

XNC1_0771	666639	667382	744	putative membrane protein	3.09
XNC1_1032	905300	906160	861	hypothetical protein	2.65
XNC1_1657	1536984	1537493	510	putative membrane protein	2.55
XNC1_1781	1720864	1721226	363	hypothetical protein	2.65
XNC1_2062	1984829	1985722	894	conserved hypothetical protein	2.81
XNC1_2271	2216142	2216915	774	conserved hypothetical protein	3.77
XNC1_3487	3374714	3375823	1110	putative membrane protein	2.54
XNC1_3490	3377887	3378033	147	hypothetical protein	5.08
XNC1_3492	3379890	3381902	2013	hypothetical protein	2.73
XNC1_4099	3973702	3974898	1197	hypothetical protein	3.20
XNC1_4170	4028949	4029095	147	hypothetical protein	5.65

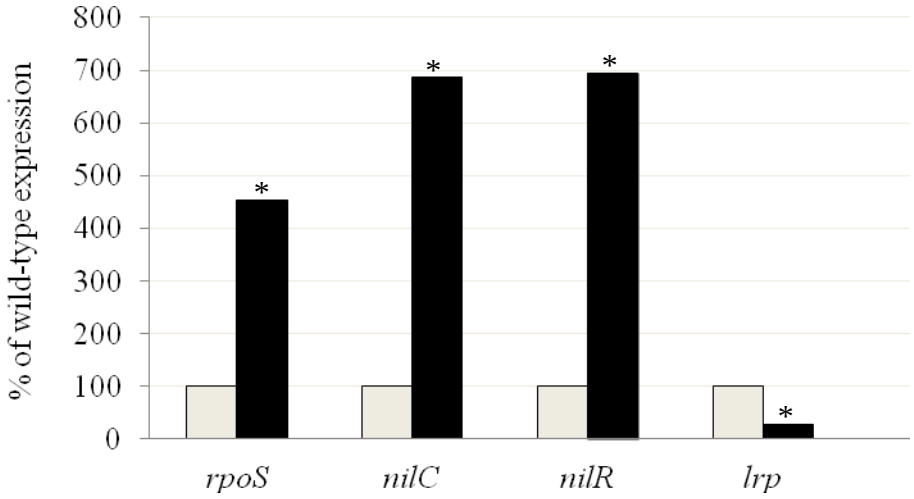

Figure 3.1. Effects of *lrp* mutation on gene transcript levels detected by microarray analysis of cells in early stationary phase. Transcript levels are shown as percent levels compared to wild-type: wild-type *X. nematophila* HGB800 (gray bars), *lrp* mutant HGB1059 (black bars). Asterisks indicate statistically significant differences from wild-type levels. $P<0.05$. Statistics were done by Student's T Test.

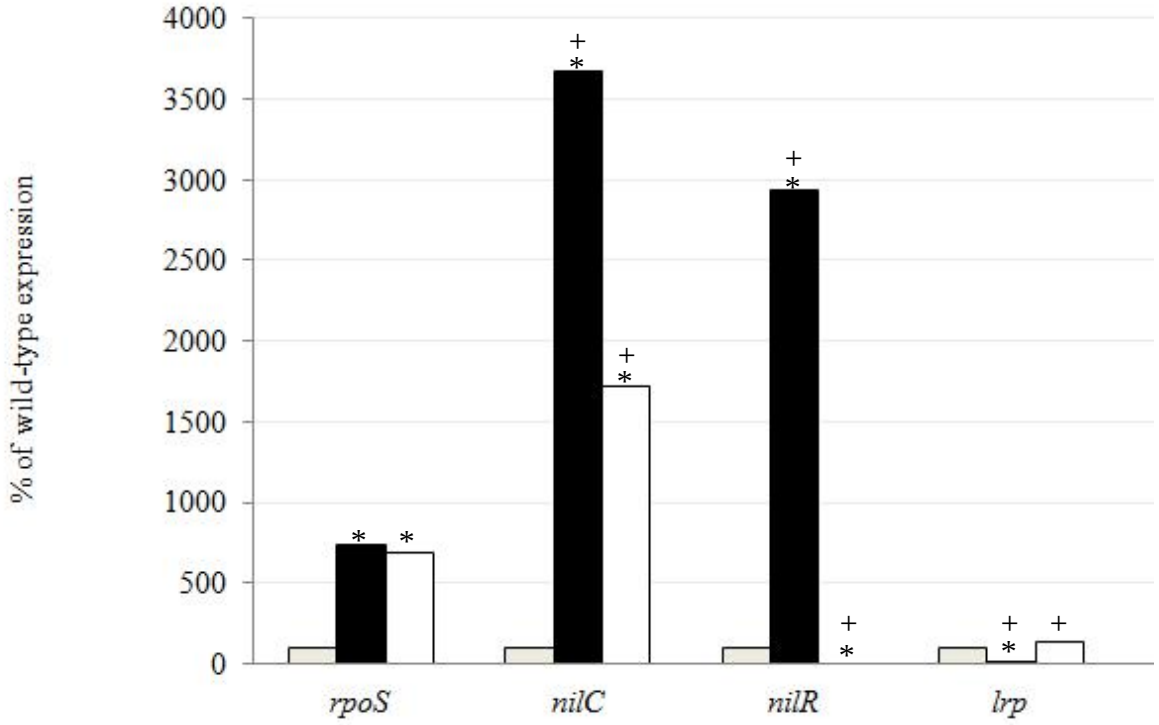

Figure 3.2. Effects of *lrp* and *nilR* mutations on transcript levels at early stationary phase. Transcript levels are shown as percent levels compared to wild-type: wild-type *X. nematophila* HGB800 (gray bars), *lrp* mutant HGB1059 (black bars), and *nilR* mutant HGB1103 (white bars). Asterisks indicate statistically significant differences from wild-type levels, $P<0.05$; Pluses indicate statistically significant differences between *lrp* mutant and *nilR* mutant, $P<0.05$. Statistics were done by One-Way ANOVA.

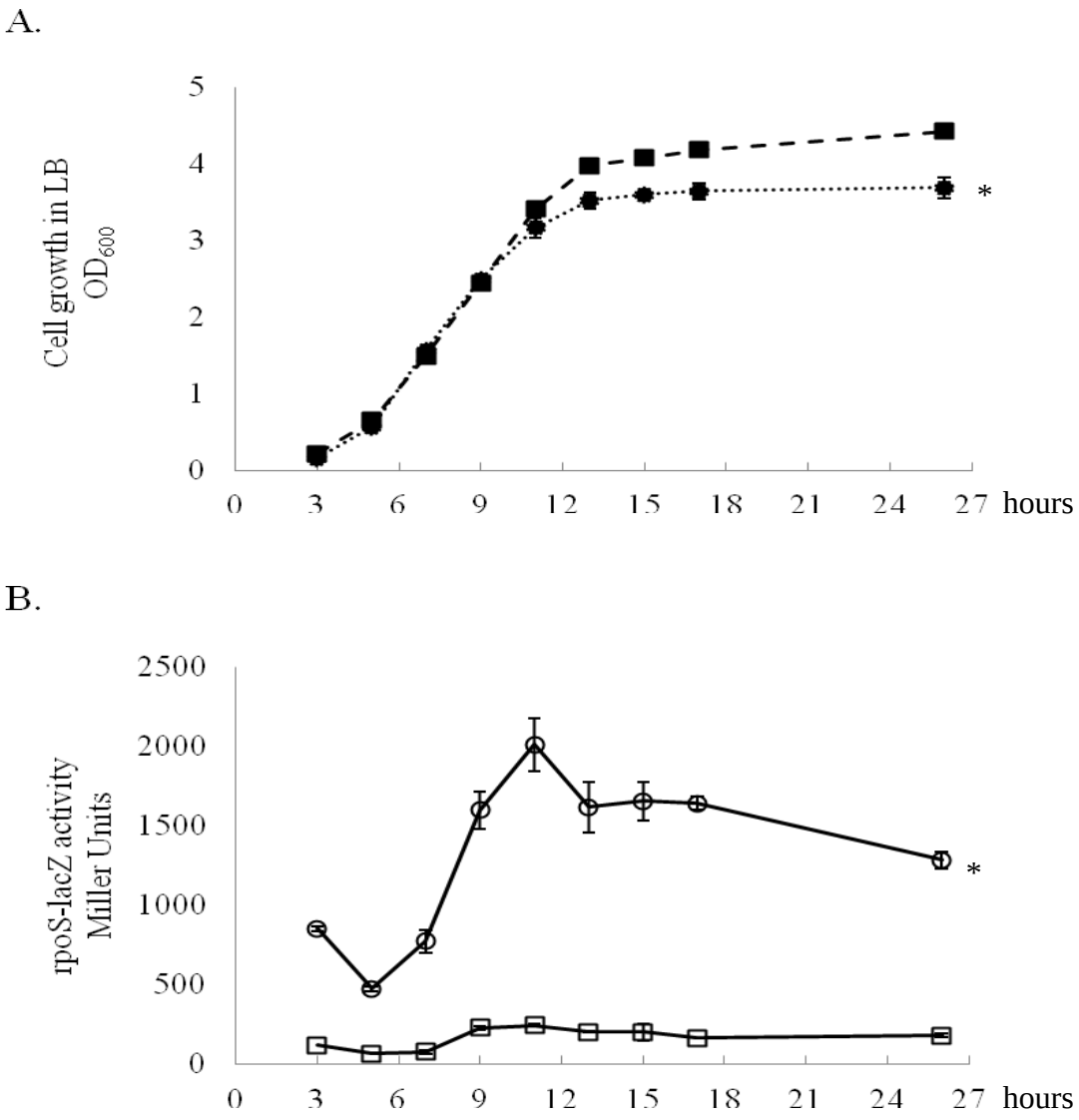

Fig 3.3 A, B. Effects of *lrp* mutant on RpoS expression in LB. Cell growth measured at OD_{600} (A) and *rpoS* promoter activity measured by β-galactosidase assay (B) for wild-type *X. nematophila* (squares) and the *lrp* mutant (circles) carrying an *rpoS'-'lacZ* translational fusion (○). Wild-type *X. nematophila* and the *lrp* mutant with empty Tn*7* insertions had no significant level of β-galactosidase activities and are not shown. Asterisks indicate statistically significant differences from wild-type levels. $P<0.05$. Statistics were done by Student's T-Test.

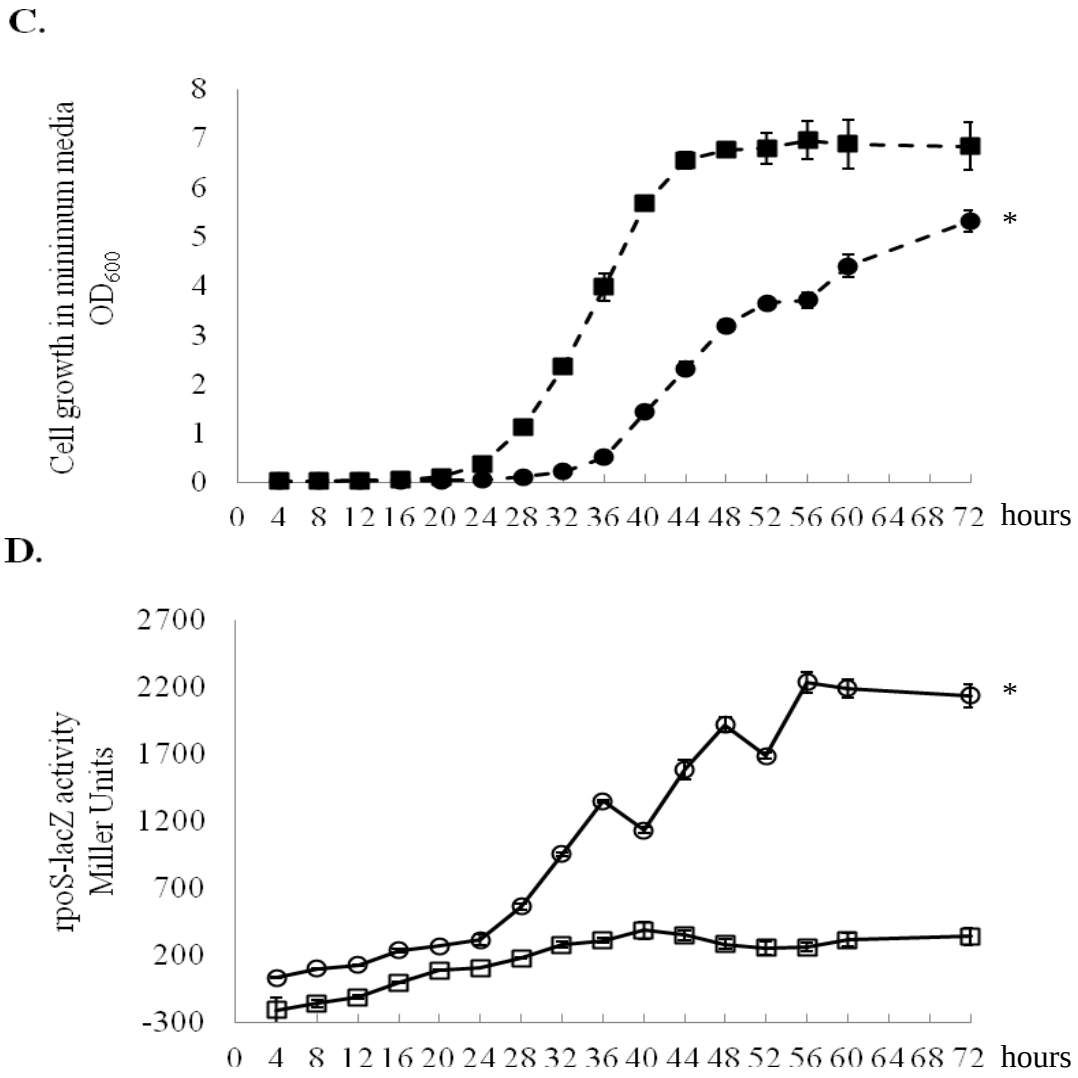

Fig 3.3 C, D. Effects of *lrp* mutant on RpoS expression in minimum medium. Cell growth measured at OD_{600} (C) and *rpoS* promoter activity measured by β-galactosidase assay (D) for wild-type *X. nematophila* with *rpoS-lacZ* translational fusion (□), and *lrp* mutant with *rpoS-lacZ* translational fusion(○). Wild-type *X. nematophila* and *lrp* mutant with empty Tn*7* insertions had no significant level of β-galactosidase activities and were not shown in the figures. Asterisks indicate statistically significant differences from wild-type levels. $P<0.05$. Statistics were done by Student's T-Test.

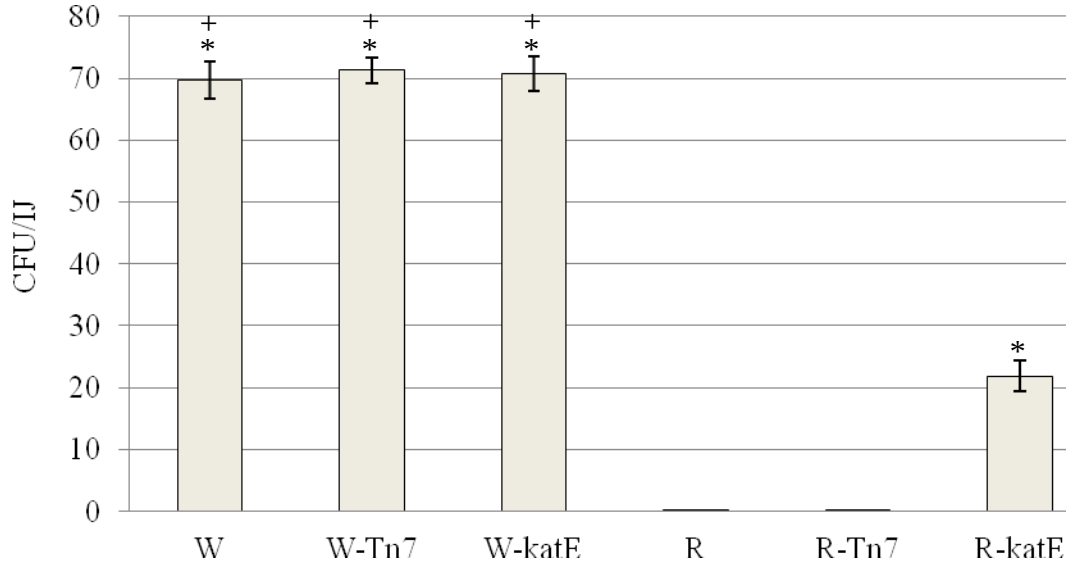

Figure 3.4. The colonization defect of the *rpoS* mutant in *S. carpocapsae* nematodes can be partially rescued by the presence of *E. coli katE* encoding catalase. Wild-type *X. nematophila* HGB007 (W), wild-type *X. nematophila* with empty Tn*7* insertion HGB763 (W-Tn7), wild-type *X. nematophila* with Tn*7-katE* insertion (W-katE), *rpoS* mutant HGB151 (R), *rpoS* mutant with empty Tn*7* insertion HGB765 (R-Tn7), and *rpoS* mutant with Tn*7-katE* insertion (R-katE). Asterisks indicate statistically significant differences from *rpoS* mutant level, $P<0.05$; Pluses indicate statistically significant differences from the level of *rpoS* mutant with Tn*7-katE* insertion, $P<0.05$. Statistics were done by One-Way ANOVA.

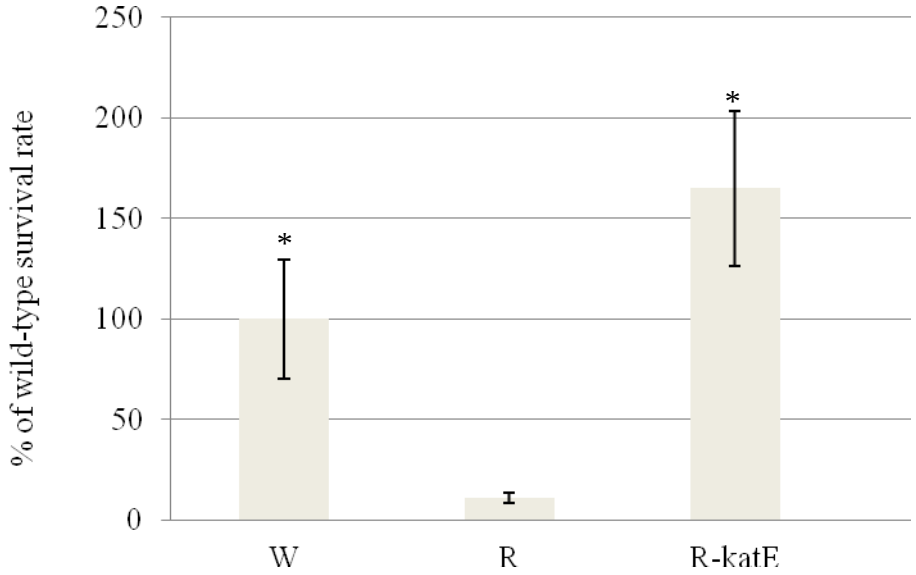

Figure 3.5. UV resistance defect of the *rpoS* mutant can be rescued by expressing *E. coli* catalase gene *katE*. Survival rates are shown as percent levels compared to wild-type: wild-type *X. nematophila* HGB007 (W), *rpoS* mutant HGB151 (R), and *rpoS* mutant with Tn*7-katE* insertion (R-katE). Asterisks indicate statistically significant differences from *rpoS* mutant level. $P<0.05$. Statistics were done by Student's T-Test.

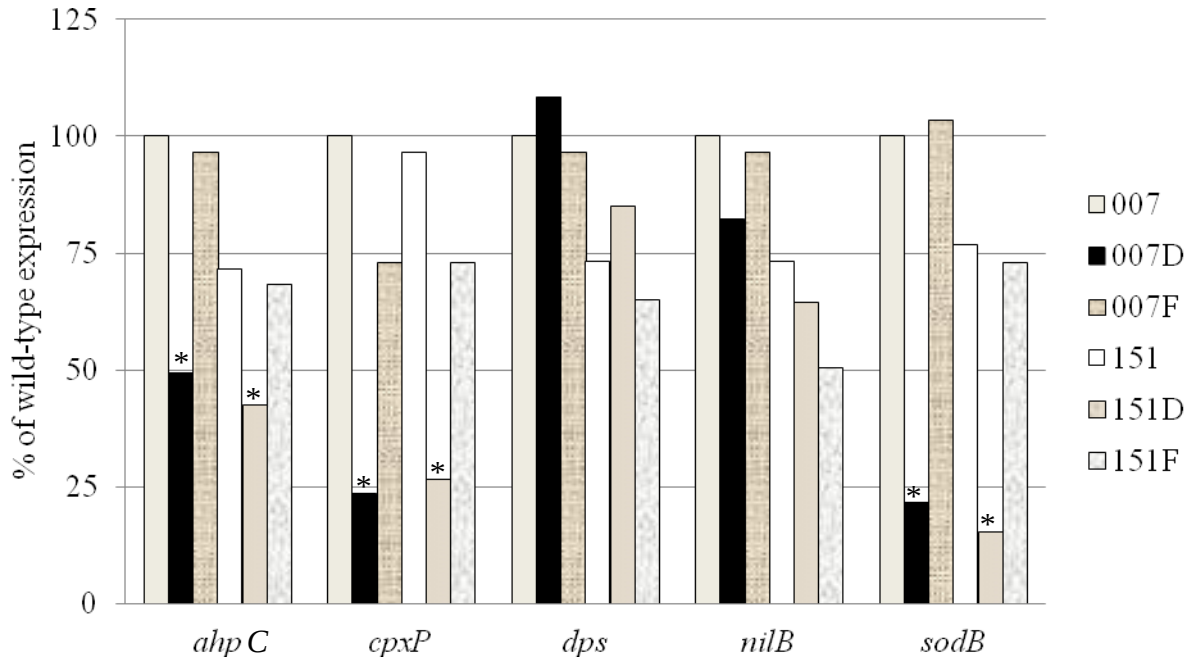

Figure 3.6. Effects of *rpoS* mutant on potential anti-ROS genes. Iron depleted conditions were achieved by adding 25mM deferoxamine in LB medium (D). Iron re-supplemented conditions were achieved by adding 500mM $FeSO_4$ to iron depleted medium (F). Transcript levels are shown as percent levels compared to wild-type: wild type *X. nematophila* HGB007 (007) and *rpoS* mutant HGB151 (151). Asterisks indicate statistically significant differences from wild-type levels. $P<0.05$. Statistics were done by Student's T-Tests.

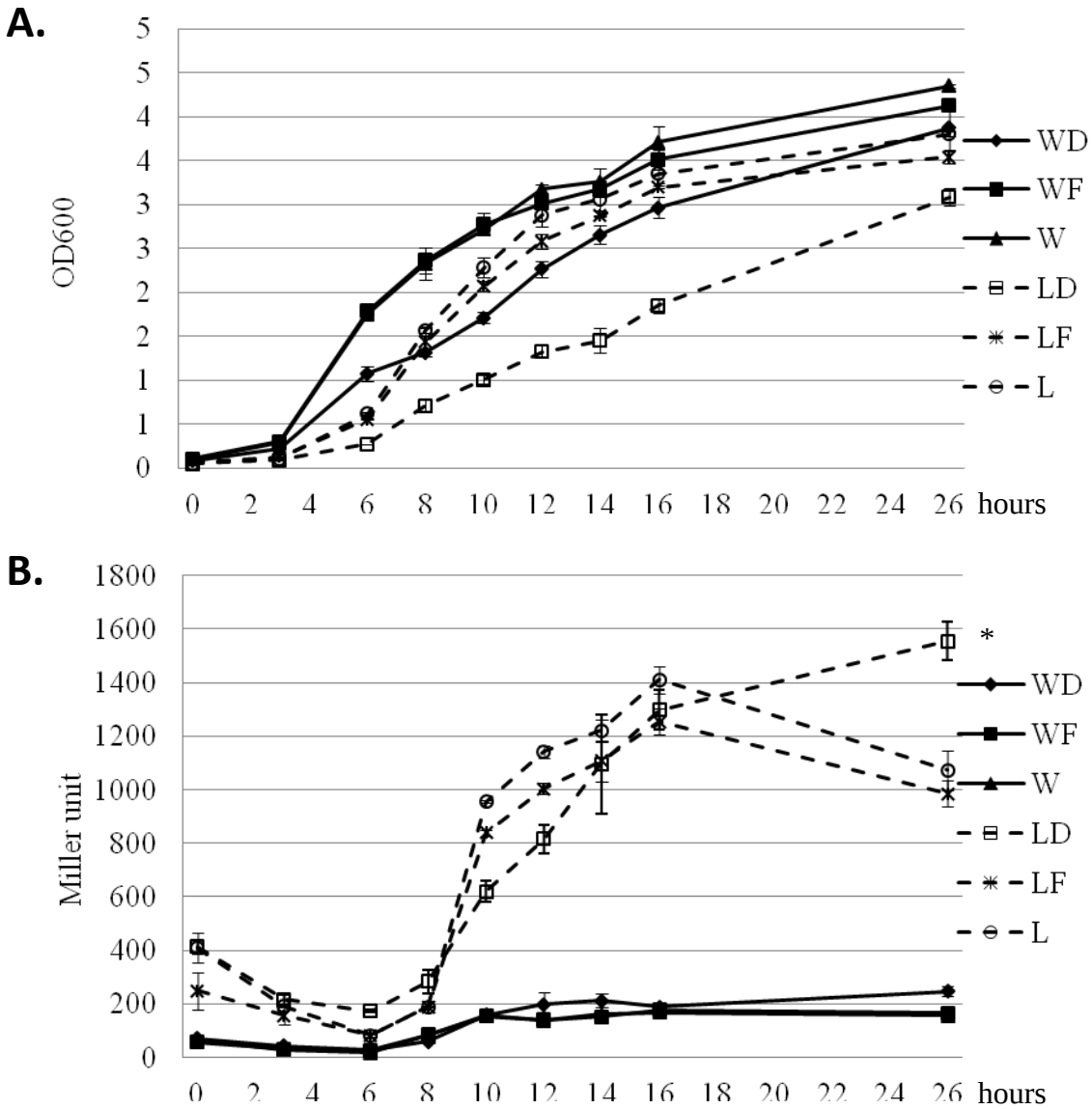

Figure 3.7 A, B. Effects of iron on Lrp-dependent *rpoS* expression. Cell growth measured at OD_{600} (A) and *rpoS* promoter activity measured by β-galactosidase assay (B). Iron depleted conditions were achieved by adding 25mM deferoxamine in LB medium (D). Iron re-supplemented conditions were achieved by adding 500 mM $FeSO_4$ to iron depleted medium (F). Wild type *X. nematophila* HGB800 (W) and the *lrp* mutant HGB1059 (L). Asterisks indicate statistically significant differences from untreated sample (L). $P<0.05$. Statistics were done by Student's T-Tests.

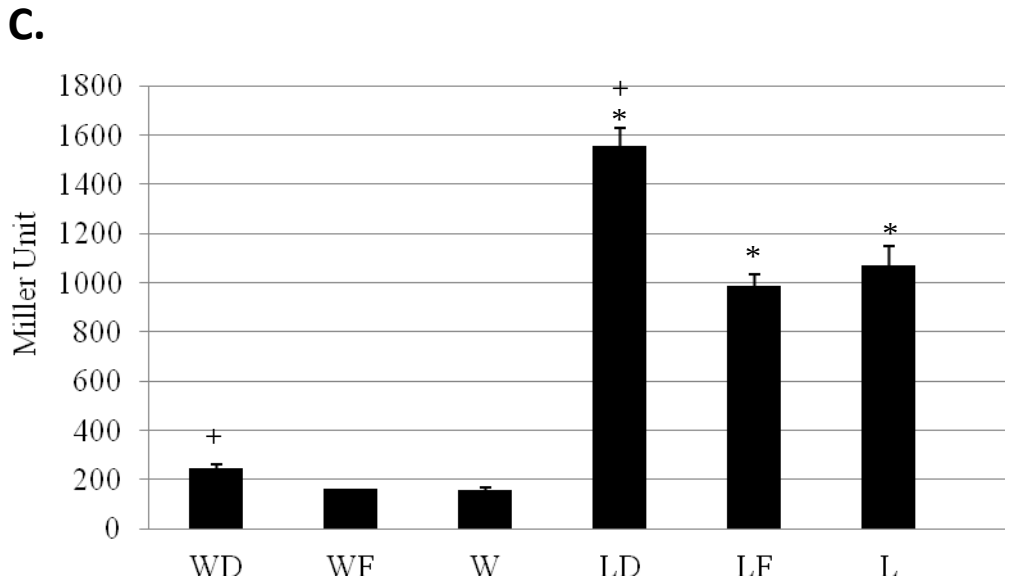

Figure 3.7 C. Effects of iron on Lrp-dependent *rpoS* expression after 26 hours of incubation. *rpoS* promoter activity was measured by β-galactosidase assay. Iron depleted conditions were achieved by adding 25mM deferoxamine in LB medium (D). Iron re-supplemented conditions were achieved by adding 500 mM $FeSO_4$ to iron depleted medium (F). Wild type *X. nematophila* HGB800 (W) and the *lrp* mutant HGB1059 (L). Asterisks indicate statistically significant differences from wild-type under same conditions. Pluses indicate statistically significant differences from the untreated condition within the same strain. $P<0.05$. Statistics were done by Student's T-Tests.

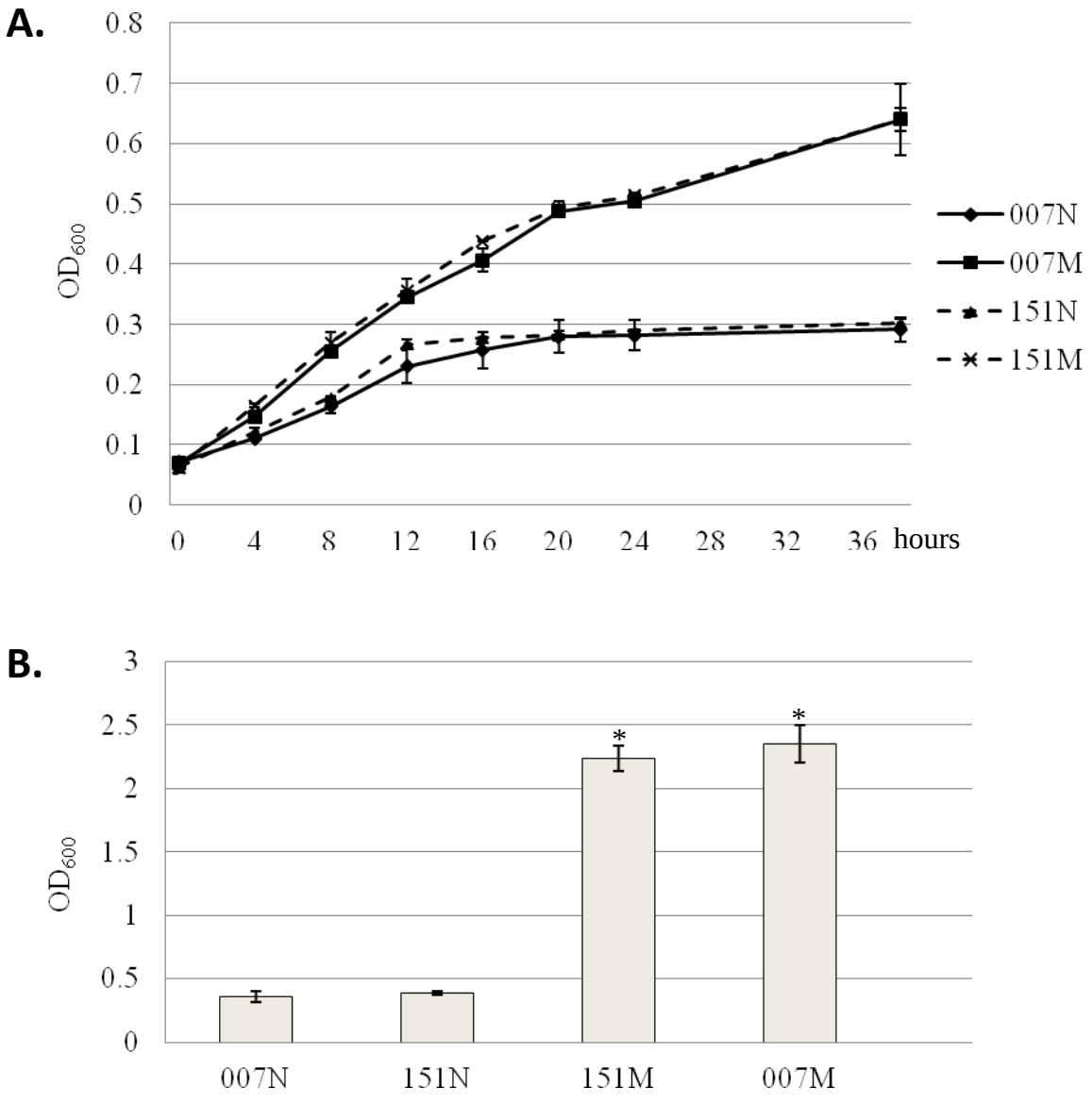

Figure 3.8. Effects of oxygen on growth of the *rpoS* mutant in LB medium. Growth curve measured at OD_{600} (A) and cell densities measured at OD_{600} after 180 hours (B). Anaerobic condition with N_2 replacing the air (N), micro-aerobic condition (M), wild-type *X. nematophila* HGB007 (007), *rpoS* mutant HGB151 (151). Asterisks indicate statistically significant differences from anaerobic condition. $P<0.05$. Statistics were done by Student's T-Tests.

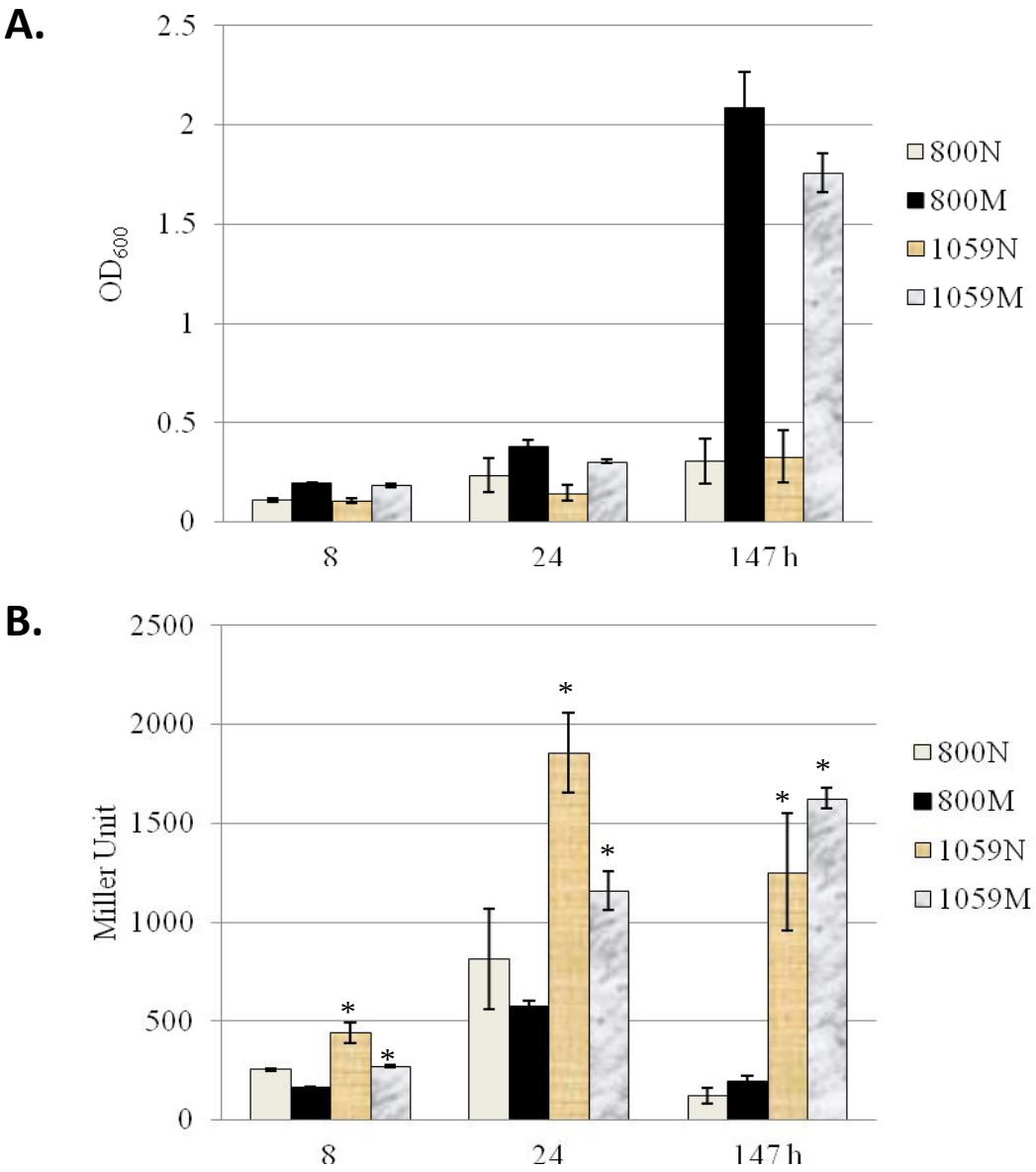

Figure 3.9 A, B. Effects of oxygen avaliability on Lrp-dependent *rpoS* expression. Cell densities measured at OD_{600} (A) and *rpoS* promoter activity measured by β-galactosidase assay (B). Anaerobic condition with N_2 replacing the air (N), micro-aerobic condition (M), wild type *X. nematophila* HGB800 (800), *lrp* mutant HGB1059 (1059). Asterisks indicate statistically significant differences from wild-type levels under same growth conditions. $P<0.05$. Statistics were done by Student's T-Tests.

C.

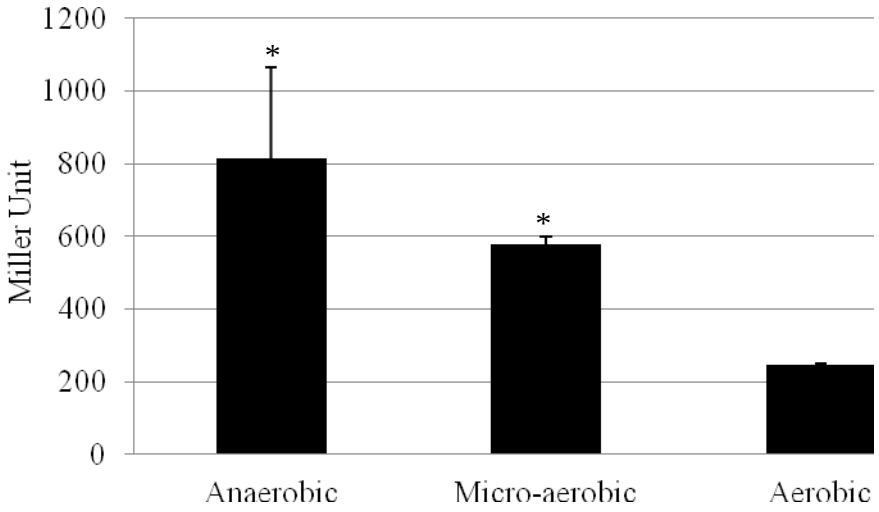

Figure 3.9 C. Effects of oxygen avaliability on the highest levels of Lrp-dependent *rpoS* expression in wild-type *X. nematophila* HGB800. *rpoS* promoter activity measured by β-galactosidase assay. Asterisks indicate statistically significant differences from aerobic condition. $P<0.05$. Statistics were done by Student's T-Tests.

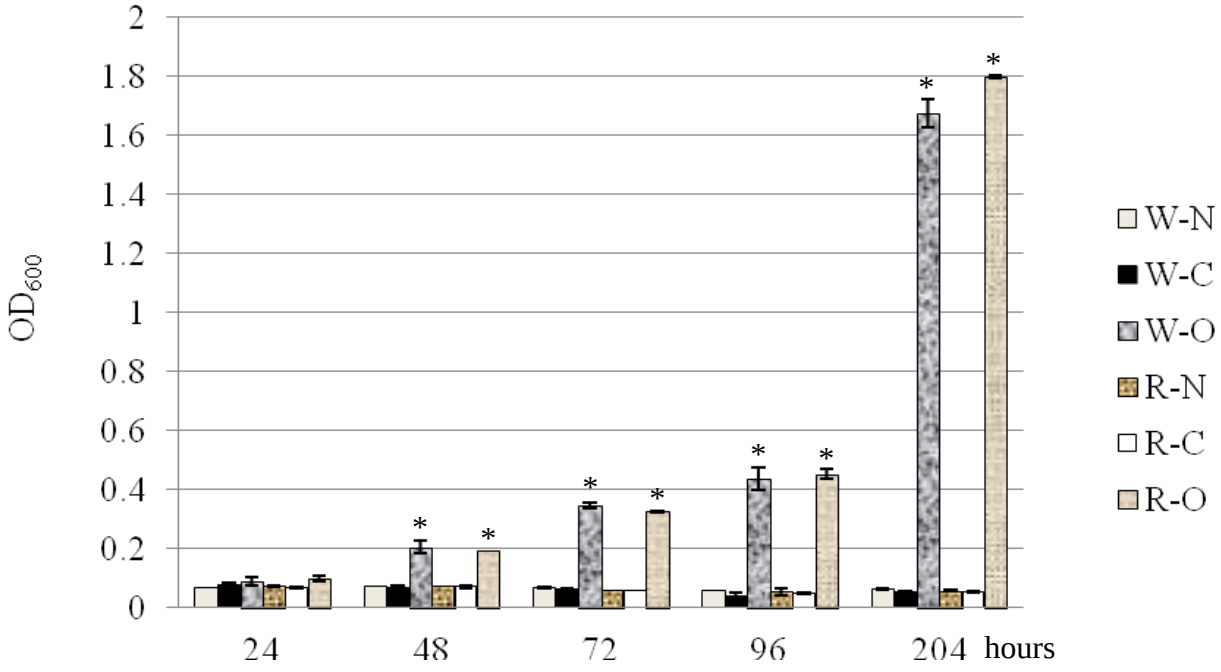

Figure 3.10. Effects of *rpoS* mutant on bicarbonate utilization. Anaerobic condition with N_2 replacing the air (N), anaerobic condition with CO_2 replacing the air (C), aerobic condition with limited O_2 (O), wild-type *X. nematophila* HGB007 (W), *rpoS* mutant HGB151 (R). Asterisks indicate statistically significant differences from levels under anaerobic conditions. $P<0.05$. Statistics were done by Student's T-Tests.

DISCUSSION

In this study we demonstrated that the expression of exogenous *E. coli* catalase gene in *X. nematophila* rescues the mutualistic colonization defect and the near UV sensitivity of the *rpoS* mutant (Figure 3.4, 3.5). This finding suggests that ROS-dependent stress inhibits bacterial colonization in the nematode host, and RpoS is responsible for mediating the anti-ROS function of the bacterium. This hypothesis is further supported by the fact that *rpoS* mutant is more sensitive to hydrogen peroxide treatments (Vivas and Goodrich-Blair, 2001). The ability of *X. nematophila rpoS* mutant to colonize *S. anatoliense* and *S. websteri* (Anderson, unpublished) but not its own natural host *S. carpocapsae* indicates that the source of the ROS during mutualistic colonization is the nematode host, and thus the ability of the hosts to generate ROS is a factor that affects bacterium-host specificity. *S. anatoliense* and *S. websteri* may produce lower levels of ROS than *S. carpocapsae*, which allows the colonization of *X. nematophila*. Although a study in *Caenorhabditis elegans* showed that exposing the nematode to bacteria can stimulate host ROS production, which can be detected by Amplex Red Assay (Chávez *et al*., 2007), attempts to use this method to determine ROS levels in the above three nematode hosts challenged with *X. nematophila* failed due to the unsynchronized development of *Steinernema* nematodes and hard-to-penetrate IJ cuticles, which made the results variable and inconclusive. The lack of catalase and a very limited number of anti-ROS function genes identified via genomic sequencing indicate that *X. nematophila* may be more sensitive to subtle differences of ROS levels in different nematode hosts, which may not be detected easily.

Surprisingly, neither microarray analysis (Table 3.1) nor qRT-PCR (Figure 3.6) detected RpoS regulation on the known anti-ROS factors *ahpC*, *sodB* and *dps*. The possible explanations

for such unexpected results are: a. RpoS regulates anti-ROS functions via unknown factors or mechanisms, or it can only regulate those genes under conditions that were not represented in the tests; b. RpoS regulates other cellular functions which when disrupted can stimulate nematode host to produce ROS; c. the dysfunction of the RpoS dependent functions in combination with existing ROS stress are enough to cause colonization defect in mutualism and introduction of catalase reduces overall stress level, and thus rescues the colonization defect. The partial rescue of bacterial colonization by *E.coli* catalase is in favor of the latter two hypotheses although the first hypothesis cannot be totally ruled out.

Microarray analysis done on aerobically grown early stationary phase cultures revealed that RpoS induces a small set of genes mainly involved in anaerobic metabolism and represses a large number of genes for nutrient transport and aerobic metabolism (Table 3.1). This indicates that RpoS, as a stationary phase induced regulator, may affect bacterial colonization in nematode host by mediating the response to stresses incurred during environmental and nutrient transitions. The inability of the bacterium to grow anaerobically (Figure 3.8) and being affected by high bicarbonate/CO_2 concentration (Figure 3.10), and the induction of RpoS in stationary phase and under oxygen limiting conditions (Figure 3.9) indirectly indicates that the confined nematode receptacle may provide a micro-aerobic environment in which the bacterial cells may be in a semi-active or dormant state. Unfortunately, the microarray analysis on *rpoS* mutant done in this study was performed under aerobic condition in rich medium, which provided limited indications on how RpoS may function in its host.

Among the suppressed transporters identified in microarray analysis, the *oppBCDFA1A2* operon encodes an oligopeptide permease. *opp* mutants have no detectable defect in pathogenicity, but *oppB* mutant has a competitive advantage over wild type in colonizing the

nematode host (Orchard and Goodrich-Blair, 2004). This suggests that proper suppression of nutrient uptake within nematode host is necessary for bacterial colonization and persistence in mutualism, and RpoS is mediating such function by repressing various transporters for nutrient uptake. Another unexpected finding through microarray analysis is that RpoS negatively regulates the fatty acid degradation (*fad* genes) genes, indicating these genes may not be expressed during colonization of or persistence within the nematode host. This at first seems to contradict the LrhA microarray data in which *fad* genes were shown to be repressed by LrhA, and such repression was believed to be released during mutualism and activation of *fad* genes may help the bacterium to utilize host source nutrients. One explanation for this contradiction is that both RpoS and LrhA negatively regulate the function of fatty acid degradation during mutualism to ensure a balance between bacterial utilization of host nutrients and host survival. In this model, during mutualism while inactivation of LrhA allows expression of *fad* genes, induced higher level of RpoS ensures that the expression of those genes is kept below a certain level so the bacterium will not overdraw the nutrients from nematode host.

Through the qRT-PCR it demonstrated that RpoS is negatively regulated by both Lrp and NilR (Figure 3.2), and it does not affect the expression of *nil* genes (Figure 3.6) that are involved in nematode colonization initiation and host specificity (Cowles and Goodrich-Blair, 2004, 2006). The separation of RpoS from the regulation of mutualistic genes while itself being regulated by mutualistic regulator NilR and global regulator Lrp, and the relatively small RpoS regulon identified via microarray analysis indicate that RpoS, unlike LrhA and Lrp, is not a global transcription factor in *X. nematophila*, but instead has a limited regulon compared to the RpoS regulon of *E. coli* (Dong and Schellhorn, 2009; Figure 3.11).

In summary, our work demonstrates that *X. nematophila* Lrp negatively regulates the general stress response regulator RpoS in a mutualistic system and demonstrates that RpoS is, directly or indirectly, involved in the *X. nematophila* anti-ROS function which is essential for bacterial colonization in nematode hosts. We also provide indirect evidence that RpoS expression may be specifically induced in the nematode host to help bacterial cells adapt and survive in a stressful host environment. Further characterization of RpoS dependent gene expression under other conditions that better mimic the host environment may provide more knowledge on how RpoS affects microbe-host interactions in a mutualistic background. Also recent unpublished studies on mutualistic colonization initiation showed that prior to IJ development, a few ingested *X. nematophila* cells colonize the pharyngeal-intestinal valve, then move to and proliferate in the receptacle (J. Chaston and H. Goodrich-Blair, unpubl.). Thus determining at which stage of the mutualistic colonization the *rpoS* mutant fails to succeed will provide further indication on the mechanisms of the effects of RpoS on bacterial mutualism.

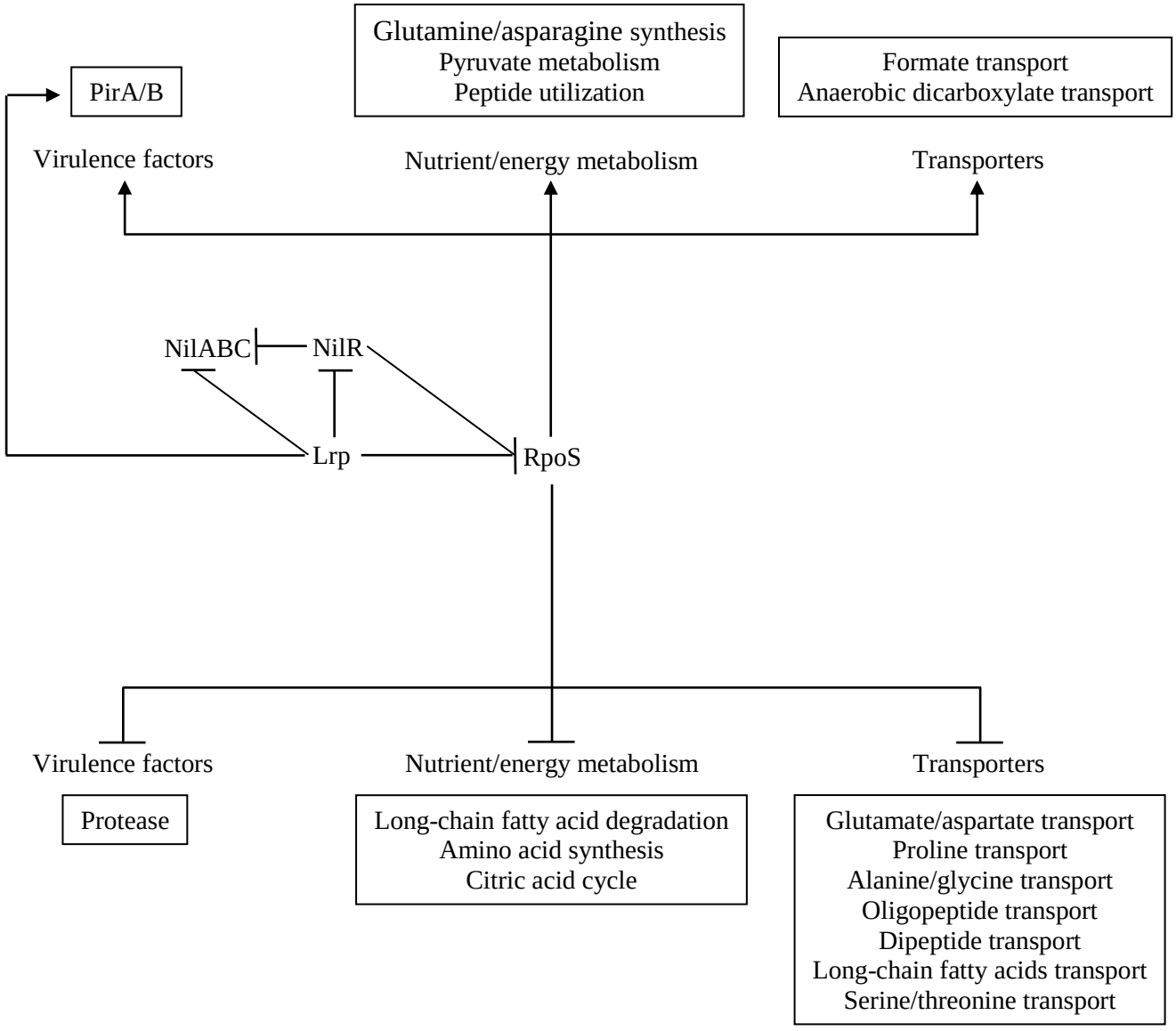

Figure 3.11. Summary of the effects of RpoS on cellular functions in *X. nematophila*.

MATERIALS AND METHODS

Bacterial and nematode strains, plasmids, and culture conditions

Table 3.2 lists strains and plasmids for this study. Unless specifically mentioned, *E.coli* were grown in LB broth or on LB plates at 37℃; *X. nematophila* were grown in LB broth or on LB plates supplemented with 0.1% pyruvate at 30℃ and kept in dark. Where appropriate, the following antibiotic concentrations were used: ampicillin, 150 μg/ml for *E.coli* and 50 μg/ml for *X. nematophila*; chloramphenicol, 30 μg/ml; erythromycin, 200 μg/ml; kanamycin, 50 μg/ml and streptomycin, 25 μg/ml. *E. coli* donor strain S17 (λ*pir*) or *Δasd* strain BW29427 was used to conjugate plasmids into *X. nematophila*. When necessary tri-parental conjugation using *E.coli* donor strain DH5α (λ*pir*) and helper *Δasd* strain BW3064 was performed to conjugate plasmids into *X. nematophila*. For growing BW29427 and BW3064, 100 μg/ml diaminopimelic acid (Sigma, St. Louis, MO) was added to the media. Nematodes were raised at 25^{o}C on bacterial lawns on lipid agar plates.

Molecular biological methods

Standard molecular biological methods were used in this study. Restriction enzymes (Promega, Madison, WI) and plasmid purification, gel extraction, and PCR purification kits (Zymo Research, Orange, CA) were used according to the manufacturers' recommendations. Constructs were sequenced at the UW-Madison Biotechnology Center using ABI Big Dye, version 3.1 (Applied Biosystems, Foster City, CA). PCR products for cloning were amplified using *Pfu* polymerase (Invitrogen, Carlsbad, CA). All other PCR amplifications were performed with

Ex*Taq* according to the manufacturer's directions (Takara, Otsu, Shiga, Japan). 0.5 μM of each appropriate primer was used for PCR amplifications. Table 3.3 lists the primers used in this study (Integrated DNA Technologies, Coralville, IA; UW-Madison Biotechnology Center, Madison, WI).

Microarray experiment

Bacteria cultures were grown overnight in 3 ml of LB supplemented with 0.1% pyruvate and appropriate antibiotics in culture tubes at 30^{o}C on roller, subcultured 1:100 into 30 ml of LB supplemented with 0.1% pyruvate and 50 μg/ml ampicilin in 125 ml glass flasks and grown for 12 hours to early stationary phase (OD 2-2.1) at 30^{o}C at 150 rpm on shaker. 1 ml of each culture was used to extract total RNA using Qiagen RNeasy Mini Kit, and on-column DNA digestion was performed using Qiagen RNase-Free DNase Set according to manufacturer's protocol (Qiagen, Valencia, CA). The RNA purity was tested by measuring 260 nm/280 nm and 260 nm/230 nm ratios in TE buffer and the values should be over 1.8. RNA integrity was verified by running 2 μg of RNA samples on 1% denaturing agarose gel. The samples were then submitted to Roche NimbleGen.for processing and microarray analysis.

Microarray data analysis

For each strain, the average signal strength of all random probes was used as the baseline signal level. The baseline signal strength value was subtracted from the average signal strength of each gene, and the resulted values were normalized using the values for *recA* gene across the strains. The normalized values were then used for comparison between different strains, and 2.5-fold

change in average signal strength was used as the cut-off level for determining the significance of changes in gene transcript levels.

Creation of *rpoS-lacZ* translational fusion strains. To create a translational *lacZ* fusion to the *rpoS* promoter, *gfp* containing *Xba*I-*BamH*I fragment from pQB163 was cloned into the *Xba*I and *BamH*I sites of pBCSK(+) to generate pBC*gfp*; the *nlpD'-rpoS*' fragment containing *rpoS* promoter was PCR amplified from wild-type *X. nematophila* genomic DNA with primers nlpDpro and rpoS2/3 harboring *Xba*I site and cloned into *Xba*I site of pBC*gfp* to create pBC*rpoS::gfp*; the *Kpn*I-*Xba*I fragment containing *rpoS::gfp* translational fusion was then cloned into Tn*7* vector pEVSCm digested with *Kpn*I and *Spe*I to give pTRSGII; promoterless *lacZ* fragment was isolated from pTOP*lacZ* as a *Kpn*I-*Nhe*I fragment and cloned into *Kpn*I and *Nhe*I sites of pTRSGII to give pTRSL. The plasmid was then conjugated from DH5α (λ*pir*) into *X. nematophila* wild-type strain HGB007 and *lrp* mutant HGB1059 to introduce a chromosome copy of the *lacZ-rpoS* translational fusion at the Tn*7* site.

β-galactosidase assays. Fresh overnight *X. nematophila* cultures were subcultured 1:100 into 40 ml LB broth in 125 ml flasks and shaked at 150 rpm at 30^{o}C in the dark. Samples were taken over the time and β-galactosidase assays were performed as following: 500 μl (OD_{600}<0.6) or 50 μl (OD_{600}>0.6) of each sample was added to Z-buffer to a final volume of 1 ml, 40 μl of chloroform was added and mixture was vortexed for 10 seconds to break the cells, 200 μl of freshly made 4 mg/ml Ortho-Nitrophenyl-β-Galactoside (ONPG) in Z-buffer was added to each sample and incubated at 25^{o}C, reaction was stopped by adding 500 μl 1 M Na_2CO_3 when

reaction turned yellow, OD_{420} and OD_{550} of the stopped reaction were measured by spectrophotometer, β-galactosidase activities in Miller units were calculated as 1000 X [OD_{420}-(1.75 X OD_{550})]/(Volume X Time X OD_{600}). For assays done in minimal medium, overnight cultures were washed and resuspended with minimal medium before subculturing. To create ion-deplete condition, deferoxamine (Sigma, St. Louis, MO) was added to LB at a concentration of 25 mM. 500 mM of ferrous sulphate was used to restore ion-replete condition when necessary. All experiments were done in duplicates.

qRT-PCR analysis

Total RNA from wild-type and mutant *X. nematophila* strains were isolated at OD_{600} 2.1~2.2 using Qiagen RNeasy Mini Kit, treated with RQ1 DNase I (Promega, Madison, WI), and used to make cDNA with random hexamer primers (Integrated DNA Technologies, Coralville, IA) and AMV Reverse Transcriptase (Promega, Madison, WI). qRT-PCR reactions were performed in duplicate in 20 μl volume with iQ™ SYBR® Green Supermix (Bio-Rad, Hercules, CA), cDNA template and appropriate primers. Reactions were carried out with a two-step cycling protocol on a Bio-Rad iCycler and results were analyzed with Bio-Rad iCycler iQ™ software. qRT-PCR primers for individual genes are listed in table 2.2. Reactions using water and DNase-treated RNA as template instead of cDNA were performed as negative controls. As expected, no product was detected in negative control samples. Cycle threshold results for each sample were normalized using *recA* levels and the average expression levels in wild-type were designated as 100%.

Nematode colonization assays

Fresh overnight *X. nematophila* cultures were diluted 1:10 in LB, cell density was normalized using OD600, and diluted cultures were plated on three replicate lipid agar plates per strain per experiment. The plates were incubated at 30℃ in the dark for 24 hours to allow bacterial lawns to form. The nematode eggs were then added on the bacterial lawns and the plates were incubated in the dark at 25℃ for 7 days before transferred into water trap. IJs were collected 14 days after eggs were added to the plates, surface-sterilized and stored in sterile water. To measure the average number of colonized bacterial cells per IJ, IJ concentrations were adjusted to 20,000 IJs/ml, 1 ml of each IJ sample was mixed with 1 ml of LB broth and sonicated for 1 minute in a 10 ml glass culture tube using Branson 1510 water bath sonicator to release bacterial cells from IJs. Sonicated samples were then diluted and plated on LB plates supplemented with 0.1% pyruvate and appropriate antibiotics and incubated in the dark at 30℃ for 24 hours. In each experiment, the average wild-type value was defined as 100% colonization. All values were normalized to the designated wild-type value.

UV exposure tests

Fresh overnight *X. nematophila* cultures were subcultured 1:100 into LB and grown for desired length of time to exponential or stationary phases. Cell densities were measured by spectrophotometer and 1 OD of each culture was span down to remove the medium. Cells were washed twice with PBS and re-suspended in PBS. Serial dilutions of the cells were made using PBS and 10 μl of each dilution was plated on LB plate and completed dried. The plates were then exposed to UV radiation on a UV crosslinker for desired length of time and incubated over

night at 30^{o}C in the dark. Colony forming units per plate were accounted and percentages of viability were calculated.

Statistics

Unless otherwise specified, experiments were done twice with 2 biological replicates for each experiment. Statistics were done with Student's T-Test for single comparison, and with One-Way ANOVA for multi-comparisons. For qRT-PCR, statistics were done using arbitrary RNA units, and the results were presented as percentage of wild-type levels for comparison.

Table 3.2. List of strains and plasmids.

Strain or plasmid	Description	Reference
HGB007	Amp^r; *X. nematophila* wild-type ATCC 19061	ATCC in 1996; Vivas and Goodrich-Blair, 2001
HGB139	Amp^r; Cm^r; HGB007 pBCSK(+)	Vivas and Goodrich-Blair, 2001
HGB140	Amp^r; Cm^r; HGB007 pBCrpoS	Vivas and Goodrich-Blair, 2001
HGB141	Amp^r; Cm^r; Kan^r; HGB151, pBCSK(+)	Vivas and Goodrich-Blair, 2001
HGB142	Amp^r; Cm^r; Kan^r; HGB151, pBCrpoS	Vivas and Goodrich-Blair, 2001
HGB151	Amp^r; Kan^r; HGB007 *rpoS3::kan*	Vivas and Goodrich-Blair, 2001
HGB763	Amp^r; Erm ^{r};HGB007 *att*Tn*7::*Tn*7*	E.I. Vivas, University of Wisconsin-Madison
HGB1936	Amp^r;Erm^r; HGB007 *att*Tn*7*::Tn*7*/*katE*	This study
HGB764	Amp^r; Kan^r; Erm ^{r}; HGB151 *att*Tn*7*::Tn*7*	E.I. Vivas, University of Wisconsin-Madison
HGB1937	Amp^r;Kan^r;Erm^r; HG151 *att*Tn*7*::Tn*7/katE*	
HGB800	Amp^r; *X. nematophila* wild-type ATCC	ATCC in 2003;

	19061	Chaston *et al*., 2011
HGB1059	Amp^r; Kan^r; HGB800 *lrp-2::kan*	Cowles *et al*., 2006; 2007
HGB1103	Amp^r; Kan^r; HGB800 *ΔnilR17::kan*	Cowles and Goodrich-Blair, 2006
HGB1262	Cm^r; Kan^r; *E. coli* BW29427 *Δasd*; donor strain for conjugations	B. Wanner
HGB2012	Amp^r;Erm^r; HGB800 *att*Tn*7*::Tn*7/rpoS'-'lacZ*	This study
HGB2013	Amp^r; Erm^r; HGB800 *att*Tn*7*::Tn*7*	This study
HGB2014	Amp^r; Kan^r; Erm^r; HGB1059 *lrp-2::kan*; *att*Tn*7*::Tn*7/rpoS'-'lacZ*	This study
HGB2015	Amp^r; Kan^r; Erm^r; HGB1059 *lrp-2::kan*; *att*Tn*7*::Tn*7*	This study
DH5α (λ*pir*)	*E. coli* general cloning and donor strain	Sambrook *et al.*, 1989
S17-1 (λ*pir*)	Str^r; *E. coli* donor strain for conjugations	Simon *et al.*, 1983
BW3064	Amp^r; *E. coli Δasd*; pUX-BF13; helper strain for conjugations	B. Wanner
pKNG101	Str^r; *oriR6K* suicide vector	Kaniga *et al.*, 1991
pBCSK(+)	Cm^r; Kan^r	Stratagene
pBC*gfp*	Cm^r; Kan^r; pBCSK(+) with *gfp* gene	E.I. Vivas, University of Wisconsin-Madison
pBC*rpoS::gfp*	Cm^r; Kan^r; pBCSK(+) with *rpoS::gfp*	E.I. Vivas, University

	translational fusion	of Wisconsin-Madison
pEVSCm	Derivative of pEVS107; Tn*7* transposon vector	Herbert *et al*., 2007
pTRSGII	Str^r; Cm^r; Erm^r; pEVSCm with a *X. nematophila rpoS::gfp* translational fusion	This study
pTOP*lacZ*	Source of promoterless *lacZ*	This study
pTRSL	Str^r; Cm^r; Erm^r; pEVSCm with a *X. nematophila rpoS'-'lacZ* translational fusion	This study
pUX-BF13	Amp^r; Triparental conjugation helper plasmid	Bao *et al*., 1991
pQB163	Source of rsGFP	Q-Biogene

Table 3.3. List of primers

Primer	Sequences 5' to 3'	Use
nilCFwd1 qPCR	AGCTCTCGCACTGGTACTTTCTG	qRT-PCR *nilC*
nilCRev1 qPCR	CCAGGCTGCTTACCTGTTTCA	qRT-PCR *nilC*
nilRFwd1 qPCR	TGGACAACGCATTCAGACCA	qRT-PCR *nilR*
nilRRev1 qPCR	GAGTTGTTGCTGACTGATGCCA	qRT-PCR *nilR*
sodBFwd1 qPCR	TGCCAAAGATGCCTTGGAAC	qRT-PCR *sodB*
sodBRev1 qPCR	GTAGGCATTGTGGTGTTTGCC	qRT-PCR *sodB*
ahpCFwd1 qPCR	ATCGCTTTCGATCACCGCT	qRT-PCR *ahpC*
ahpCRev1 qPCR	TTACGCCATGCGTTGTGAAC	qRT-PCR *ahpC*
dpsCFwd1 qPCR	TCGACCTGTCTATGGTAACGAAAC	qRT-PCR *dpsC*
dpsCRev1 qPCR	GTGCTGCGAAAAGTATCCAGC	qRT-PCR *dpsC*
rpoSFwd1 qPCR	ACCCGCACAATTCGTCTGC	qRT-PCR *rpoS*
rpoSRev1 qPCR	CCGCAATTTCTTCAACCGTG	qRT-PCR *rpoS*
lrpFwd qPCR	GCGAGTAGGTCTGTCACCAACA	qRT-PCR *lrp*
lrpRev qPCR	ACATCTGCTGCACCACGATTC	qRT-PCR *lrp*
cpxPFwd1 qPCR	CTGAACAACAGCGCCAGCA	qRT-PCR *cpxR*
cpxPRev1 qPCR	TTCTGACGTTCAACCCGCAT	qRT-PCR *cpxR*

REFERENCES

Battesti A, Majdalani N, Gottesman S. 2011. The RpoS-mediated general stress response in *Escherichia coli*. Annu Rev Microbiol. 65:189-213

Bird, AF and Akhurst RJ. 1983. The nature of the intestinal vesicle in nematodes of the family *Steinernematidae*. Int. J. Parasitol. 13:599–606

Chávez V, Mohri-Shiomi A, Maadani A, Vega LA, Garsin DA. 2007. Oxidative stress enzymes are required for DAF-16-mediated immunity due to generation of reactive oxygen species by *Caenorhabditis elegans*. Genetics. 176(3):1567-77

Chaston JM, Suen G, Tucker SL, Andersen AW, Bhasin A, Bode E, Bode HB, Brachmann AO, Cowles CE, Cowles KN, Darby C, de León L, Drace K, Du Z, Givaudan A, Herbert Tran EE, Jewell KA, Knack JJ, Krasomil-Osterfeld KC, Kukor R, Lanois A, Latreille P, Leimgruber NK, Lipke CM, Liu R, Lu X, Martens EC, Marri PR, Médigue C, Menard ML, Miller NM, Morales-Soto N, Norton S, Ogier JC, Orchard SS, Park D, Park Y, Qurollo BA, Sugar DR, Richards GR, Rouy Z, Slominski B, Slominski K, Snyder H, Tjaden BC, van der Hoeven R, Welch RD, Wheeler C, Xiang B, Barbazuk B, Gaudriault S, Goodner B, Slater SC, Forst S, Goldman BS, Goodrich-Blair H. 2011. The entomopathogenic bacterial endosymbionts *Xenorhabdus* and *Photorhabdus*: convergent lifestyles from divergent genomes. PLoS ONE 6(11):e27909

Cowles CE, Goodrich-Blair H. 2004. Characterization of a lipoprotein, NilC, required by *Xenorhabdus nematophila* for mutualism with its nematode host. Mol. Microbiol. 54(2):464-77

Cowles CE, Goodrich-Blair H. 2006. *nilR* is necessary for co-ordinate repression of *Xenorhabdus nematophila* mutualism genes. Mol. Microbiol. 62(3):760-71

Dong T, Schellhorn HE. 2009. Control of RpoS in global gene expression of *Escherichia coli* in minimal media. Mol Genet Genomics. 281(1):19-33

Eisenstark A, Calcutt MJ, Becker-Hapak M, Ivanova A. 1996. Role of *Escherichia coli rpoS* and associated genes in defense against oxidative damage. Free Radic Biol Med. 21(7):975-93

Herbert EE, Cowles KN, Goodrich-Blair H. 2007. CpxRA Regulates Mutualism and Pathogenesis in *Xenorhabdus nematophila*. Appl Environ Microbiol. 73(24): 7826–7836.

Fones H, Preston GM. 2012. Reactive oxygen and oxidative stress tolerance in plant pathogenic *Pseudomonas*. FEMS Microbiol Lett. 327(1):1-8

Forst S, Dowds B, Boemare N, Stackebrandt E. 1997. *Xenorhabdus* and *Photorhabdus* spp.: bugs that kill bugs. Annu Rev Microbiol. 51:47-72

Goodrich-Blair H, Clarke DJ. 2007. Mutualism and pathogenesis in *Xenorhabdus* and *Photorhabdus*: two roads to the same destination. Mol. Microbiol. 64(2):260-8

Hengge-Aronis R. 1993. Survival of hunger and stress: the role of *rpoS* in early stationary phase gene regulation in *E. coli*. Cell. 72(2):165-8

Herbert EE, Goodrich-Blair H. 2007. Friend and foe: the two faces of *Xenorhabdus nematophila*. Nat. Rev. Microbiol. 5(8):634-46

Hirsch M, Elliott T. 2005. Stationary-phase regulation of RpoS translation in *Escherichia coli*. J Bacteriol. 187(21):7204-13

Imlay JA, Linn S. 1988. DNA damage and oxygen radical toxicity. Science 240:1302–1309

Imlay JA. 2006. Iron-sulphur clusters and the problem with oxygen. Mol. Microbiol. 59:1073–1082

King T, Ferenci T. 2005. Divergent roles of RpoS in Escherichia coli under aerobic and anaerobic conditions. FEMS Microbiol Lett. 244(2):323-7.

Kozliak EI, Fuchs JA, Guilloton MB, Anderson PM. 1995. Role of bicarbonate/CO2 in the inhibition of Escherichia coli growth by cyanate. J Bacteriol. 177(11):3213-9.

Lloyd DR, Carmichael PL, Phillips DH. 1998. Comparison of the formation of 8-hydroxy-2′-deoxyguanosine and single- and double-strand breaks in DNA mediated by Fenton reactions. Chem. Res. Toxicol. 11:420–427

Loewen PC, Triggs BL. 1984. Genetic mapping of *katF*, a locus that with *katE* affects the synthesis of a second catalase species in *Escherichia coli*. J Bacteriol 160:668–675

Orchard SS, Goodrich-Blair H. 2004. Identification and functional characterization of a *Xenorhabdus nematophila* oligopeptide permease. Appl. Environ. Microbiol. 70(9):5621-7

Orchard SS, Goodrich-Blair H. 2005. Pyrimidine nucleoside salvage confers an advantage to *Xenorhabdus nematophila* in its host interactions. Appl. Environ. Microbiol. 71(10):6254-9

Ruby, EG, McFall-Ngai, MJ. 1999. Oxygen-utilizing reactions and symbiotic colonization of the squid light organ by *Vibrio fischeri*. Trends Microbiol. 7(10):414-20

Sambrook J, Fritsch EF, Maniatis T. 1989. Molecular cloning: a laboratory manual, 2nd ed. Cold Spring Harbor Laboratory Press, Cold Spring Harbor, NY

Sammartano LJ, Tuveson RW, Davenport R. 1986. Control of sensitivity to inactivation by H_2O_2 and broad-spectrum near-UV radiation by the *Escherichia coli katF* locus. J Bacteriol 168:13–21

Simon R, Priefer U, Pu ̈hler A. 1983. A broad host range mobilization system for *in vivo* genetic engineering: transposon mutagenesis in gram negative bacteria. Biotechnology 1:784–791

Soto MJ, Dom ́nguez-Ferreras A, P ́rez-Mendoza D, Sanju ́n J, Olivares J. 2009. Mutualism versus pathogenesis: the give-and-take in plant-bacteria interactions. Cell Microbiol.

11(3):381-8

Tarassova K, Tegova R, Tover A, Teras R, Tark M, Saumaa S, Kivisaar M. 2009. Elevated mutation frequency in surviving populations of carbon-starved *rpoS*-deficient *Pseudomonas putida* is caused by reduced expression of superoxide dismutase and catalase. J Bacteriol. 191(11):3604-14

Touati E, Dassa E, Boquet PL. 1986. Pleiotropic mutations in *appR* reduce pH 2.5 acid phosphatase expression and restore succinate utilisation in CRP-deficient strains of *Escherichia coli*. Mol Gen Genet 202:257–264

Tuveson RW. 1981. The interaction of a gene (*nur*) controlling near-UV sensitivity and the polA1 gene in strains of *E. coli* K12. Photochem Photobiol. 33(6):919-23

Vivas EI, Goodrich-Blair H. 2001. *Xenorhabdus nematophilus* as a model for host-bacterium interactions*: rpoS* is necessary for mutualism with nematodes. J Bacteriol. 183(16):4687-93

Xu J and Hurlbert RE. 1990. Toxicity of irradiated media for *Xenorhabdus* spp. Appl Environ Microbiol. 56(3):815-8.

CHAPTER 4

The *Xenorhabdus nematophila* CRISPR-Cas system affects bacterial colonization of the nematode *Steinernema carpocapsae*

All the works described in this chapter were performed by me with the support and guidance from Dr. Heidi Goodrich-Blair.

INTRODUCTION

The Gram-negative bacterium *Xenorhabdus nematophila* mutualistically associates with the entomopathogenic nematode *Steinernema carpocapsae*. A monoculture of *X. nematophila* colonizes the intestine of an infective juvenile (IJ) stage of *S. carpocapsae*, and this nematode-bacterium complex invades insect hosts, which are rapidly killed after bacterial release from the nematode triggered by unknown factors in insect blood (Forst *et al*., 1997; Snyder *et al*., 2007). Within the insect cadaver the nematode reproduces through juvenile and adult stages with the assistance from the bacterial symbiont. When nutrients derived from the insect cadaver are depleted, the nematodes re-associate with the symbiotic bacteria and develop into IJs that exit the insect cadaver to search for a new host (Bird and Akhurst, 1983). In nature, *X. nematophila* cannot live without insect or nematode hosts and require the nematode for transmission between insects (Chaston *et al*., 2011; Herbert and Goodrich-Blair, 2007). Previous studies have shown that *X. nematophila* exists in two phenotypically variant forms termed primary and secondary (Volgyi *et al*., 1998; Forst and Clarke, 2002). Although it varies by strain, in general both forms are virulent to insect hosts and are also capable of colonizing the nematode host. Although the primary form bacterium is the typical form isolated from *S. carpocapsae* nematodes in nature, stable secondary form of the *X. nematophila* generated by prolonged stationary-phase incubation and multiple passages has a competitive advantage in association with nematode host when co-injected into insect hosts with primary form bacterium (Sicard *et al*., 2005). But in the tests using unstable reversible secondary form *X. nematophila* cells isolated from colonized IJs were predominantly in the secondary form (C.E. Cowles, Ph.D. thesis, UW-Madison). This difference of primary and secondary forms in competing for colonization indicates that the phenotypic

variation of *X. nematophila* might be a mechanism used by the bacterium for adapting in different hosts.

To date, many endeavors have been made to understand the mechanisms underlying *X. nematophila* phenotypic variation and the regulation of its pathogenic and mutualistic functions. Studies have shown that Lrp, a leucine responsive regulatory protein, serves as a global regulator affecting mutualism, pathogenesis and phenotypic variation. An *lrp* mutant displays attenuated virulence in *Manduca sexta* insects and a defect in colonization of the nematode host (Cowles *et al*., 2007). Microarray analysis of gene expression profiles of the *lrp* mutant revealed that in addition to genes known or predicted to be involved in bacterial virulence, mutualism and phenotypic variation, Lrp also regulates expression of CRISPR associated sequences (*cas*) genes. (Chapter 2) that in some organisms function in adaptive bacterial defense of invading bacteriophages and plasmids (Bhaya *et al*., 2011). The CRISPR-Cas system (CCS) is widely distributed among bacteria and archaea and requires the presence of conserved repeat sequences separated by fixed-size spacer sequences known as clustered regularly interspaced short palindromic repeats (CRISPR). Certain spacer sequences within the CRISPR arrays exhibit identity to phage or other mobile DNA elements (termed proto-spacers) and can provide resistance to phage infection and silencing of exogenous plasmids. CRISPR arrays are transcribed as long RNAs that are processed, but virtue of Cas proteins, into short (~50-80 nt) CRISPR RNA (crRNA) oligonucleotides that in conjunction with Cas proteins target proto-spacer containing DNA or RNA molecules resulting in silencing and, in some case, degradation of the target molecule. Although *cas* gene families are very diverse, CCS can be generally divided into three types based on their functional components, namely Types I-III. All three CCS types encode the *cas1* and *cas2* core genes but are differentiated by the components of other core

cas genes (Bhaya *et al*., 2011). The CCS identified in *X. nematophila* through genome sequencing is compositionally and structurally similar to the Type I system of *E. coli* (Figure 4.1), which encodes five *cas* genes (*casABCDE*). This similarity indicates similar functions and working mechanisms of *X. nematophila* and *E. coli* CCS. In *E. coli*, the *casABCDE* products form a complex called Cascade, which mediates both CRISPR processing and proto-spacer targeting by the crRNAs. CasE, a putative RNA binding protein, is the active subunit responsible for processing of the large CRISPR transcript into crRNAs while Cas3-chaperoned interactions between the crRNA and target phage/plasmid genes result in target gene silencing. Removal of *casE* or *cas3* alone causes a severe defect in anti-phage functions in *E. coli* (Pougach *et al*., 2010; Bhaya *et al*., 2011; Brouns *et al*., 2008). In *X. nematophila*, a putative CRISPR locus called *nilD* was identified in a screen for transposon mutants defective in colonization (Heungens *et al*., 2002). The *nilD* RNA has no significant similarity to other sequences in the *X. nematophila* genome sequence, nor in the public sequence database (A. Andersen, J. Veesenmeyer, and H. Goodrich-Blair, unpubl; Heungens *et al*., 2002), and while *nilD* mutation causes a nematode host colonization defect it has no effect on virulence in insects or bacterial survival (Heungens *et al*., 2002). *nilD* is expressed as a ~58-nt small RNA with CRISPR-like characteristics (A. Andersen and H. Goodrich-Blair, unpubl.). However, no evidence to date has shown that NilD RNA is a component of the CCS.

While many spacer sequences have identity to phage genes or other mobile DNA elements, others exhibit identity to endogenously encoded sequences, implicating CCS in cellular gene regulation (Aklujkar and Lovley, 2010). These potential endogenous targets can be recognized by crRNA-Cas complexes not only by identity with the CRISPR spacer sequence, but also by their flanking repeat regions, which are different from those of the spacers for exogenous

targets (Bhaya *et al*., 2011). Recognition of endogenous genomic targets by CSS is thought to lead to gene expression changes. For example, an *E. coli*-type CRISPR spacer within *Pelobacter carbinolicus* was identified that matches a region of the endogenous histidinyl-tRNA synthetase gene, *hisS*. The study demonstrated an evolutionary trend within *Pelobacter* towards either the loss or mutation of genes encoding histidine-rich proteins or proteins with closely spaced histidine residues, indicating that the presence of CRISPR spacers against the histidinyl tRNA synthetase decreases its expression or function (Aklujkar and Lovley, 2010). In *X. nematophila*, two genes with proto-spacers (32-bp regions of 100% identity to their respective spacers) were identified via genome sequencing: an ORF (XNC1_3681) with similarity to putative plasmid-related proteins and *xptE1*, a gene predicted to encode a subunit of an insecticidal toxin and which is found adjacent to a phage-like region (H. Goodrich-Blair, unpubl.). In both cases the predicted mature crRNA spacer sequence is complementary to the target mRNA, which indicates CCS may be involved in regulating endogenous gene expression in *X. nematophila*.

CCS have been suggested to play a role in other cellular processes including chromosome partitioning, DNA repair, chromosomal rearrangements and, in *Myxococcus xanthus*, the formation of fruiting bodies (Viswanathan *et al*., 2007; Babu *et al*., 2011; Bhaya *et al*., 2011), indicating they play diverse roles in bacterial physiology. However, the mechanisms by which CCS mediate these diverse functions, and as addressed by this study, whether or not CCS affects bacterial virulence, mutualism and phenotypic variation in *X. nematophila* remains to be elucidated.

Here we demonstrate that *X. nematophila cas3* or *casE* mutants have wild type virulence in insects, but have a competitive disadvantage when mutualistically colonizing the nematode

host. CCS also impacts endogenous gene expression in *X. nematophila* and a lower transcript level of CCS target gene *Xn3631* was observed in secondary form of the bacterium.

A.

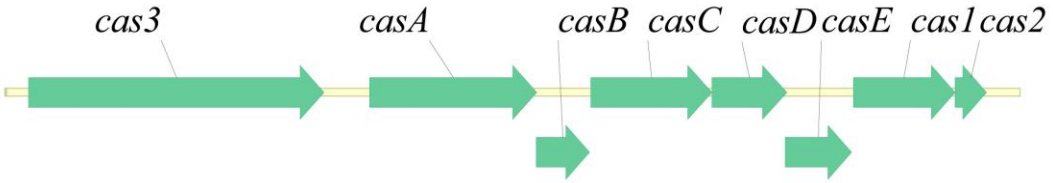

B.

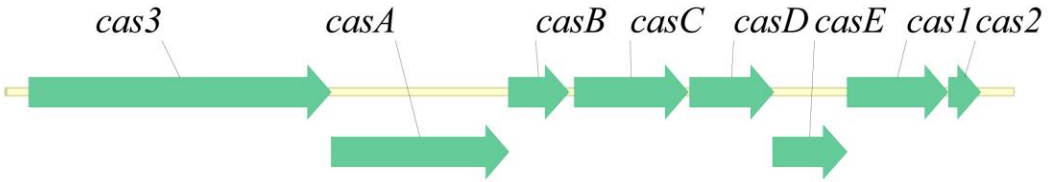

Figure 4.1. *cas* operon in *E.coli* (A) and *X. nematophila* (B). Lower arrows indicate genes overlapping with adjacent gene(s).

RESULTS

Lrp regulates transcript levels of *cas* genes.

Microarray analysis of *lrp* and *lrhA* mutants revealed that the global regulator Lrp suppresses *cas* gene expression while the transcription factor LrhA, which is positively regulated by Lrp, has no effect on transcript levels of *cas* genes (Figure 4.2). To confirm Lrp regulation of *cas* genes and test if *cas* gene expression is also affected by the colonization gene regulator NilR, which is a synergistic repressor with Lrp of colonization genes and is itself negatively regulated by Lrp, qRT-PCR was performed to measure *cas3* transcript levels in *lrp* and *nilR* mutants. The test showed that *lrp* and *nilR* mutants each had elevated *cas3* mRNA levels relative to wild type (with *lrp* mutants having twice as much as *nilR* mutants) indicating both transcription factors negatively regulate *cas3* gene expression (Figure 4.3). Other genes negatively regulated by both Lrp and NilR (e.g. *rpoS*, *nilA*, *nilB*, *nilC*) are required for colonization of nematodes (Chapter 3; Vivas and Goodrich-Blair, 2001; Heungens *et al.*, 2002; Cowles and Goodrich-Blair, 2006), raising the possibility that the CCS system is as well.

cas3 and *casE* mutants are defective in competitive bacterial colonization both *in vitro* and *in vivo* in *Galleria mellonella* insects.

To test if the Cas system is involved in colonization of the nematode, colonization competition assays were performed between wild type *X. nematophila* and *cas* insertion-deletion mutants *in vitro* on bacterial lawns or *in vivo* inside *Galleria mellonella* insects. The assay showed that wild-type bacteria and *cas* mutants alone colonized nematode host at a similar level, indicating that unlike the *rpoS* and *nil* genes, the *cas* genes are not essential for colonization.

However, in competition with wild type *X. nematophila in vitro*, the *cas3* mutant represented 16% of the total bacterial population isolated from IJs, and the *casE* mutant only represented 3% of the colonizing bacteria (Figure 4.4). When competing with wild type *X. nematophila in vivo* in *Galleria mellonella* larvae, both *cas3* and *casE* mutants were outcompeted by wild-type bacteria and no mutants were found in the bacterial population isolated from IJs. Also, the *casE* mutant alone colonized nematode IJs at a lower level in the insect host compared with wild-type bacteria while the *cas3* mutant alone had no significant defect in nematode colonization (Figure 4.5), suggesting the *casE* defect is more severe. The *in vivo* competitive colonization defect of the *casE* mutant, but not the *cas3* mtuant, was partially rescued by the presence of *casE* or *cas3* respectively in the context of their native predicted promoter regions (Figure 4.6).

Effects of phenotypic variation and CCS on endogenous gene expression.

We tested if CCS affects expression of *X. nematophila* genes involved in virulence or mutualism, and whether the effects, if any, are influenced by phenotypic variation. Transcript levels, in primary and secondary forms of *X. nematophila* wild type and *cas3* mutant, of 8 genes were monitored by qRT-PCR. *rpoS* and *nilC* were chosen because like *cas3*, they are negatively regulated by NilR and Lrp and are involved in colonization. *flgF, Xn3681,* and *xptE1* were chosen because they each contain a proto-spacer sequence. *xptA1* was included because, like *xptE1* it is predicted to encode a subunit of the Tc toxin (Sergeant *et al*., 2006). Finally, we monitored expression of *cas3* itself. Although not all comparisons were statistically significant, six of the tested genes could be categorized into two general expression trends: those with elevated transcript levels in secondary form relative to primary in wild type but not the *cas3* mutant (*rpoS, nilC,* and *xptE1*) and those with lower transcript levels in secondary form relative

to primary form in wild type but not the *cas3* mutant (*nilR, Xn3681,* and *flgF*) (Figure 4.7). These trends suggest that Cas3 is necessary for increased or decreased expression of each set of genes respectively, in secondary form cells relative to primary form cells. Consistent with this idea, *nilR* and *nilC* expression is inversely correlated, and NilR encodes a repressor of *nilC* expression. While *xptE1*, one of the two potential endogenous targets of CCS, had no statistically significant differences in transcript levels among strains, it did show a trend of being slightly lower in secondary *cas3* mutant. More strikingly, transcript levels of another potential CCS target, *XNC1_3681*, were significantly lower in secondary form in a *cas3*-dependent manner. Also noteworthy is the finding that the primary form *cas3* mutant showed significantly lower *rpoS* and *nilC* transcript levels than primary form wild type, indicating that *cas3* has a positive influence the expression or stability of these transcripts even in primary form cells. (Figure 4.7).

cas3 and _casE_ mutations do not affect _lrp_ phenotype

To test if the Cas system affects other aspects of *X. nematophila* physiology a series of phenotypic tests were performed. Since *lrp* mutants are similar to secondary form cells, Lrp negatively regulates *cas* genes (Figure 4.2) and phenotypic differences in gene expression are *cas3*-dependent (Figure 4.7) we determined if *cas3* is necessary for any Lrp-dependent secondary form traits. While the *lrp* mutant was defective as expected in motility and lipase, protease, antibiotic, and hemolysin activities, *cas* mutants had no apparent defect in these traits (Table 4.1), indicating *cas3* and *casE* are not necessary for cells to exhibit primary form phenotypes. To determine if any *lrp* mutant phenotypes are rescued by the absence of *cas*, we constructed and examined the phenotypes of *lrp cas* double mutants. Except for antibiotic activity against *Micrococcus luteus* all phenotypes examined, including virulence against

Manduca sexta insects were the same as the *lrp* single mutant. Some antibiotic activity against *E. coli* was observed in the *casE lrp* double mutant, indicating *casE* may be partially responsible for the lack of antibiotic activity in the *lrp* mutant.

Cas3 affects phenotypic variation.

Given the links between *cas* genes and phenotypic variation noted above, we tested if *cas3* influences the switch between primary and secondary forms of the bacteria. The ratio of primary and secondary form cells was measured for various bacterial strains after overnight culture. While the primary form of wild type, *cas3* mutant and a *nilR* mutant behaved similarly with very few cells converting to secondary form, the secondary form *cas3* mutant had a higher level of conversion to primary form compared to secondary wild type. Also, introduction of the *cas3* mutation into an *lrp* mutant, which is locked in a secondary form like state, allowed a small portion (4%) of the double mutant to switch to a primary form like state (Table 4.2). These data indicate that *cas3* contributes to the stability of the secondary form phenotype.

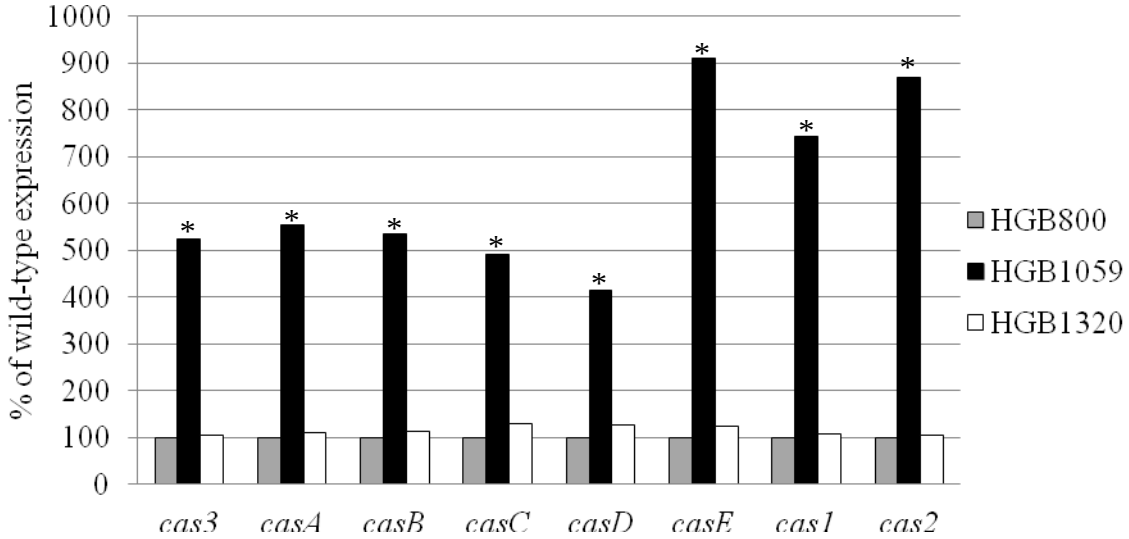

Figure 4.2. Microarray detection of transcript levels of *cas* genes in wild type *X. nematophila* (HGB800), an *lrp* mutant (HGB1059), and an *lrhA* mutant (HGB1320). Transcript levels are shown as percent levels compared to wild-type.

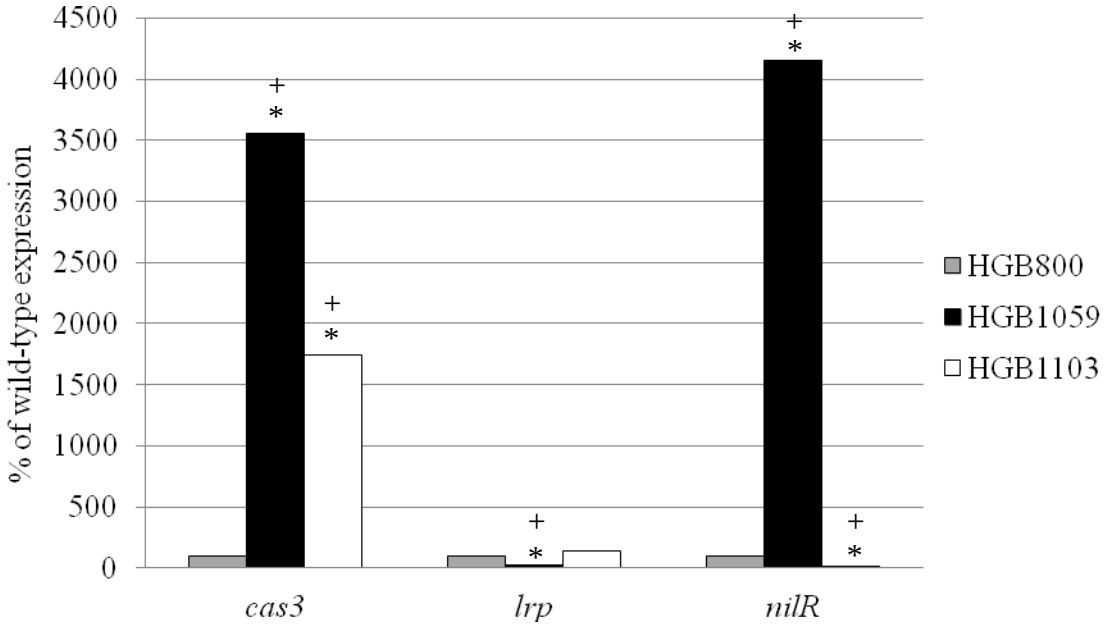

Figure 4.3. Effects of *lrp* and *nilR* mutations on *cas3* transcript levels. Transcript levels in wild type *X. nematophila* (HGB800), an *lrp* mutant (HGB1059), and a *nilR* mutant (HGB1103) are shown as percent levels compared to wild-type. Asterisks indicate statistically significant differences from wild-type levels. Pluses indicate statistically significant differences between *lrp* and *nilR* mutants. $P<0.05$. Statistics were done by One-Way ANOVA. Data are from two biological replicates from each of two experiments.

Table 4.1. Phenotypic assays of *cas3*, *casE*, and *lrp* mutants.

	HGB800 (Wild-type)	HGB1577 (*cas3*)	HGB1694 (*casE*)	HGB1059 (*lrp*)	HGB2000 (*cas3 lrp*)	HGB2001 (*casE lrp*)
Lipase	+	+	+	-	-	-
Antibiotics (*M. luteus*)	++	++	++	-	-	+
Antibiotics (*B. subtilis*)	++	++	++	+	+	+
Motility	++	++	++	+/-	+/-	+/-
Hemolysin	++	++	++	-	-	-
Insect killing	+	+	+	N/A	N/A	N/A

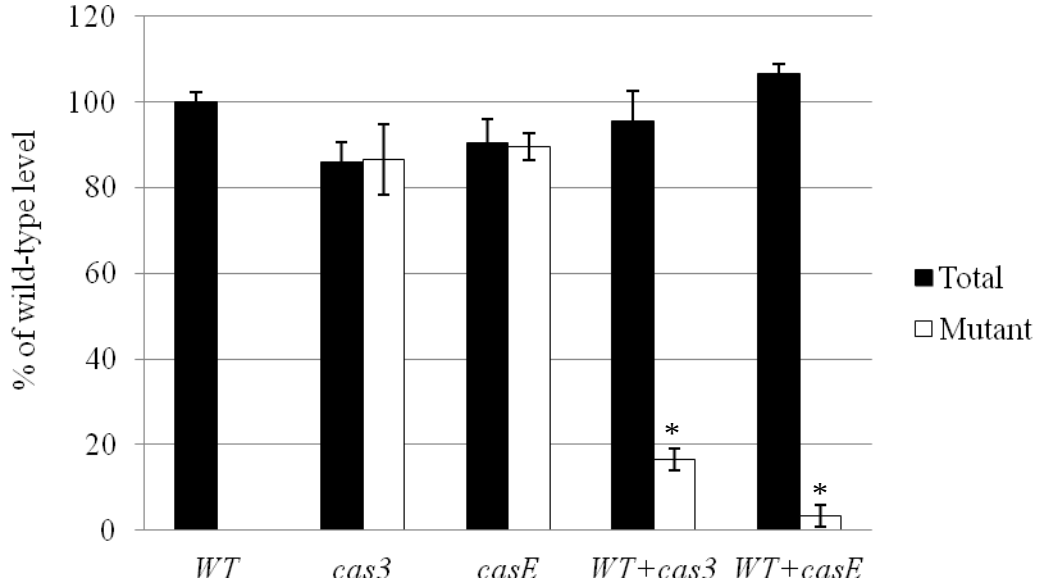

Figure 4.4. Competitive colonization phenotype of *cas* mutants in *in vitro* cultivation conditions. Colonization levels are shown as percent wild type levels for wild type (HGB800), the *cas3* mutant (HGB1577), and the *casE* mutant (HGB1694) cultivated with nematodes individually or in combination. Black and white bars show total and mutant colonization levels respectively, compared to wild type. Asterisks indicate statistically significant differences from wild-type levels. $P<0.05$. Statistics were done by Student's T-Test. Data are from two biological replicates from each of two experiments. Errors bars reprenent +/- SD.

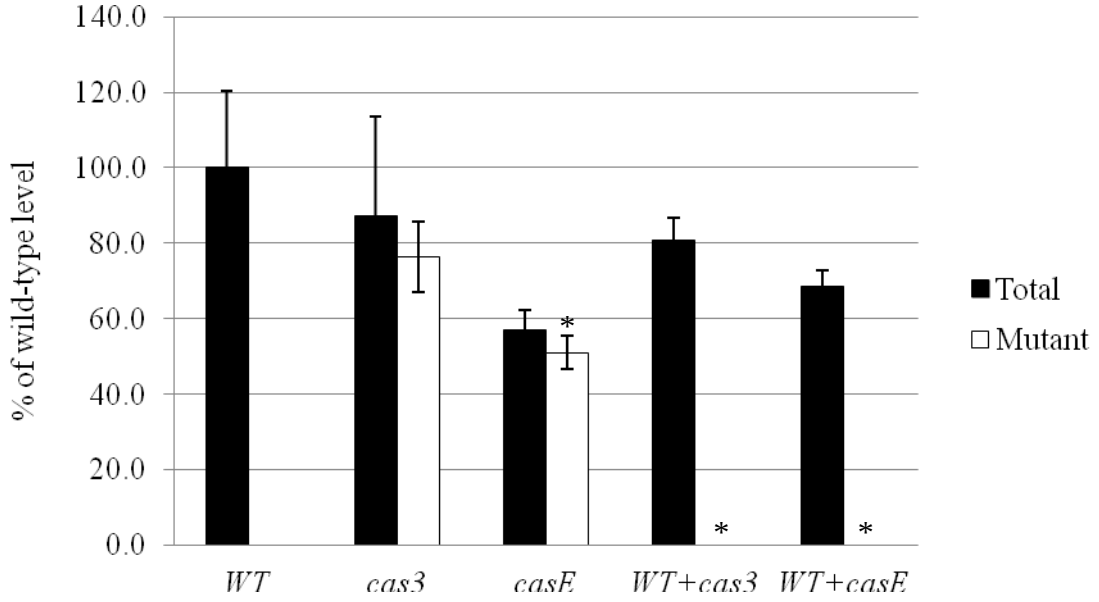

Figure 4.5. Competitive colonization phenotype of *cas* mutants in *in vivo* cultivation conditions. Colonization levels are shown as percent wild type levels for wild type (HGB800), the *cas3* mutant (HGB1577), and the *casE* mutant (HGB1694) cultivated with nematodes individually or in combination. Black and white bars show total and mutant colonization levels respectively, compared to wild type. Asterisks indicate statistically significant differences from wild-type levels. $P<0.05$. Statistics were done by Student's T-Test. Data are from two biological replicates from each of two experiments. Errors bars reprenent +/- SD.

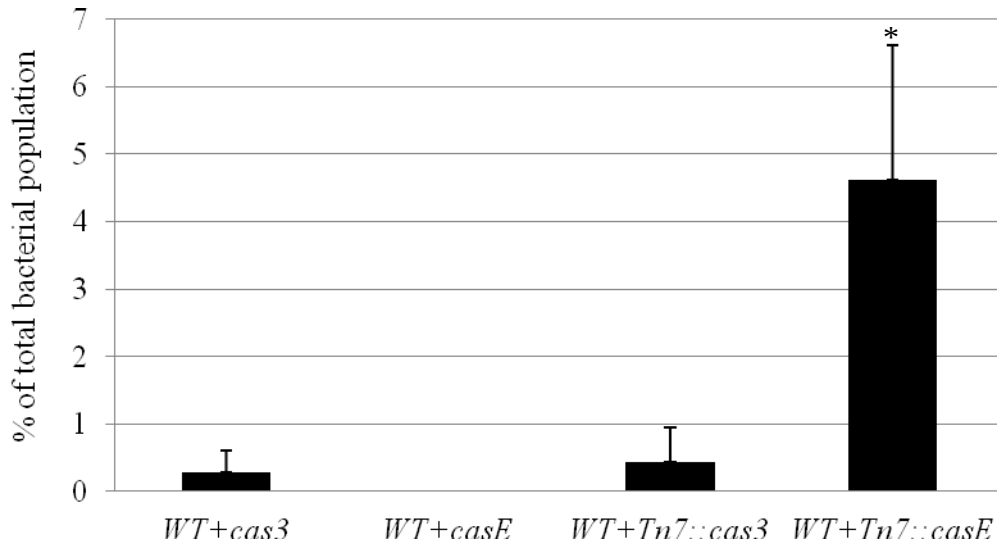

Figure 4.6. The competitive colonization phenotype of *cas3* and *casE* mutants complemented with *cas3* or *casE* in trans. Wild-type *X. nematophila* (HGB800), the *cas3* mutant (HGB1577), the *casE* mutant (HGB1694), *cas3* Tn*7*/*cas3* (HGB2028), and *casE* Tn*7*/*casE* (HGB2029). Black bars show the percentages of colonized *cas* mutants in the bacterial population isolated from IJs. Asterisks indicate statistically significant differences from uncomplemented levels. $P<0.05$. Statistics were done by Student's T-Test. Data are from two biological replicates from one experiment. Errors bars reprenent +/- SD.

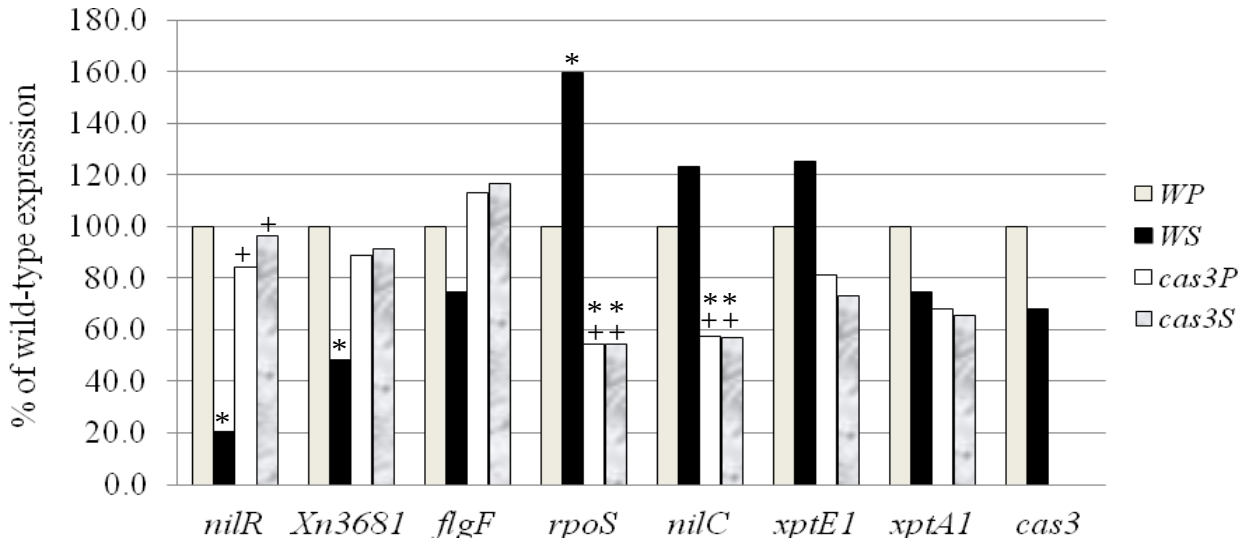

Figure 4.7. Effects of *cas3* on expression of select chromosomal genes in primary and secondary forms of *X. nematophila*. Transcript levels are shown as percent levels compared to wild-type. Primary wild-type *X. nematophila* HGB800 (*WP*), secondary wild-type *X. nematophila* HGB1061 (*WS*), primary *cas3* mutant HGB1577 (*cas3P*), and secondary *cas3* mutant of HGB1577 (the unstable secondary form tested was isolated by restreaking the secondary form colonies on NBTA plates 3 times) (*cas3S*). Asterisks indicate statistically significant differences from primary wild-type levels. $P<0.05$. Pluses indicate statistically significant differences from secondary wild-type levels. $P<0.05$. Statistics were done by One-Way ANOVA. Data are from two biological replicates from each of two experiments. Levels of *cas3* gene transcripts in *cas3* mutant were undetectable.

Bacterial strain	% of primary form
HGB800 wild-type primary	98.4 +/- 0.01
HGB1061 wild-type secondary	22.7 +/- 4.08
HGB1577 *cas3* mutant primary	97.6 +/- 2.28
HGB1577 *cas3* mutant secondary	38.7 +/- 1.88
HGB1874 *cas3 lrp* double mutant secondary	4.1 +/- 2.62
HGB1059 *lrp* mutant secondary	0
HGB1103 *nilR* mutant primary	99.6 +/- 0.54

Table 4.2. Percent primary form colonies from 13 hour cultures of *cas* and *lrp* mutant strains. Primary and secondary form colonies used for inoculating the cultures were freshly isolated by repetitive streaking on NBTA plates. The predominant phenotype (primary or secondary) of the starting culture is indicated. Overnight cultures from single colonies were diluted 1:1000 and 100 μl of the diluted culture were plated on NBTA and assessed for blue (primary) or red (secondary) color (3 plates per strain, the experiment was done twice). Errors bars reprenent +/- SD.

DISCUSSION

CCS have been widely identified in archaea and bacteria and are used by microbes for various purposes, including defending against invading phages and exogenous DNA elements, regulating endogenous gene expression and cellular functions (Bhaya *et al*., 2011). In this study, we first demonstrated the regulatory function of CCS on *X. nematophila* colonization in its mutualistic nematode host, and the potential involvement of CCS in regulating phenotypic variation in this bacterium. Microarray analysis (Chapter 2, Figure 4.2) showed that *X. nematophila cas* operon is suppressed by global regulator Lrp, and such regulation was also found in other microbes such as *Salmonella enterica* serovar Typhi and *E. coli* (Medina-Aparicio *et al*., 2011).

The lack of defects in virulence (Table 4.1) in *cas* mutants and the suppression of *cas* genes by colonization gene suppresser NilR (Figure 4.3) led to the idea that CSS is involved in *X. nematophila* mutualism. The competitive colonization defects of *cas* mutants both *in vitro* and *in vivo* when co-cultivated with wild-type bacteria (Figure 4.4, 4.5) further support the above assumption. The more severe colonization defects *in vivo* than *in vitro* (Figure 4.4, 4.5) also indicate that host specific factors affect the functions of *X. nematophila* CCS, and CCS is necessary for *X. nematophila* adaptation to both pathogenic and mutualistic host environments. Although *casE* mutant has a more severe defect than *cas3* mutant in colonization competition with wild-type, it had a higher level of recovery in such defect than *cas3* mutuant when complemented (Figure 4.6). This effect may due to the shorter promoter sequence used for *cas3* complementation, which may not allow an efficient complementation of *cas3* mutant. The partial recovery of the colonization competition defect of the *cas* mutants also indicates that the *cas*

genes may need to be coordinately expressed as an operon to obtain their full functions in mutualism. Further tests using the whole *cas* operon for complementation may help address this question.

When tested against *M. luteus*, the partial rescue of the inhibition defect of *lrp* mutant by *casE-lrp* double mutant indicates that *casE* is involved in the production of antibiotic xenocoumacin. The inability of the *casE-lrp* double mutant to rescue the inhibition defect against *B. subtilus* may because the bacterium is more resistant to xenocoumacin and the partial rescue cannot produce enough compound to reach the inhibitory level.

The higher phenotypic variation ratio of *cas3* mutant from secondary form to primary form (Table 4.2) indicates that CCS may affect bacterial mutualism by mediating the phenotypic switches between two forms. Previous studies have shown that the stable secondary form bacteria are the mostly isolated form from colonized IJs when competing with primary form bacteria (Sicard *et al*., 2005; Cowles *et al*., 2007). By increasing the frequency of primary form cells, *cas* mutants may become less favorable in nematode host during colonization process or for surviving in the host since the primary form is usually more virulent. This is supported by the fact that secondary *cas3* mutant cannot suppress *nilR* expression as in secondary wild-type (Figure 4.7) which causes the suppression of genes needed for nematode colonization. It also fails to increase the expression of *rpoS* that is known to be necessary for bacterial colonization in nematode host. As a general stress response regulator, RpoS may help bacterial cells deal with host-generated stress, such as reactive oxygen species, limitation of nutrients (Chapter 2). Thus failure to induce *rpoS* may set the *cas3* mutant at a disadvantage when competing with wild-type bacteria.

The more significant colonization defect of the *casE* mutant, predicted to be defective in crRNA processing relative to the *cas3* mutant, predicted to lack helicase activity for disassociation and annealing of RNA-DNA hybrids, also indicates a difference in *X. nematophila* CCS regulation from *E. coli*, where both components are essential for anti-phage functions (Pougach *et al*., 2010; Sinkunas *et al*., 2011). While the *nilD*-encoded CRISPR RNA, which has no apparent endogenous target, is essential for bacterial colonization indicating an involvement of potential anti-foreign RNA/DNA function in mutualism, the suppression of *Xn3681*, a gene encoded on an integrative and conjugative element, in secondary form by Cas3 (Figure 4.7) but not other endogenous genes (*flgF* and *xptE1*) that have CRISPR RNA sequences hinted that *X. nematophila* CCS may also regulate endogenous gene functions in a very specific manner. The partial rescue of antibiotic defect of *lrp* mutant by *casE* mutant but not *cas3* mutant further supports the above predication that *X. nematophila* Cas system is acting differently from *E.coli* Cas system (Pougach *et al*., 2010; Sinkunas *et al*., 2011). It also indicates that Cas system may affect cellular functions like antibiotic synthesis or secretion.

Although evidence is mounting that CCS plays a role in *X. nematophila* mutualism regulation, potentially via mediating phenotypic variation, further studies on the functions of individual Cas system components, identification of exogenous targets, especially in nematode and insect hosts, and understanding the conditions and mechanisms mediating endogenous gene regulation will provide valuable insight on CCS mediated microbe-host interactions.

MATERIALS AND METHODS

Bacterial and nematode strains, plasmids, and culture conditions

Table 4.3 lists strains and plasmids for this study. Unless specifically mentioned, *E.coli* were grown in LB broth or on LB plates at 37℃; *X. nematophila* were grown in LB broth or on LB plates supplemented with 0.1% pyruvate at 30℃ and kept in dark. Where appropriate, the following antibiotic concentrations were used: ampicillin, 150 μg/ml for *E.coli* and 50 μg/ml for *X. nematophila*; chloramphenicol, 30 μg/ml; erythromycin, 200 μg/ml; kanamycin, 50 μg/ml and streptomycin, 25 μg/ml. *E. coli* donor strain S17 (λ*pir*) or *Δasd* strain BW29427 was used to conjugate plasmids into *X. nematophila*. When necessary tri-parental conjugation using *E.coli* donor strain DH5α (λ*pir*) and helper *Δasd* strain BW3064 was performed to conjugate plasmids into *X. nematophila*. For growing BW29427 and BW3064, 100 μg/ml diaminopimelic acid (Sigma, St. Louis, MO) was added to the media. Nematodes were raised at 25^{o}C on bacterial lawns on lipid agar plates.

Molecular biological methods

Standard molecular biological methods were used in this study. Restriction enzymes (Promega, Madison, WI) and plasmid purification, gel extraction, and PCR purification kits (Zymo Research, Orange, CA) were used according to the manufacturers' recommendations. Constructs were sequenced at the UW-Madison Biotechnology Center using ABI Big Dye, version 3.1 (Applied Biosystems, Foster City, CA). PCR products for cloning were amplified using *Pfu* polymerase (Invitrogen, Carlsbad, CA). All other PCR amplifications were performed with

Ex*Taq* according to the manufacturer's directions (Takara, Otsu, Shiga, Japan). 0.5 μM of each appropriate primer was used for PCR amplifications. Table 4.4 lists the primers used in this study (Integrated DNA Technologies, Coralville, IA; UW-Madison Biotechnology Center, Madison, WI).

pCR2.1-TOPOmini construction

Primers TOPO2.1mini_Fwd_NcoI and TOPO2.1mini_Rev_NcoI were used to amplify the backbone of the plasmid pCR2.1-TOPO. The amplified product was cut with *Nco*I and self-ligated to form pCR2.1-TOPOmini, which had kan^r gene removed.

***cas-3* deletion mutant construction**

The 4,857 bp DNA fragment containing 2,751 bp *cas-3* gene and its up-stream (1,213 bp) and down-stream (893 bp) sequences was amplified from HGB800 chromosome DNA by using *Pfu* DNA polymerase (Stratagene, Santa Clara, CA) and primers cas3UpFwd_SpeI and cas3DownRev_XbaI. The fragment was digested with *Xba*I and *Spe*I and cloned into plasmid pCR2.1-TOPOmini between *Xba*I and *Spe*I sites. The kan^r gene with its promoter region was amplified from plasmid pEVS107 by using primers Kan-CleanRev_EcoRV_NEW and Kan-FullFwd_NheI_NEW, digested with *Nhe*I and *EcoR*V, and used to replace the 2,362 bp *Nhe*I-*EcoR*V region (89-2451 bp) within *cas3* gene to form to form pCR2.1mini *Δcas3::kan*. The *Spe*I-*Xba*I *cas3*::*Kan* fragment was then cloned into the *Spe*I site of the mobilizable suicide plasmid pKNG101 to generate pKNG*Δcas-3::kan*. The resulting construct was conjugated from *E.coli* S17-1 (*λpir*) into HGB800. Str^r exconjugants sensitive to 5% sucrose were grown on LB

agar containing 25μg/ml streptomycin overnight and subsequently grown on LB agar plus 5% sucrose to select for sucrose-resistant exconjugants that had excised the vector. The Sm^s phenotype was verified, and deletion of the *cas3* fragment was confirmed by PCR amplification.

casE deletion mutant construction

The 2,553 bp DNA fragment containing 678 bp *casE* gene and its up-stream (1,233 bp) and down-stream (642 bp) sequences was amplified from HGB800 chromosome DNA by using *Pfu* DNA polymerase and primers casEUpF_SpeI and casEDownR_ XbaI. The fragment was digested with *Xba*I and *Spe*I and cloned into plasmid pCR2.1-TOPOmini between *Xba*I and *Spe*I sites. The up-stream and down-stream sequences of *casE* along with the plasmid backbone were then amplified using primers casEDownF_EcoRV and casEUpR2_NheI. The product was digested with *Nhe*I and *EcoR*V and ligated with Kan^r cassette amplified from plasmid pEVS107 using primers Kan-CleanRev_EcoRV_NEW and Kan-FullFwd_NheI_NEW to form pCR2.1mini *ΔcasE::kan*. This deleted the 26-321 bp region of the *casE* gene. The *Spe*I-*Xba*I *casE::Kan* fragment was cloned into the *Spe*I site of plasmid pKNG101 to give pKNG*ΔcasE::kan*. The resulting construct was then conjugated into HGB800, and the exconjugants were selected as described above.

cas3 and _casE_ complementation strains construction

cas3 and *casE* genes with their native promoter sequences (53bp upstream of *cas3* and 192bp upstream of *casE*) were amplified from HGB800 chromosome DNA by using *Pfu* DNA polymerase and primer sets cas3FwdShortApaI and cas3RevSpeI, and casEFwdShortApaI and

casERevSpeI respectively. The PCR products were digested with *Spe*I and *Apa*I, and inserted between the *Spe*I and *Apa*I sites of pEVS107. The resulting constructs were then conjugated into *cas3* mutant (HGB2009 generated by conjugating pKNG*Δcas3::s*tr into HGB800) and *casE* mutant (HGB2008 generated by conjugating pKNG*ΔcasE::s*tr into HGB800) respectively using *E.coli* S17-1 (λ*pir*) as the donor strain. The exconjugants with the complementation constructs inserted at the Tn*7* site were selected on LB + Kan, and verified by PCR.

cas3 and _lrp_ double mutant construction

The *kan* cassette in pCR2.1mini *Δcas3::kan* was removed by cutting with *EcoR*V and *Nhe*I, the remaining backbone of the plasmid was ligated with the *str* cassette cut out from pKNG101 using *EcoR*V and *Spe*I, which forms pCR2.1mini *Δcas3::str*. The *Δcas3::str* cassette was cut out using *Spe*I and *Xba*I and ligated with pKNG101 backbone that was dephosphorylated after cut with *Xba*I and *Spe*I. The resulting plasmid pKNG*Δcas3::s*tr was then conjugated into HGB1059 to form *Δcas3::str Δlrp::kan* double mutant.

casE and _lrp_ double mutant construction

The kan cassette in pCR2.1 mini *ΔcasE::kan* was removed by cutting with *EcoR*V and *Nhe*I, the remaining backbone of the plasmid was ligated with the *str* cassette cut out from pKNG101 using *EcoR*V and *Spe*I, which forms pCR2.1mini *ΔcasE::str*. The *ΔcasE::str* cassette was cut out using *Spe*I and *Xba*I and ligated with pKNG101 backbone that was dephosphorylated after cut with *Xba*I and *Spe*I. The resulting plasmid pKNG*ΔcasE::str* was then conjugated into HGB1059 to form *ΔcasE::str Δlrp::kan* double mutant.

qRT-PCR analysis

Total RNA from wild-type and mutant *X. nematophila* strains were isolated at OD_{600} 2.1~2.2 using Qiagen RNeasy Mini Kit, treated with RQ1 DNase I (Promega, Madison, WI), and used to make cDNA with random hexamer primers (Integrated DNA Technologies, Coralville, IA) and AMV Reverse Transcriptase (Promega, Madison, WI). qRT-PCR reactions were performed in duplicate in 20 μl volume with iQ™ SYBR® Green Supermix (Bio-Rad, Hercules, CA), cDNA template and appropriate primers. Reactions were carried out with a two-step cycling protocol on a Bio-Rad iCycler and results were analyzed with Bio-Rad iCycler iQ™ software. qRT-PCR primers for individual genes are listed in table 2.2. Reactions using water and DNase-treated RNA as template instead of cDNA were performed as negative controls. As expected, no product was detected in negative control samples. Cycle threshold results for each sample were normalized using *recA* levels and the average expression levels in wild-type were designated as 100%.

Primary and secondary variation of *X. nematophila* strains

To test the phenotypic variation of different *X. nematophila* strains, overnight bacterial cultures (>20 hours) were streaked onto NBTA plates supplemented with 0.1% of pyruvate and incubated at 30°C in the dark for 2 days to allow primary and secondary forms of colonies to form. The primary or secondary form colonies of each strain were then re-streaked on NBTA plates. Newly formed primary or secondary form colonies from each plate were grown in LB + 50 mg/ml ampicillin for 13 hours, diluted in LB and plated on NBTA plates supplemented with 0.1% of pyruvate. The primary and secondary form colonies formed on each plate were counted and the percentages of primary form colonies were calculated.

Nematode colonization assays

Fresh overnight *X. nematophila* cultures were diluted 1:10 in LB, cell density was normalized using OD600, and diluted cultures were plated on three replicate lipid agar plates per strain per experiment. The plates were incubated at 30℃ in the dark for 24 hours to allow bacterial lawns to form. The nematode eggs were then added on the bacterial lawns and the plates were incubated in the dark at 25℃ for 7 days before transferred into water trap. IJs were collected 14 days after eggs were added to the plates, surface-sterilized and stored in sterile water. To measure the average number of colonized bacterial cells per IJ, IJ concentrations were adjusted to 20,000 IJs/ml, 1 ml of each IJ sample was mixed with 1 ml of LB broth and sonicated for 1 minute in a 10 ml glass culture tube using Branson 1510 water bath sonicator to release bacterial cells from IJs. Sonicated samples were then diluted and plated on LB plates supplemented with 0.1% pyruvate and appropriate antibiotics and incubated in the dark at 30℃ for 24 hours. In each experiment, the average wild-type value was defined as 100% colonization. All values were normalized to the designated wild-type value.

***In vitro* colonization competition assay**

Fresh overnight *X. nematophila* cultures were diluted 1:10 in LB, and cell density was normalized using OD600. The individual diluted cultures and mixtures of wild-type *X. nematophila* and individual mutant at 1:1 ratio were plated on three replicate lipid agar plates per strain per experiment. The plates were incubated at 30℃ in the dark for 24 hours to allow bacterial lawns to form. The nematode eggs were then added on the bacterial lawns and the plates were incubated in the dark at 25℃ for 7 days before transferred into water trap. IJs were

collected 30 days after eggs were added to the plates, surface-sterilized and stored in sterile water. To measure the average number of colonized bacterial cells per IJ, IJ concentrations were adjusted to 20,000 IJs/ml, 1 ml of each IJ sample was mixed with 1 ml of LB broth and sonicated for 1 minute in a 10 ml glass culture tube using Branson 1510 water bath sonicator to release bacterial cells from IJs. Sonicated samples were then diluted and plated on LB plates supplemented with 0.1% pyruvate and 50 μg/ml ampicillin for measuring the total CFU of colonized bacteria, and on LB plates supplemented with 0.1% pyruvate and 50 μg/ml kanamycin for measuring the CFU of colonized mutant bacteria. In each experiment, the average wild-type value was defined as 100% colonization. All values were normalized to the designated wild-type value.

***In vivo* colonization competition assay**

Cell density of fresh overnight *X. nematophila* cultures was normalized using OD600, and the normalized cultures were diluted 1:1000 in LB. 500 μl of the individual diluted cultures or mixtures of wild-type *X. nematophila* and individual mutant at 1:1 ratio were mixed with 500 μl of freshly isolated nematode eggs. 25 μl of the bacterial-egg mixture was injected into each *Galleria mellonella* larvae. In each experiment, 9 worms were injected with the bacterial-egg mixture and the experiment was done in duplicates. After 5 days the dead worms were moved into water trap. IJs were collected 30 days after injection, surface-sterilized and stored in sterile water. To measure the average number of colonized bacterial cells per IJ, IJ concentrations were adjusted to 20,000 IJs/ml, 1 ml of each IJ sample was mixed with 1 ml of LB broth and sonicated for 1 minute in a 10 ml glass culture tube using Branson 1510 water bath sonicator to release

bacterial cells from IJs. Sonicated samples were then diluted and plated on LB plates supplemented with 0.1% pyruvate and 50 μg/ml ampicillin for measuring the total CFU of colonized bacteria, and on LB plates supplemented with 0.1% pyruvate and 50 μg/ml kanamycin for measuring the CFU of colonized mutant bacteria. In each experiment, the average wild-type value was defined as 100% colonization. All values were normalized to the designated wild-type value.

Phenotypic assays

The hemolysin activity (Rowe and Welch, 1994) towards sheep and horse erythrocytes, protease activity (Boemare *et al*., 1997), lipase activity (Sierra, 1957), motility (Vivas and Goodrich-Blair, 2001), antibiotic production (Maxwell *et al*., 1994) and insect killing ability in *Manduca sexta* (Cowles and Goodrich-Blair, 2005) were tested as described in previous published literatures.

Statistics

Unless otherwise specified, experiments were done twice with 2 biological replicates for each experiment. Statistics were done with Student's T-Test for single comparison, and with One-Way ANOVA for multi-comparisons. For qRT-PCR, statistics were done using arbitrary RNA units, and the results were presented as percentage of wild-type levels for comparison.

Table 4.3. List of strains and plasmids

Strain or plasmid	Description	Reference
HGB800	Amp^r; *X. nematophila* wild-type ATCC 19061	ATCC
HGB1059	Amp^r; Kan^r; *Δlrp::kan*; HGB800	Cowles *et al.*, 2006
HGB1103	Amp^r; Kan^r; *ΔnilR::kan*; HGB800	C. Cowles
HGB1262	Cm^r; Kan^r; *Δasd*; *E. coli* BW29427 donor strain for conjugations	B. Wanner
HGB1577	Amp^r; Kan^r; *Δcas3::kan*; HGB800	This study
HGB1694	Amp^r; Kan^r; *ΔcasE::kan*; HGB800	This study
HGB1874	Amp^r; Kan^r; Str^r; *Δcas3::str*; *Δlrp::kan*; HGB800	This study
HGB1877	Amp^r; Kan^r; Str^r; *ΔcasE::str*; *Δlrp::kan*; HGB800	This study
HGB1320	Amp^r; Kan^r; *ΔlrhA::kan*; HGB800	Richards *et al.* 2009
HGB2008	Amp^r; Kan^r; Str^r; *Δcas3::str*; HGB800	This study
HGB2009	Amp^r; Kan^r; Str^r; *ΔcasE::str*; HGB800	This study
HGB2028	Amp^r; Kan^r; Str^r; *Δcas3::str*; Tn*7::cas3*; HGB800	This study
HGB2029	Amp^r; Kan^r; Str^r; *ΔcasE::str*; Tn*7::casE*; HGB800	This study

DH5α (λ*pir*)	*E. coli* general cloning and donor strain	Sambrook *et al.*, 1989
S17-1 (λ*pir*)	Str^r; *E. coli* donor strain for conjugations	Simon *et al.*, 1983
BW3064	Amp^r; *Δasd*; pUX-BF13; *E. coli* helper strain for conjugations	B. Wanner
pKNG101	Str^r; *oriR6K* suicide vector	Kaniga *et al*, 1991
pEVSCm	Derivative of pEVS107; Tn*7* transposon vector	E. Martens, University of Wisconsin-Madison
pUX-BF13	Amp^r; Triparental conjugation helper plasmid	Bao *et al*., 1991
pCR2.1-TOPO	Ap^r; Kan^r; General cloning vector	Invitrogen, Carlsbad, CA
pCR2.1-TOPOmini	Ap^r; General cloning vector	This study
pCR2.1mini *Δcas3::kan*	Kan^r; pCR2.1-TOPOmini with *Δcas3::kan*	This study
pCR2.1mini *ΔcasE::kan*	Kan^r; pCR2.1-TOPOmini with *ΔcasE::kan*	This study
pCR2.1mini *Δcas3::str*	Kan^r; pCR2.1-TOPOmini with *Δcas3::str*	This study
pCR2.1mini *ΔcasE::str*	Kan^r; pCR2.1-TOPOmini with *ΔcasE::str*	This study
pKNG*Δcas3::kan*	Kan^r; Str^r; pKNG101 with *Δcas3::kan*	This study
pKNG*ΔcasE::kan*	Kan^r; Str^r; pKNG101 with *ΔcasE::kan*	This study

pKNG*Δcas3::str*	Str^r; pKNG101 with *Δcas3::str*	This study
pKNG*ΔcasE::str*	Str^r; pKNG101 with *ΔcasE::str*	This study

Table 4.4. List of primers

Primer	Sequences 5' to 3'	Use
nilRFwd1 qPCR	TGGACAACGCATTCAGACCA	qRT-PCR *nilR*
nilRRev1 qPCR	GAGTTGTTGCTGACTGATGCCA	qRT-PCR *nilR*
rpoSFwd1 qPCR	ACCCGCACAATTCGTCTGC	qRT-PCR *rpoS*
rpoSRev1 qPCR	CCGCAATTTCTTCAACCGTG	qRT-PCR *rpoS*
lrpFwd qPCR	GCGAGTAGGTCTGTCACCAACA	qRT-PCR *lrp*
lrpRev qPCR	ACATCTGCTGCACCACGATTC	qRT-PCR *lrp*
cpxPFwd1 qPCR	CTGAACAACAGCGCCAGCA	qRT-PCR *cpxR*
cpxPRev1 qPCR	TTCTGACGTTCAACCCGCAT	qRT-PCR *cpxR*
cas3UpFwd_SpeI	ATATATACTAGTCCATGGCTACTTTGAATTTCCTTG	*cas3* mutant
cas3DownRev_XbaI	ATATATTCTAGACGGATTCCACCGATAGGGTG	*cas3* mutant
Kan-CleanRev_EcoRV_NEW	ATATATGATATCTTAGAAAAACTCATCGAGCATCAAATG	*cas3* mutant
Kan-FullFwd_NheI_NEW	ATATATGCTAGCCCACGTTGTGTCTCAAAATCTCTG	*cas* mutant
casEUpF_SpeI	ATATATACTAGTCTTTACCGCCGTGGACGAT	*casE* mutant
casEDownR_ XbaI	ATATATTCTAGAATAAAGGTTTACCCGTGTGCAGA	*casE* mutant

casEDownF_EcoRV	ATATATGATATCGATTCAGGCA AACAGCGGC	*casE* mutant
casEUpR2_NheI	ATATATGCTAGCGCAAGGTGAC TTTAGACAGATACA	*casE* mutant
TOPO2.1mini_Fwd_NcoI	ATATATCCATGGCGATGCCTGC	Vector construction
TOPO2.1mini_Rev_NcoI	ATATATCCATGGTCCATTCGCCA TTCAGGC	Vector construction

REFERENCES

Aklujkar M, Lovley DR. 2010. Interference with histidyl-tRNA synthetase by a CRISPR spacer sequence as a factor in the evolution of *Pelobacter carbinolicus*. BMC Evol Biol. 10:230

Babu M, Beloglazova N, Flick R, Graham C, Skarina T, Nocek B, Gagarinova A, Pogoutse O, Brown G, Binkowski A, Phanse S, Joachimiak A, Koonin EV, Savchenko A, Emili A, Greenblatt J, Edwards AM, Yakunin AF. 2011. A dual function of the CRISPR-Cas system in bacterial antivirus immunity and DNA repair. Mol Microbiol.79(2):484-502

Bhaya D, Davison M, Barrangou R. 2011. CRISPR-Cas systems in bacteria and archaea: versatile small RNAs for adaptive defense and regulation. Annu Rev Genet. 45:273-97

Bird, AF and Akhurst RJ. 1983. The nature of the intestinal vesicle in nematodes of the family *Steinernematidae*. Int. J. Parasitol. 13:599–606

Boemare N, Thaler JO, Lanois A. 1997. Simple bacteriological tests for phenotypic characterization of *Xenorhabdus* and *Photorhabdus* phase variants. Symbiosis. 22:167-175

Brouns SJ, Jore MM, Lundgren M, Westra ER, Slijkhuis RJ, Snijders AP, Dickman MJ, Makarova KS, Koonin EV, van der Oost J. 2008. Small CRISPR RNAs guide antiviral defense in prokaryotes. Science. 321(5891):960-4.

Chaston JM, Suen G, Tucker SL, Andersen AW, Bhasin A, Bode E, Bode HB, Brachmann AO, Cowles CE, Cowles KN, Darby C, de León L, Drace K, Du Z, Givaudan A, Herbert Tran EE, Jewell KA, Knack JJ, Krasomil-Osterfeld KC, Kukor R, Lanois A, Latreille P, Leimgruber NK, Lipke CM, Liu R, Lu X, Martens EC, Marri PR, Médigue C, Menard ML, Miller NM, Morales-Soto N, Norton S, Ogier JC, Orchard SS, Park D, Park Y, Qurollo BA, Sugar DR, Richards GR, Rouy Z, Slominski B, Slominski K, Snyder H, Tjaden BC, van

der Hoeven R, Welch RD, Wheeler C, Xiang B, Barbazuk B, Gaudriault S, Goodner B, Slater SC, Forst S, Goldman BS, Goodrich-Blair H. 2011. The entomopathogenic bacterial endosymbionts Xenorhabdus and Photorhabdus: convergent lifestyles from divergent genomes. PLoS ONE 6(11):e27909

Cowles KN, Cowles CE, Richards GR, Martens EC, Goodrich-Blair H. 2007. The global regulator Lrp contributes to mutualism, pathogenesis and phenotypic variation in the bacterium *Xenorhabdus nematophila*. Cell. Microbiol. 9(5):1311-23

Cowles KN, Goodrich-Blair H. 2005. Expression and activity of a *Xenorhabdus nematophila* haemolysin required for full virulence towards Manduca sexta insects. Cell. Microbiol. 7(2):209-19

Forst S, Dowds B, Boemare N, Stackebrandt E. 1997. *Xenorhabdus* and *Photorhabdus* spp.: bugs that kill bugs. Annu Rev Microbiol. 51:47-72

Forst S and Clarke D. 2002. Bacteria-nematode symbioses. In *Entomopathogenic Nematology*. Gaugler, R. (eds). Wallingford: CABI Publishing, pp. 57–77.

Herbert EE, Goodrich-Blair H. 2007. Friend and foe: the two faces of *Xenorhabdus nematophila*. Nat. Rev. Microbiol. 5(8):634-46

Heungens K, Cowles CE, Goodrich-Blair H. 2002. Identification of *Xenorhabdus nematophila* genes required for mutualistic colonization of *Steinernema carpocapsae* nematodes. Mol Microbiol. 45(5):1337-53.

Kaniga, K., I. Delor, and G. R. Cornelis. 1991. A wide-host-range suicide vector for improving reverse genetics in gram-negative bacteria: inactivation of the *blaA* gene of *Yersinia enterocolitica*. Gene 109**:**137–141

Maxwell PW, Chen G, Webster JM, Dunphy GB. 1994. Stability and Activities of Antibiotics Produced during Infection of the Insect Galleria mellonella by Two Isolates of *Xenorhabdus nematophilus*. Appl Environ Microbiol. 60(2):715-21

Medina-Aparicio L, Rebollar-Flores JE, Gallego-Hernández AL, Vázquez A, Olvera L, Gutiérrez-Ríos RM, Calva E, Hernández-Lucas I. 2011. The CRISPR/Cas immune system is an operon regulated by LeuO, H-NS, and leucine-responsive regulatory protein in *Salmonella enterica serovar* Typhi. J Bacteriol. 193(10):2396-407.

Morgan W, Kuntzelmann V, Tavernor S, Ousley MA, Winstanley C. 1977. Survival of *Xenorhabdus nematophilus* and *Photorhabdus luminescens* in water and soil. J. Appl. Microbiol. 83, 665–670

Pougach K, Semenova E, Bogdanova E, Datsenko KA, Djordjevic M, Wanner BL, Severinov K. 2010. Transcription, processing and function of CRISPR cassettes in *Escherichia coli*. Mol Microbiol. 77(6):1367-79

Rowe GE, Welch RA. 1994. Assays of hemolytic toxins. Methods Enzymol. 235:657-67

Sergeant M, Baxter L, Jarrett P, Shaw E, Ousley M, Winstanley C, Morgan JA. 2006. Identification, typing, and insecticidal activity of *Xenorhabdus* isolates from entomopathogenic nematodes in United Kingdom soil and characterization of the *xpt* toxin loci. Appl Environ Microbiol. 72(9):5895-907.

Sicard M, Tabart J, Boemare NE, Thaler O, Moulia C. 2005. Effect of phenotypic variation in *Xenorhabdus nematophila* on its mutualistic relationship with the entomopathogenic nematode *Steinernema carpocapsae*. Parasitology. 131(Pt 5):687-94

Sierra G. 1957. A simple method for the detection of lipolytic activity of micro-organisms and some observations on the influence of the contact between cells and fatty substrates. Antonie Van Leeuwenhoek. 23(1):15-22

Sambrook, J., E. F. Fritsch, and T. Maniatis. 1989. Molecular cloning: a laboratory manual, 2nd ed. Cold Spring Harbor Laboratory Press, Cold Spring Harbor, NY.

Simon, R., U. Priefer, and A. Pu ̈hler. 1983. A broad host range mobilization system for *in vivo* genetic engineering: transposon mutagenesis in gram negative bacteria. Biotechnology **1:**784–791.

Sinkunas T, Gasiunas G, Fremaux C, Barrangou R, Horvath P, Siksnys V. 2011. Cas3 is a single-stranded DNA nuclease and ATP-dependent helicase in the CRISPR/Cas immune system. EMBO J. 30(7):1335-42

Snyder, H., Stock, P., Kim, S., Flores-Lara, Y. and Forst, S. 2007. New Insights into the Colonization and Release Processes of *Xenorhabdus nematophila* and the Morphology and Ultrastructure of the Bacterial Receptacle of its Nematode Host, *Steinernema carpocapsae*. Appl. Environ. Microbiol. 66: 1622-1628

Viswanathan P, Murphy K, Julien B, Garza AG, Kroos L. 2007. Regulation of dev, an operon that includes genes essential for *Myxococcus xanthus* development and CRISPR-associated genes and repeats. J Bacteriol. 189(10):3738-50

Vivas EI, Goodrich-Blair H. 2001. *Xenorhabdus nematophilus* as a model for host-bacterium interactions: *rpoS* is necessary for mutualism with nematodes. J Bacteriol. 183(16):4687-93

Volgyi A, Fodor A, Szentirmai A, Forst S. 1998. Phase Variation in *Xenorhabdus nematophilus*. Appl Environ Microbiol. 64(4):1188-93

CHAPTER 5

Summary and future directions

Summary

This thesis describes the exploration of the regulatory networks involved in the mutualistic and pathogenic interactions between bacterium *Xenorhabdus nematophila* and its nematode and insect hosts. Before this work, the connections among the known regulators of bacterial mutualism and pathogensis were not fully established. Here, I employed microarray technology to further define the regulons of three known regulators: Lrp, LrhA (Chapter 2) and RpoS (Chapter 3). I indentified the connection between two known regulators Lrp and RpoS (Chapter 2 and 3) and revealed a new factor, Cas system, that is involved in bacterial mutualism and phenotypic variation (Chapter 2 and 4). I also provided insights on the role of RpoS in mutualistic bacterium-host interaction (Chapter 3). Overall, this work helped identify and connect the new factors with known regulators, and expanded our knowledge on the regulatory networks of *X. nematophila*-host interactions.

Future directions

Further define the regulons of other regulatory factors. In Chapters 2 and 3, I explored the global gene expression profiles of three regulators (Lrp, LrhA and RpoS) involved in bacterial mutualism and pethogenesis. However, the global effects of other regulators, such as NilR, CpxR and Cas system, are still not clear even though they have been shown to play important roles in bacterium-host interactions. Thus future microarray analysis of the effects of these factors will provide more insights for us to connect the functions of these factors and complete the regulatory networks in *X. nematophila*.

Explore the role of the nutrient transport/uptake function of RpoS in bacterial mutualism. Through the microarray analysis I have demonstrated that RpoS suppresses a large number of transporters for nutrient uptake and transportation (Chapter 3). The fact that *oppB* mutant, a gene of oligopeptide permease *opp* operon suppressed by RpoS, is more competitive in nematode colonization suggests that the nutrient uptake needs to be properly regulated during mutualism. This may help explain the colonization defect of *rpoS* mutant as disrupted suppression of excessive nutrient uptake may make the mutant less adaptive in nematode host. Future work testing possible rescue of colonization defect of *rpoS* mutant by introducing transporter mutations will help answer this question.

Identify when the *rpoS* mutant fails to colonize nematode host. Studies have shown that the bacterium needs to go through a series of stages for colonizing nematode host, involving host recognition, attachment to the pharyngeal-intestinal valve of pre-IJs, and outgrowth and

persistence in receptacle. By using GFP labeled strains to monitor the *in vivo* behavior of *rpoS* mutant we can gain useful information on the underlying mechanisms of RpoS-dependent mutualism. Further characterization of RpoS dependent gene expression profile under conditions that mimic host environment will provide more knowledge on how RpoS affects microbe-host interactions in a mutualistic background.

Futher characterize *X. nematophila* Cas system in mutualistic and pathogenic bacterium-host interactions. In this work I have provided evidences that indicate the role of Cas system in bacterial mutualism and pathogenesis, potentially via mediating phenotypic variation. Further studies on the functions of individual Cas system components, identification of exogenous targets, especially in nematode and insect hosts, and understanding the conditions and mechanisms mediating endogenous gene regulation will provide valuable insight on Cas sytem mediated microbe-host interactions.